UNIVERSITY OF ALBERTA
LIBRARY

Regulations Regarding Theses and Dissertations

Typescript copies of theses and dissertations for Master's and Doctor's degrees deposited in the University of Alberta Library, as the official Copy of the Faculty of Graduate Studies, may be consulted in the Reference Reading Room only.

A second copy is on deposit in the Department under whose supervision the work was done. Some Departments are willing to loan their copy to libraries, through the inter-library loan service of the University of Alberta Library.

These theses and dissertations are to be used only with due regard to the rights of the author. Written permission of the author and of the Department must be obtained through the University of Alberta Library when extended passages are copied. When permission has been granted, acknowledgement must appear in the published work.

This thesis or dissertation has been used in accordance with the above regulations by the persons listed below. The borrowing library is obligated to secure the signature of each user.

Please sign below:

Date	Signature	Institution

THE UNIVERSITY OF ALBERTA

CATALYSIS WITH AN ION EXCHANGE RESIN - THE HYDROLYSIS OF ETHYL ACETATE IN A CONTINUOUS - FLOW - STIRRED TANK REACTOR

BY

DINESH B. GANDHI

A THESIS

SUBMITTED TO THE FACULTY OF GRADUATE STUDIES

IN PARTIAL FULFILMENT OF THE REQUIREMENTS FOR THE

DEGREE OF MASTER OF SCIENCE

IN

CHEMICAL ENGINEERING

FACULTY OF ENGINEERING

DEPARTMENT OF CHEMICAL AND PETROLEUM ENGINEERING

EDMONTON, ALBERTA

FEBRUARY, 1966

UNIVERSITY OF ALBERTA

FACULTY OF GRADUATE STUDIES

The undersigned certify that they have read, and recommend to the Faculty of Graduate Studies for acceptance, a thesis entitled "Catalysis with an Ion Exchange Resin - The Hydrolysis of Ethyl Acetate in a Continuous - Flow - Stirred Tank Reactor" submitted by Dinesh B. Gandhi in partial fulfulment of the requirements for the degree of Master of Science in Chemical Engineering.

ACKNOWLEDGEMENTS

The author wishes to express his sincere appreciation for the guidance and encouragement of Dr. F.D. Otto, under whose supervision this investigation was performed.

The financial assistance provided by the National Research Council of Canada and the University of Alberta is gratefully acknowledged.

The author also thanks Miss B. Penner for typing this thesis.

ABSTRACT

A mathematical model is proposed for a solid-liquid catalytic reaction carried out in a nonideal continuous-flow-stirred-tank reactor (CFSTR). The model considers a nonideal CFSTR as a combination of a perfectly backmixed reactor and a by-pass region and describes the effect of external mass transfer, intraparticle diffusion and chemical reaction (first order, irreversible) and the nonideality in the reactor operation on the overall reaction rate. The derived rate expression permits evaluation of the various parameters which characterize the individual phenomena.

Attempts were made to verify the model experimentally. The experimental set up consisted of a glass CFSTR and the related accessories. The reaction employed was the hydrolysis of ethyl acetate catalysed by a cation exchange resin. The experimental work was performed in three parts.

The first part involved the determination of the response of the reactor to a step change in the feed. This was done to evaluate the extent of nonideality at different agitator speeds. The results indicate that the reactor exhibited no nonideality in operation under the experimental conditions employed.

The second part was concerned with the evaluation, of the significance of the external film diffusion by carrying out the reaction at various agitation rates. The problem was, however, complicated due to settling of the resin particles at low stirrer speeds. For all stirrer speeds at which the particles were completely in the bulk phase, the external film mass transfer resistance was negligible.

In the last and more extensive phase of the study the rate constant, k, and the effective diffusivity, D, for ethyl acetate in the resin phase were determined at different temperatures by carrying out the reaction at high stirrer speeds. Effectiveness factors for the catalyst were calculated for different temperatures and particle diameters. The results indicate that the chemical reaction is the rate limiting step for the hydrolysis of ethyl acetate under the experimental conditions employed.

These results are discussed in light of the work done by previous investigators. Though only a partial verification of the model was achieved, significant knowledge was gained on various aspects of the system.

TABLE OF CONTENTS

LIST OF TABLES

LIST OF FIGURES

CHAPTER I

INTRODUCTION

The investigation of a heterogeneous catalytic reaction is complicated by the fact that in such a system there is an interplay between the true chemical reaction rate and the physical transport phenomenon. Depending on the reaction system and the operating conditions either one may contribute the dominating influence on the overall rate process.

It is postulated that in the presence of a relative motion between a solid particle and the ambient fluid, a thin film of the liquid envelopes the particle. The reactants diffuse through this film and then into the catalytic particle where chemical reaction takes place. To isolate only one of these rate processes for study, it is necessary to devise conditions so that all the other effects play no role in the observed kinetics. However, these extremes are not always experimentally accessible. Often within the range of conditions for a chemical reaction the individual rate processes are coupled and then it is necessary to account for their combined effects on the reaction rate.

With a given reaction system, the effect of varying turbulence, catalyst size and temperature in an experimental study should indicate, respectively, the importance of external film diffusion, intra-particle diffusion and chemical reaction. It is convenient to study these aspects in a Continuous-Flow-Stirred-Tank Reactor (CFSTR). The experimental data do not require differentiation or integration, nor is an especially precise analysis required. Unlike tubular reactors the intensity of turbulence is independent of the flow rate and can be easily controlled by the degree of agitation. Therefore the effect of film mass transfer may be more easily evaluated or eliminated in a CFSTR. Similarly, the temperature gradients within the bulk phase can be eliminated.

By definition, the contents of an ideal CFSTR are perfectly mixed; they are at uniform composition and temperature. At steady state the exit stream has the same composition as the fluid within the reactor. However, deviations from the ideal behaviour may occur at low stirrer speeds which give imperfect mixing. This nonideality results in nonuniform composition in the reactor and causes changes in the extent of the reaction.

The particular system chosen for experimental study was the hydrolysis of Ethyl Acetate using a suspension of acidic ion exchange resin paricles as catalyst. The ester hydrolysis proceeds according to the reaction:

$$C_2H_5COOCH_3 + H_2O \longrightarrow CH_3COOH + C_2H_5OH$$

The reaction is fairly rapid at moderate temperatures in the presence of the catalyst and proceeds at a negligible rate without the catalyst. By employing a large excess of water the rate of the reaction can be approximated by the linear relation

$$\text{Rate} = kC$$

This, in addition, ensures low concentrations of the products in the resulting mixture. The reaction can therefore be assumed as virtually irreversible.

Previous experiments with similar systems show wide disagreement: some investigators reported significant film-diffusion effects while others found simultaneous intra-particle-diffusion and chemical reaction as the rate controlling process. Again, while there exists considerable literature on the theoretical aspects of nonideal behaviour of backmix reactors, some workers have reported only minor deviations even in the absence of any stirring.

In face of these seemingly divergent observations, the aim of this investigation, then, was to establish the relative importance of different rate processes under varying operating conditions for the reaction under study, to ascertain to what extent nonideality in flow exists and also to investigate a means of accounting for this nonideality in prediction of the actual conversion in the reactor.

CHAPTER II

THEORY

II.- A. GENERAL

A catalyst is a substance which by virtue of its presence in the reaction mixture, changes the rate of chemical reactions but is not consumed stoichiometrically in the reactions. Catalysts offer an alternate route for the reactions to take place. This property of a catalyst is advantageously employed in reactions which otherwise require extreme operating conditions.

In a heterogeneous system, a catalyst is instrumental in the chemical conversion in the sense that the reaction takes place at or near the solid surface. Therefore the reactants present in the ambient fluid have to be transferred to the interface and the products away from it. In the main body of a well-agitated fluid, the transport takes place by a rapid eddy diffusion. However, due to frictional effects near the solid surface, the catalyst particle is surrounded by a thin film of the liquid. Mass transfer through this relatively stagnant film occurs only by molecular diffusion and convection.

It is recognized that in a heterogeneous catalysic reaction, the following steps occur successively:

(a) The reactants diffuse through the liquid film to the particle surface,

(b) The reactants then diffuse into the interior of the catalyst,

(c) Chemical reaction takes place, and

(d) The products diffuse outwards through the surrounding liquid film to the bulk of the fluid.

As the chemical reaction occurs simultaneously with the intra-particle diffusion, they provide resistances in parallel and they both offer resistance in series with the liquid film mass transfer resistance. Whenever one of the steps offers major resistance, that step may be considered as the rate controlling step. Resistances of the different steps can and do vary greatly from each other. Also their relative importance varies with the operating conditions. The individual resistances and their dependence on the operating conditions must be known in order to express the overall rate expression in terms of the concentrations in the bulk fluid stream.

II-B. LIQUID FILM DIFFUSION

Many mechanisms have been postulated to explain the mass transfer of solute from the bulk fluid to the particle surface. That this transfer of material is very closely related to the

existing flow pattern in the vicinity of the particles and to the fluid properties is at once obvious. The present qualitative picture is of continuous increase in turbulence from the interface to the main body of liquid. The concept of a film as proposed by Lewis & Whitman (1924) can be used as a convenient basis for a mental picture of the localization of diffusional resistance in a region near the interface. Beyond this the theory has serious limitations. Later developments of the penetration and the boundary layer theories have provided more realistic models.

For convenience and by usage it has been customary to express the mass transfer rate by the equation

$$N = K(C_b - C_s) \qquad \text{(II.1)}$$

where, N = Rate, $\text{gmmoles}\cdot\text{hr}^{-1}\cdot\text{cm}^{-2}$

K = Mass Transfer Coefficient, $\text{cm}\cdot\text{hr}^{-1}$

C_b = Bulk concentration, $\text{gmmoles}\cdot\text{ml}^{-1}$ of solute

C_s = Interface concentration, $\text{gmmoles}\cdot\text{ml}^{-1}$ of solute

This equation itself is a mathematical definition of the mass transfer coefficient and this coefficient remains to be related, theoretically and experimentally, to the basic properties of the fluid and the flow conditions.

Usually the experimental data on mass transfer coefficient are related with the apparent variables of a system by a semi-

empirical equation of the form

$$\frac{Kl}{D_l} = c\left(\frac{d_s N \cdot l \rho}{\mu}\right)^a \left(\frac{\mu}{\rho D_l}\right)^b \qquad \text{(II.2)}$$

where, D_l = Diffusivity in the liquid phase

l = A characteristic length

d_s = Agitator diameter

The equation can be derived by dimensional analysis. The constants a, b and c of the equation are determined from experimental results. Though applicable only under limited conditions, the equation has been widely used to predict the mass transfer coefficient.

II- C. INTRA-PARTICLE DIFFUSION AND SURFACE REACTION

From the particle surface reactants must diffuse into the catalyst particle through the pore structure. The pores are substantially interconnected channels of irregular shapes and varying cross-sections. Any mathematical treatment of intra-particle diffusion remains largely emperical because the pore geometry of most catalysts cannot be adequately defined. A simple approach has been to represent the complex diffusion process by a single effective diffusion coefficient, D, which satisfies the equation

$$N = D\left(\frac{dC}{dx}\right) \qquad \text{(II. 3)}$$

at any location in the particle.

where, N = Flux of the flow of diffusing species, gmmoles·min^{-1}· cm^{-2}

C = Local concentration of the diffusing species in the porous solid, gmmoles·cm^{-3}

x = Distance parameter, cms

D = Effective diffusivity in the solid phase, cm^{2}·min^{-1}

It should be noted that the effective diffusivity is based on the unit geometric area of the solid particle.

As the reactants reach the interface, chemical reaction takes place. Many theories have been developed in an attempt to explain the nature of surface reaction. Very detailed mechanisms have been proposed. The most commonly accepted theory postulates that the reaction takes place on active sites on the surface of the catalyst. The reaction is therefore accompanied by adsorption and desorption processes. The rate expressions resulting from these mechanisms involve many arbitary constants. Many a times a number of alternative mechanisms fit the data equally well and the choice of the correct reaction scheme is not obvious. For this

reason some authors have advocated the use of simple equations of the form

$$\text{Rate} = kC^n$$

or

$$\text{Rate} = \frac{aC}{1+bC}$$

to correlate rate data. This type of rate expression simplifies the mathematical treatment.

The simultaneous mass transfer and chemical reaction establishes a concentration gradient within the catalyst particle. The interior surfaces are then exposed to reactant concentrations lower than the ambient fluid and the overall reaction rate throughout the catalyst particle under isothermal conditions is less than it would be if there were no intra-particle diffusion limitations. In this sense the internal surface is not effectively utilized. An 'Effectiveness Factor', η, can be defined as the ratio of the actual reaction rate to that which would occur if all the internal surface were exposed to reactant of the same concentration and temperature as that existing at the outside surface of the particle.

$$\eta = \frac{\text{Rate observed}}{\text{Rate in absence of internal diffusion}} \qquad \text{(II.4)}$$

The effectiveness factor describes the rate of reaction in terms of the values of the concentration and temperature at the external surface.

For simple cases the effectiveness factor can be quantitatively expressed as a function of the catalyst size and intrinsic reaction parameters; e.g., for spherical particles with no internal temperature gradients and first order reaction (See Appendix A)

$$\eta = \frac{3}{w^2R^2}\,(wR\cdot\coth(wR) - 1) \qquad \text{(II.5)}$$

where,

$$w^2 = \frac{k}{D}$$

This equation has important practical implications

: If wR is small - that is small k and/or R, and/or large D - η approaches unity. All the active surface is exposed to the same reactant concentration; internal diffusional effects are insignificant.

: If wR is large - in a system with low diffusivity and/or fast reaction and/or large particle diameter - the effectiveness, η , becomes small, i.e., the internal area is not effectively utilized.

Thus very active catalysts (large k) tend to have low effectiveness factors. In this case, maximum use is made of a catalyst by employing the smallest practical particle size.

CHAPTER III

LITERATURE REVIEW

Ion exchange resins have been found to catalyse numerous reactions (40). Ester hydrolysis using a cation exchange resin has been subject to considerable investigation. The fact that an acidic ion exchange resin can catalyse the hydrolysis of an ester was observed by Sussman (55) and Thomas and Davies (57).

Hammett et al (4,29) studied the hydrolysis of ten esters, including Methyl and Ethyl Acetates, in 70% aqueous acetone at 25° C. They used IR-120 as the catalyst. Their batch experiments in test tubes indicated that

- The resin catalyst was less effective than using a mineral acid as catalyst, e.g. for ethyl acetate

$$\frac{k(\text{resin})}{k(HCl)} = 0.326$$

- Diffusion rates were fast:
  - (a) reaction rate was insensitive to the degree of agitation,
  - (b) particle diameter of the resin did not seem to have an effect on the reaction rate

i.e., the chemical reaction rate was the limiting step.

- The reaction rate was proportional to the resin mass.
- The rate constant k decreases with increase in molecular weight of the ester. For ethyl acetate

$$k = 1.5 \times 10^{-5} \quad \text{litre} \cdot \text{gmmole}^{-1}\ \text{sec}^{-1} \text{ at } 25^{\circ}\text{ C}$$

In variance with these results, Davies and Thomas (16) observed that a cation exchange resin was more efficient than a homogeneous system for the hydrolysis of various esters including ethyl acetate. They attributed the discrepancy with Hammett (4) to the presence of acetone in the latter's reaction mixture. They reported the following rate constants for ethyl acetate, using IR-100 as the catalyst.

Temperature $^{\circ}$C	15	25	35	45	55
$k \times 10^{6}$ $gm^{-1} \cdot sec^{-1}$	3.5	9.4	22.7	49.2	97.8

and $E = 15{,}540$ $cal \cdot gmmole^{-1}$

$$\frac{k(\text{resin})}{k(HCl)} = 2.3 \text{ at } 25^{\circ}\text{ C}$$

They confirmed that the particle diameter had no effect on the reaction rates.

Bernhard and Hammett (5) studied the hydrolysis of methyl and ethyl acetates in aqueous solutions using ion exchange resins. They showed that reaction rates depend on the resin type. While

a highly crosslinked resin like Dowex - 50 x 8 was less effective than HCl as the catalyst, the lightly crosslinked resin, DVB - 4, was more effective. They reported the following rate constants for ethyl acetate.

	$k \times 10^5$ litre·gmmole^{-1} sec^{-1}			E cal·gmmole^{-1}
Temperature °C	10	20	30	
Catalyst				
HCl (0.466N)	2.32	6.60	17.20	17.20
DVB - 4	3.20	9.21	24.00	17.40
DOWEX - 50	2.09	5.99	16.00	17.50

Hammett et al (6,50) made a detailed investigation of the specificity of the reactions and showed that the catalytic specificity of a resin catalyst can be altered by fundamentally two different ways: varying the degree of crosslinking and changing the nature of the functional group.

Levesque and Craig (42) while studying the esterification of some alcohols claimed that the reaction rates were proportional to the resin surface and not the mass, thus indicating the presence of strong internal diffusion.

Saletan and White (52) studied a continuous process for the esterification of ethanol with acetic acid by passing the reactants through beds of a cation exchanger, Dowex - 50, of varying particle size at different flow rates and temperatures.

Their results showed that the reaction rate was nearly independent of the liquid flow rate even in the laminar region. Hence liquid film diffusion effects were insignificant. Their second-order rate expression gave the average volumetric rate of reaction in a spherical catalyst particle as the product of the reaction rate at the resin surface and the effectiveness factor, η, as given by equation (II.5):

$$\eta = \frac{3}{w^2R^2} (wR \cdot \coth(wR) - 1) \qquad \text{(II.5)}$$

They suggested that the above expression applied to close approximation to second-order reactions in spherical particles. In their experiments the particle diameter was varied from 0.009 to 0.05 cms and the temperature from 30 to 70 degrees C; the calculated effectiveness factors varied from 0.4 to 1.0. The results show that unlike other porous catalysts, the diffusivity, D, was an exponential function of temperature. The rate of increase of the specific reaction velocity constant with temperature was, however, greater than the rate of increase of diffusivity with temperature. Therefore at high temperatures the internal diffusion was the rate limiting step, particularly for the larger particle size of the catalyst.

In a similar study Barker and White (2) measured conversions for the alcoholysis reaction of ethanol and n-butyl-acetate. They

confirmed, in general, the observations of the previous investigators. However, three entirely different mechanisms correlated their data within the experimental error.

Smith and Amundson (54) considered the problem of intra-particle diffusion for catalytic, simple reversible reaction, first-order in each direction. In the theoretical study they derived equations to relate the conversion with the apparent variables of the system. Taking into account the effects of mass transfer and chemical reaction rate in the resin phase, they obtained expressions for conversion in CFSTR, fixed bed and batch reactors. The mathematical models were experimentally verified for the CFSTR and batch reactor. The reaction employed was the hydrolysis of ethyl formate catalysed by the Dowex - 50 resins. The reaction was carried out at 25 degrees C and 600 r.p.m. in a one-liter glass reactor. The intense agitation eliminated the possible effects of external film diffusion and non-ideality of mixing.

For the irreversible reaction of pseudo-first order, they verified the linear dependence of C_i/A_o, inlet ester concentration divided by the acid concentration in outlet, upon the flow rate, q (See equation (IV.18)). Four particle sizes from 0.005 to 0.08 cms were used. Their data indicate that the effectiveness factor, η, was nearly unity for the smaller particles and it decreased with an increase in the particle size. For the hydrolysis of ethyl formate they reported

$k = 0.962 \quad min^{-1}$

$D = 5.0 \times 10^{-5} \quad cm^2 \cdot min^{-1}$ at 25° C

Engel and Hougen (18) carried out hydrolysis of amyl acetate in a batch reactor using three different sizes of acidic ion exchange resins. They resolved the total resistance to the overall reaction into the liquid phase resistance and intra-particle resistance. Their data were correlated by an equation of the form

$$\text{Overall Resistance} = A' (N_{Re})^{a} (N_{Sc})^{b} + \frac{B'}{d_p^{c}} \exp\left(\frac{C'}{RT}\right)$$

where,

A', B', C', c, a and b are constants

d_p = Particle size

and

$$\text{Reaction rate} = \frac{\text{Ester concentration in the bulk phase}}{\text{Overall Resistance}}$$

They observed that only for the particle size of 0.026 mms was the liquid film diffusion significant and for larger particles the constant A' was negligible. They defined a contactor efficiency, $\emptyset$, as a measure of the effectiveness of agitation. As $\emptyset$ approaches unity, the external mass transfer resistance decreases and the internal diffusion and chemical reaction become the rate controlling step.

For a heterogeneous reaction in a CFSTR the effect of agitation upon reaction rate could be complicated by the occurrence of nonideal flow, i.e., deviation from the assumption of complete mixing. This aspect has not been studied previously.

The first systematic attempt to develop a theory of residence time distributions was made by Gilliland and Mason (22, 23) and by Dankwerts (13), who introduced some quantitative measures relating to various features of flow systems. Since then considerable work has been done on this aspect (11, 14, 15, 46, 60). Levenspiel (41) has summarized the theories of residence time distributions, the methods of interpretation of the actual experimental flow patterns and the approach of postulating flow models for prediction of the reactor performance. Cholette and Cloutier (10) considered various types of models for a CFSTR, derived related theoretical equations and experimentally verified one of the simpler models.

Not many experimental observations have been reported on the measurement of actual residence time distributions for CFSTR measured as the response to a known stimulus. However, the techniques of measuring the residence time distributions and the relative advantages of various methods are extensively treated by Levenspiel (41) and Naor and Shinnar (46). Cholette and Cloutier (10) explored the nonideal behaviour of a 30 inches dia. x 30 inches height stirred tank and found that their data was best

described by combination of a backmix and a dead water region with a portion of the feed short-circuiting the vessel. They measured the response of the stirred tank to a step demand of water in a 0.05 N NaCl solution. The NaCl concentrations were measured at regular time intervals by volumetric titration. For their experimental conditions nearly ideal flow prevailed at agitator speeds of more than 200 rpm. No other reference can be cited in support of the above work. In contrast, Wolf and Manning (59) measured the residence time distributions of a stirred tank over the range of 0-500 rpm and the data indicate that it changes very little with the stirrer speed. Also, Worrell and Engleston (61) noticed insignificant difference between the residence time distributions for no mixing and perfect mixing; they measured the response of a pulse injection of 10 % KCl solution in the flow of distilled water. Other investigators (7, 38) have shown that homogeneity can be achieved in as short a time as one second at 20-50 rpm in a laboratory sized stirred tank.

In the field of external film diffusion, Harriott (27, 28), Hyman (36) and Miller (44) have given critical reviews of the theoretical studies on solid-liquid mass transfer in agitated vessels. Miller (44) and Marangozis and Johnson (43) have collected available experimental data on the solid-liquid systems and compared various correlations proposed in the literature (2, 9, 21, 25, 28, 35, 37, 45, 62).

Most of the measurements have been made on the processes involving the dissolution of a solute which was in the form of freely suspended particles. Harriott (27) and Calderbank and Moo-Young (9) measured the mass transfer coefficients with ion exchangers. The effect of vessel geometry and the properties of the solid-liquid systems used have been studied and the experiments cover a wide range of variables. The data have been mostly correlated by the Gilliland - Sherwood equation

$$N_{sh} = C(N_{Re})^{a} (N_{Sc})^{b} \qquad (II.2)$$

In most of the correlations the exponent b has been assumed to be equal to 0.5 to concur with the penetration theory. However, Marangozis and Johnson (43) have shown that most of the data can also be fitted by $b = 1/3$, as predicted by the boundary layer theory. Both the theories seem to apply.

The exponent a varies from 0.4 to 0.9 among different investigators. Harriott (27) has proposed an alternate approach. He argues that the use of stirrer diameter as the characteristic length in the Reynold and Sherwood numbers is basically erroneous and consequently these correlations have no fundamental significance. He justifies the use of particle diameter instead. Mass transfer to and from suspended solids depends primarily on slip velocity, with the terminal velocity yielding the maximum value of the mass

transfer coefficient, which can be calculated by using Frossling's semi-theoretical equation

$$\frac{K^*1}{D} = 2 + 0.55(N_{Re})^{1/2}(N_{Sc})^{1/3}$$

The actual mass transfer coefficient for a given system can then be calculated from his graphs for K/K* versus power input.

Presently available correlations are uncertain because of the discrepancies in the values of the constants, the accompanying scatter of the data and the wide differences in the reported effects of the variables like particle size (3, 18, 28, 30-35, 58), stirrer speed (3, 24, 35), stirrer location (28, 37) and baffles etc (3, 19, 21, 30, 36, 37).

Following the classical work of Thiele (56) numerous articles have appeared on the subject of internal diffusion and chemical reaction in porous catalysts. From this vast literature has evolved a mathematical treatment which has now become a standard approach to the problem. Excellent books have also appeared on the subject (47, 53). As a result, no detailed review of the literature was undertaken. While on the theoretical side massive work is being done to explain the phenomenon of catalysis (1, 39) and in deriving rate expressions for complex reaction mechanisms and pore geometries (12, 20, 39, 47) the most common approach on the engineering side has been to use an average effective diffusivity and a simple rate expression.

CHAPTER IV

REACTION SYSTEM MODEL

When a solid-liquid catalytic reaction is carried out in a CFSTR the intensity of turbulence in the flow field affects simultaneously the processes of transport and mixing, the former being the transfer of matter under a concentration gradient and the latter the rate of progress of the system toward the equilibrium state of complete randomness at the molecular level. Implicit with the concept of an ideal CFSTR is the assumption that the contents of the reactor are so thoroughly mixed that they are at uniform concentration and temperature throughout. However, insufficient mixing may occur at low impeller speeds which causes deviations from the ideal behaviour of the reactor. The concentrations are then not uniform in the reaction mixture and the observed rate of the reaction differs from that obtainable in an ideal CFSTR.

Many models have been proposed to characterize nonideal flow patterns so that quantitative prediction of the performance of real equipment can be made. The usual procedure is to obtain the actual residence time distribution for the vessel and to use this information for applying correction to the ideal flow. The residence time distribution gives a measure of the time individual

molecules stay in the vessel. A residence time distribution function F(t) of a continuous flow system is defined as the volume fraction of the fluid at the outlet which has resided in the system for a time less than t. This function F(t) represents the probability that an element of volume which has entered the system at t=0, has left it within a period of time t; the probability that it will leave a moment later than t is 1 - F(t). Therefore, dF(t) is the volume fraction of the outgoing stream which has a residence time between t and t + dt.

Clearly,

$$t = 0; \quad F(t)=0$$

$$t = \; ; \quad F(t)=1$$

and average residence time $$\bar{t} = \int_0^\infty t\,dF(t)$$

Levenspial (41) discusses other residence time distribution functions. For idealized systems these functions can be derived mathematically. In principle, all the information is embodied in any one of the various functions and in systems where steady state conditions prevail the relations among them are uniquely determined by mathematical equations.

For an ideal backmixed vessel it can be shown that

$$\text{if } \Theta = t/\bar{t}$$

$$F(\Theta) = 1 - e^{-\Theta} \qquad \text{(IV.1)}$$

Experimental measurements of the residence time distribution are done by the stimulus-response technique, that is measuring the response of the vessel to a known input signal of a tracer. Most commonly a step function or a delta function is used. It can be shown that for a perfectly backmixed vessel, the response to an imposed step function, measured as the concentration time curve at the vessel outlet is $F(\Theta)$.

i.e.,

$$F(\Theta) = \frac{CN(\Theta)}{CN(0)} = 1 - e^{-\Theta} \qquad \text{(IV.2)}$$

where,

$CN(\Theta)$ = Tracer concentration at time Θ

This information can be used directly only for first order homogeneous reactions. For nonlinear reaction rates it is necessary to hypothesize what is considered to be a reasonable model for the behaviour of the fluid in the vessel and then in conjunction with the residence time distribution information calculate the conversions. The flow model approach consists in visualizing the vessel with imperfect mixing as made up of two or more flow regions such as

Plug flow regions

Backmix regions

Dead water regions

By-pass regions, etc.

For each combination there exists a theoretical response curve. It can be derived mathematically in terms of the parameters which express the magnitude of the constituent regions of the reactor model. The theoretical response curve is then matched as closely as possible to the experimental response curve. This yields the values of the various parameters.

The problem of nonideality in a heterogeneous system could be complicated. In a backmix reactor with no through passage of solids nonideal behaviour can exist due to nonuniform distribution of solids in the reactor, in addition to the nonideal flow of liquid. Emperically this can be taken into account by proposing a flow model. A simple model is proposed for the system under study. A fraction, m, of the feed is assumed to by-pass the solids, while in the rest of the reactor volume the solids are uniformly distributed; that is to say that the reactor is composed of a by-pass zone in which there are no solids and a perfectly backmixed zone which contains all the catalyst. There is no conversion in the by-pass stream, while in the other stream the conversion is that obtainable in an ideal backmix reactor. At the outlet, it is hypothesized, the two streams mix and the resulting composition can be calculated by material balance. A pictorial representation of the model is shown in FIGURE (IV-1).

With the simple model of by-pass plus backmix flow, it is possible to derive expressions which can be used to determine the

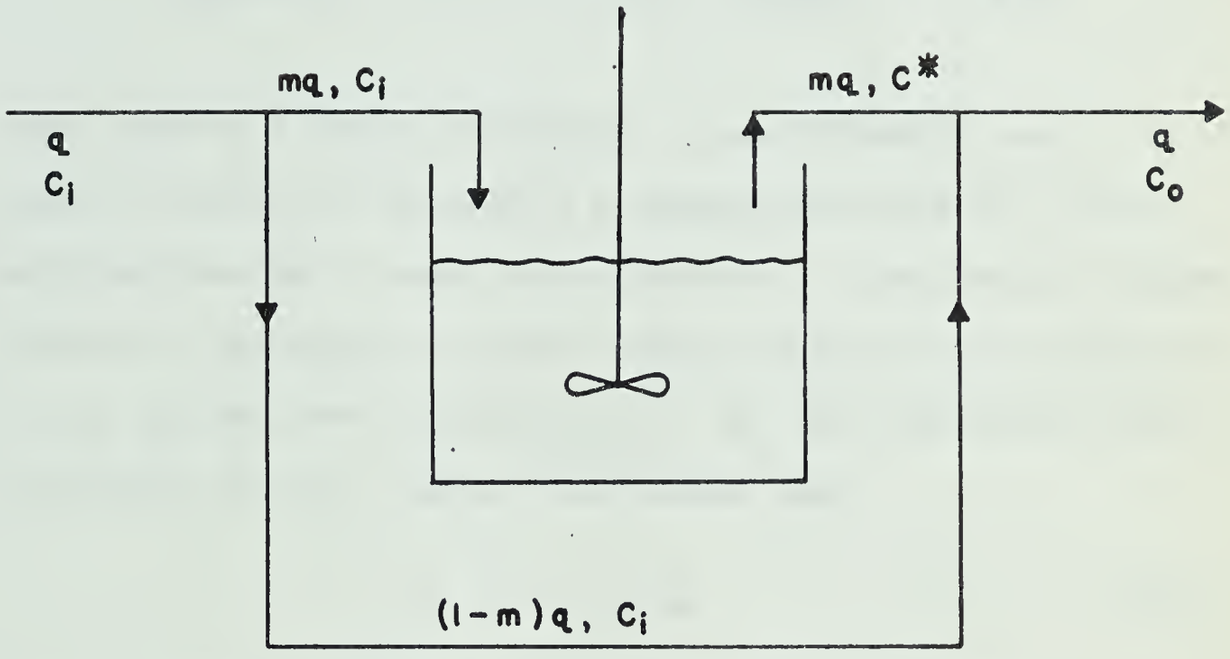

FIGURE IV-1 : REACTOR MODEL

parameters of the reaction system. In the following analysis the reaction

$$CH_3COOC_2H_5 + H_2O \xrightarrow{\text{Resin}} CH_3COOH + C_2H_5OH$$

takes place in a reactor containing W gms of catalyst and V liters of solution. The feed is introduced at a rate of q mls per minute and has an ester concentration of C_i gmmoles/ml. Effluent solution is withdrawn at the same rate but with an acid concentration of A_o and the ester concentration of C_o. The feed solution does not contain any acid, therefore, at steady state

$$C_i = C_o + A_o \qquad \text{(IV.3)}$$

According to the model proposed, only a fraction m of the feed enters the zone of perfect mixing, while the other fraction $(1 - m)$ is assumed to be short-circuited directly to the outlet. The concentration, at steady state, in the zone of perfect mixing is assumed to be C^* . The material issuing from this zone is mixed with that portion of the feed which short-circuits the system; the mixture of the two giving a liquid of composition C_o at the outlet.

A material balance at the outlet gives

$$C_o = (1 - m)C_i + mC^* \qquad \text{(IV.4)}$$

The reaction is considered to be elementary, irreversible and represented kinetically by

$$\text{Rate} = kC \qquad \text{(IV.5)}$$

C = Concentration of the ester $\quad gmmoles \cdot ml^{-1}$

k = Chemical rate constant, min^{-1}; it is characterized by the catalyst.

For a single sphere, a material balance at steady state over a spherical shell of thickness dr gives

$$\left(4\pi r^2 D \frac{dC}{dr}\right)_{r + dr} - \left(4\pi r^2 D \frac{dC}{dr}\right)_{r}$$

$$- \left(4\pi r^2 dr \cdot kC\right)_{\bar{r}} = 0$$

where,

D = Effective diffusivity of ethyl acetate in the resin phase, $cm^2 \cdot min^{-1}$

as dr $\longrightarrow$ 0, this equation reduces to

$$\frac{d^2C}{dr^2} + \frac{2}{r}\left(\frac{dC}{dr}\right) - \frac{kC}{D} = 0 \qquad \text{(IV.6)}$$

Substituting

$$u = rC$$

and $$\frac{k}{D} = w^2$$

in the above equation

$$\frac{d^2u}{dr^2} - w^2u = 0 \qquad \text{(IV.7)}$$

A General solution of the equation (IV.7) is

$$u = A\cosh(wr) + B\sinh(wr)$$

or

$$C = \frac{A}{r}\cosh(wr) + \frac{B}{r}\sinh(wr)$$

Boundary conditions for the equation are

(1) At the centre of the catalyst particle

$$\left(\frac{dC}{dr}\right)_{r=0} = 0 \qquad \text{(IV.9)}$$

(2) At the catalyst surface, the ester diffusing through the liquid film enters the particle.

$$\therefore \quad D\left(\frac{dC}{dr}\right)_{r=R} = K(C^* - C_s) \qquad \text{(IV.10)}$$

where

K = Mass transfer coefficient, cms·min^{-1}

C_s = Concentration of ester on the particle surface, gmmoles·ml^{-1}

R = Average radius of the catalyst particles as defined by equation (V.1), cms

The rate at which the ester enters a single sphere is

$$4\pi R^2 D\left(\frac{dC}{dr}\right)_{r=R}$$

and the rate at which it enters W gms of spheres is

$$\frac{3WD}{R\varsigma}\left(\frac{dC}{dr}\right)_{r=R} \qquad \text{(IV.11)}$$

where

$$\varsigma = \frac{W}{\text{Volume of } W \text{ gms of wet resins}} \quad \frac{\text{gms}}{\text{ml}}$$

Hence, this is the rate at which the main body of the solution is being depleted in ester by diffusion into the particles.

$$\therefore \quad mq(C_i - C^*) = \frac{3WD}{R\varsigma}\left(\frac{dC}{dr}\right)_{r=R} \qquad \text{(IV.12)}$$

Eliminating C^* from equations (IV.12) and (IV.10)

$$C_i - C_s = \left[\frac{3W\,D}{R\varsigma mq} + \frac{D}{K}\right]\left(\frac{dC}{dr}\right)_{r=R} \qquad \text{(IV.13)}$$

The differential equation (IV.6), in conjunction with the boundary conditions (IV.9) and (IV.13) yields the solution in the following form (See Appendix A).

$$\frac{C_i}{A_o} = q\left[\frac{1}{Q} + \frac{R\varsigma}{3KW}\right] + \frac{1}{m} \qquad \text{(IV.14)}$$

where,

$$Q = \frac{3WD}{R^2 \rho} (wR \cdot \coth(wR) - 1) \qquad \text{(IV.15)}$$

where,

$$w^2 = \frac{k}{D}$$

It is possible, in principle, to evaluate all the four parameters K, m, k and D from more than four experimental values of $\frac{C_i}{A_o}$ at varying R, W and q and constant N and T, by using equation (IV.14). Mathematically, however, it would be a staggering task due to the complexity of the equation. A simpler and more reliable method of evaluating the parameters consists of two steps: First determine k and D and then evaluate K and m at desired conditions. The method is elaborated below.

When the ratio of the inlet ester concentration to the exit acid concentration, $\frac{C_i}{A_o}$, in an experimental run is plotted versus the flow rate, q, equation (IV.14) gives a straight line with

$$\text{Slope} = \frac{1}{Q} + \frac{R\rho}{3KW} \qquad \text{(IV.16)}$$

and

$$\text{Intercept} = \frac{1}{m} \qquad \text{(IV.17)}$$

As can be seen from the equation (IV.15), for a given quantity of a catalyst, Q is a function of only temperature

and the particle diameter and is independent of the reactor geometry and the flow conditions. To evaluate the constants k & D, two conditions in the reactor operation need to be satisfied:

(a) The reactor behaves as an ideal CFSTR, and

(b) The mass transfer in the external film is very rapid.

If one or both of the above conditions are not met, the reaction rate would be considerably affected by changes in the intensity of turbulence in the fluid field. A simple method of ensuring that the above conditions are met is based on the expectation that at high agitation rates the increased turbulence must eventually become adequate to supply reactant at the rate at which it would be sufficient for consumption at the catalyst surface and also to give complete mixing of the reactor contents so that an ideal backmix flow is approximated. When the reaction rate is constant as agitation is varied, the concentration in the bulk phase is assumed to be uniform and it is reported that no nonideality in flow exists, i.e., $m = 1$; it is also assumed to be the same as at the catalyst surface and it is reported that no film mass transfer resistance exists, i.e., $K = \infty$.

When the above conditions are met, the equation (IV.14) simplifies to

$$\frac{C_i}{A_o} = 1 + \frac{q}{Q} \qquad \text{(IV.18)}$$

The plot of $\frac{C_i}{A_o}$ versus the flow rate, q, should give a straight line with

$$\text{Slope} = \frac{1}{Q}$$

$$\text{Intercept} = 1$$

From a given set of the experimental values of Q , the parameters k & D can then be calculated from the equation

$$Q = \frac{3WD}{R^2 \varsigma} (wR \cdot \coth(wR) - 1) \qquad \text{(IV.15)}$$

By varying the temperature in the above procedure the rate constants can be calculated as a function of temperature.

The experiments can now be performed under any desired conditions and, as stated above, the equation (IV.14) plotted to determine the slope and the intercept. Q calculated from equation (IV.15) is substituted in the expression

$$\text{Slope} = \frac{1}{Q} + \frac{R\varsigma}{3KW} \qquad \text{(IV.16)}$$

to calculate the mass transfer coefficient, K. The

$$\text{Intercept} = \frac{1}{m} \qquad \text{(IV.17)}$$

directly gives the parameter m. These quantities can be determined in relation to any important variable of the system, e.g., stirrer speed, particle diameter etc.

The values of K & m thus obtained can be compared with those evaluated in a different manner. The coefficient of mass transfer can be calculated, as stated previously, by a suitable equation of the form

$$N_{sh} = c(N_{Re})^{a}(N_{Sc})^{b} \qquad \text{(II.2)}$$

The parameter m can be evaluated directly by the stimulus-response technique. It has been shown (41) that, for the proposed model, the theoretical response curve to a step function in the inlet concentration is

$$F(\theta) = \frac{CN(\theta)}{CN(0)} = 1 - me^{-m\theta} \qquad \text{(IV.19)}$$

The function $F(\theta)$ is obtained experimentally.

Once the adequacy of the proposed model is established for an actual reactor, equation (IV.14) can be used for various purposes, e.g.

(1) To predict the actual conversion in the reactor by using known K, m, k and D for given R, W and q.

(2) To determine the rate parameters k and D from experimental observations at any stirrer speed if values of K and m under the experimental conditions are available by independent means.

CHAPTER V

EXPERIMENTAL

The experimental program was planned to

(1) establish the extent of nonideality in the reactor operation at various stirrer speeds,

(2) investigate the significance of liquid-film mass transfer resistance on the overall rate process,

(3) evaluate the rate constants k and D and if the above effects are significant to test the validity of the equation (IV.14):

$$\frac{C_i}{A_o} = q\left[\frac{1}{Q} + \frac{R\beta}{3KW}\right] + \frac{1}{m} \qquad \text{(IV.14)}$$

V-A EXPERIMENTAL EQUIPMENT

The experimental set up was designed so that known quantities of ethyl acetate and water could be introduced into a CFSTR in which a solid catalyst was dispersed and the product stream could be withdrawn from the reactor at the same rate, retaining the catalyst inside the reactor by employing a filter.

The equipment consisted principally of feed reservoirs, feed-pumps, rotameters, associated tubings, a glass reactor placed in a constant-temperature water bath and a proportioning pump. A schematic

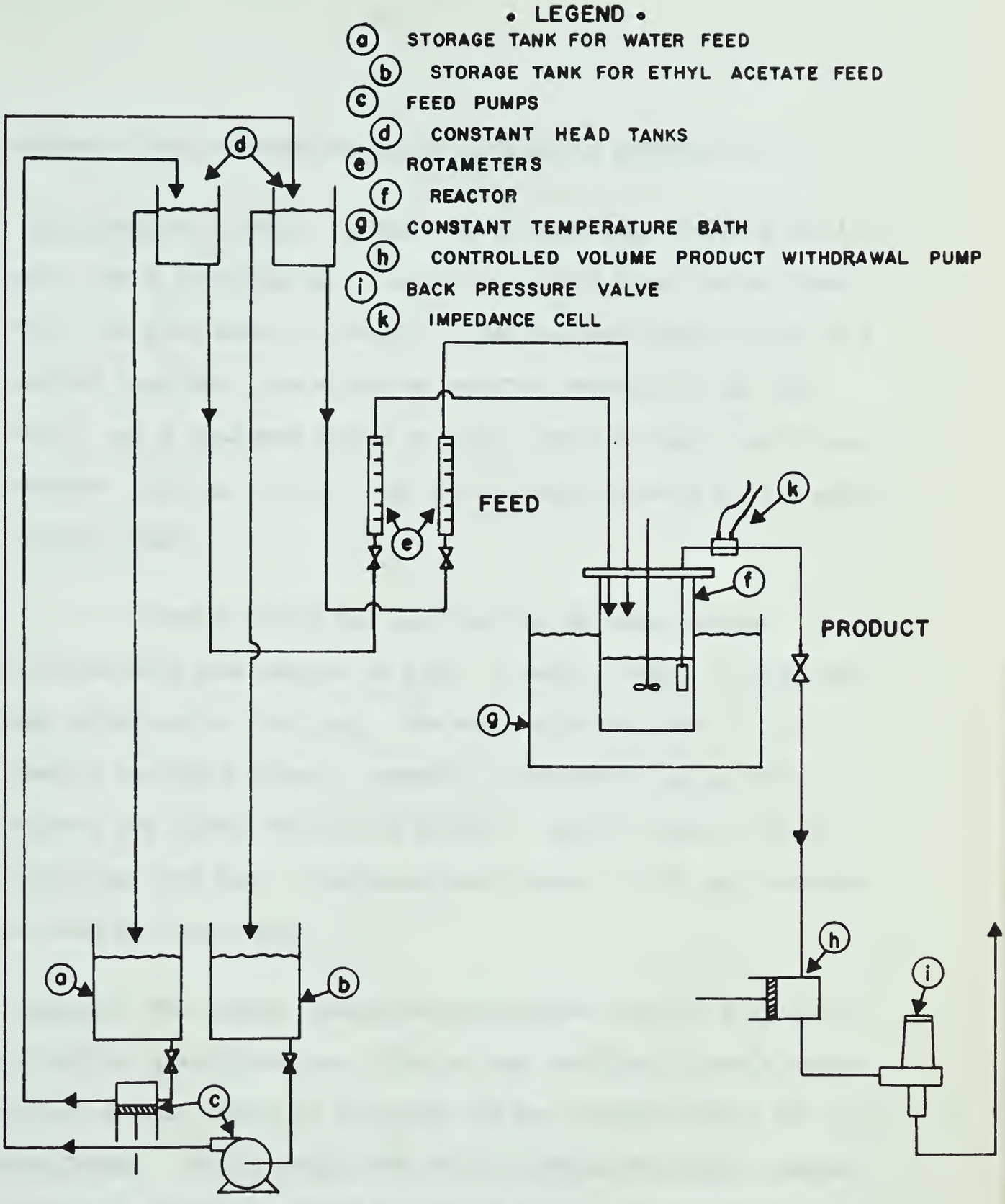

FIGURE V-1 : SCHEMATIC DIAGRAM OF THE EXPERIMENTAL SET-UP

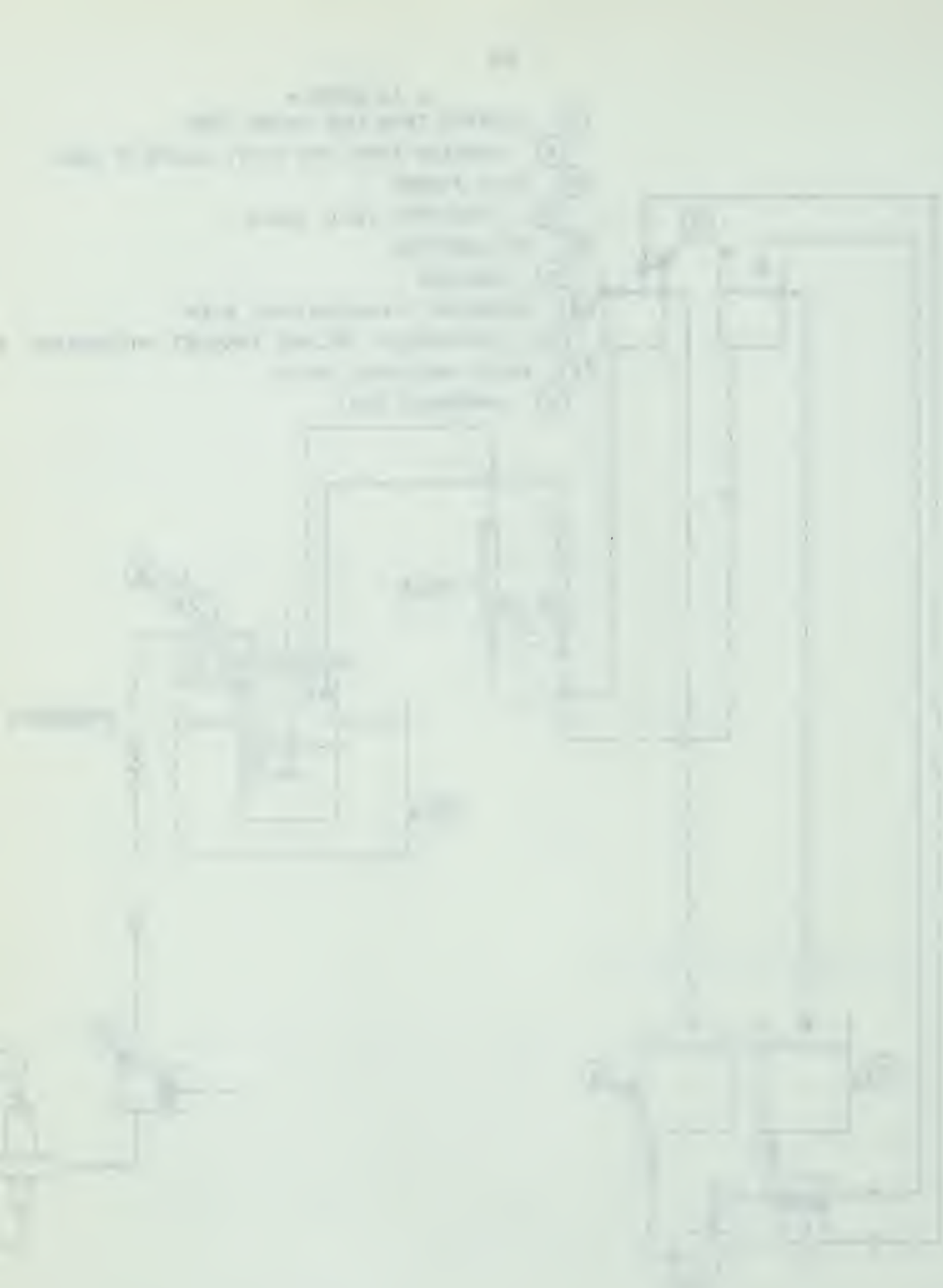

diagram of the experimental set up is shown in FIGURE (V-1)

Introduction of feed: A small centrifugal pump supplied distilled water from a 12-gallon glass bottle to a small glass bottle placed about four feet above the reactor. The overhead bottle served as a constant head tank from which the overflow returned to the feed bottle, and a regulated stream of water flowed through a calibrated rotameter into the reactor. The tubing employed was $\frac{1}{4}$ inch diameter, stainless steel.

A similar set up was provided for the ester stream. However, the reservoirs were smaller in size. A small positive displacement pump served as the feed pump. The ester dissolves most of the commonly available rubbers; therefore, connections using rubber stoppers and plastic tubes were avoided. Special glass-to-steel connections were used. Stainless steel tubing of 1/8 inch diameter was used for this stream.

Reactor: The reactor vessel was constructed from a 6 x 12 inch cylindrical pyrex glass jar. The jar was modified to give a vessel with an overall length of $9\frac{1}{2}$ inches and was provided with a 3/4 inch wide flange. The jar could then be held between two metal flanges. Rubber gaskets were employed to provide a seal. The metal cover of the reactor served as the complimentary part to a stainless steel ring, $6\frac{1}{4}$ inches i.d. and $1\frac{3}{8}$ inches wide, which served as the lower flange. The top cover was made of a $\frac{1}{4}$ inch thick stainless steel

plate, 9 inches in diameter and it accomodated suitable connections for inlet and outlet stream lines and a centrally placed stirrer shaft. Four symmetrically located stainless steel baffles $9\frac{1}{4}$ inches long and $\frac{1}{2}$ inch wide were attached to the top cover such that when it covered the glass reactor the clearance between the glass wall and the baffles was about 1/16 inch. In addition, the top cover supported the stirrer assembly at a fixed position so that the stirrer shaft was centrally positioned and accurately aligned with the bushing and that the occasional removal of the top cover did not disturb the alignment.

The geometrical features of the reactor were chosen as being typical of previous practice (36). The dimensional and other details are given in FIGURE (V-2) and Appendix B. Some important dimensions were:

I.d. of the reactor	=	$5\frac{1}{2}$ inches
Liquid depth	=	$5\frac{1}{2}$ inches-equal to the reactor i.d.
Volume of reaction mixture	=	2 litres.
Impeller diameter	=	1 3/4 inches - equal to 1/3 to $\frac{1}{4}$ of the reactor i.d.
Impeller position	=	1 3/4 inches from the reactor bottom - at about 1/3 the liquid depth
Baffle width	=	$\frac{1}{2}$ inch - equal to 1/10 to 1/12 the reactor i.d.

LEGEND

- (a) BAFFLES, NO 4
- (b) ESTER FEED LINE, 1/8"
- (c) THERMOWELL
- (d) WATER FEED LINE, 1/4"
- (e) EFFLUENT LINE, 1/4"
- (f) FLANGE RING
- (g) FILTER
- (h) BOLTS, 3/8, NO 6
- (k) GLASS REACTOR

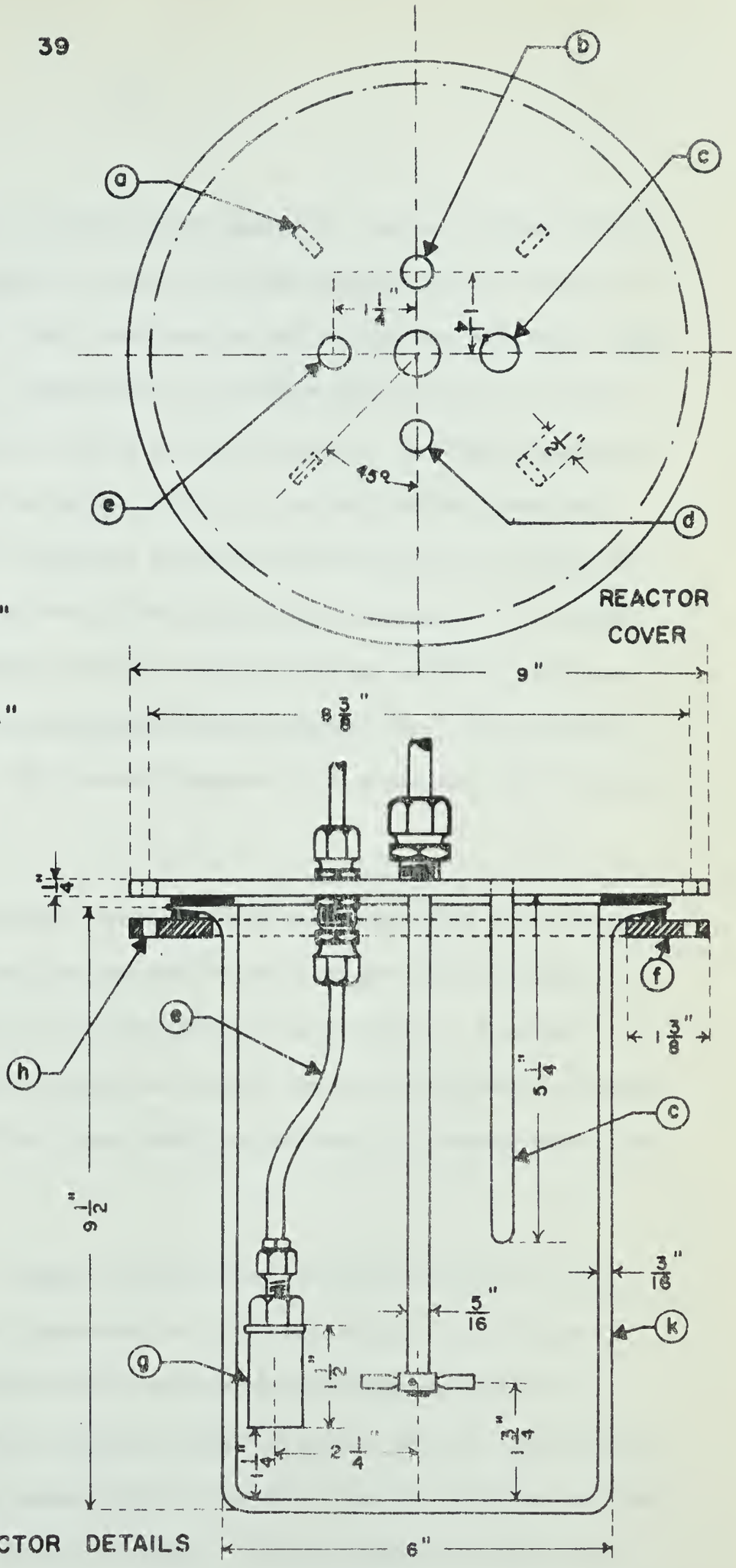

FIGURE V - 2 : REACTOR DETAILS

Two types of stirrers were employed. An air driven stirrer was used for high impeller speeds. It was supported on a frame of aluminum T-section. The frame was bolted to the reactor top. This stirrer was, however, unsuitable for experiments at low r.p.m. for it provided very little torque at these speeds. For this purpose a stirrer driven by an enclosed 1/50 h.p. electric motor, provided with a shaft of 36:1 reduction and which could deliver a torque of 9 inch-pound at speeds from 20 to 175 r.p.m., was used. The motor was supported by a cast aluminum control housing which in turn was clamped to a support rod mounted on the reactor top. The agitator was a three blade, 1 3/4 inches diameter, 316 stainless steel turbine impeller.

A thermometer well made of 5/16 inch stainless steel tube sealed at the lower end was welded to the reacter top to project about 2 inches below the liquid level in the reactor. A mercury thermometer was placed inside the tube to measure the reaction temperature. The feed tubes terminated approximately 2 inches above the liquid level.

Product removal: A small sintered brass filter with pores of 12-50 micron size was connected to a $\frac{1}{4}$ inch stainless steel tube and placed in the bulk of the reaction mixture approximately 2 inches above the bottom and $\frac{1}{2}$ inch away from the wall of the reactor. At this location the strong liquid currents from the impeller reduced the possibilities of filter-choking. A $\frac{1}{4}$ inch tube-to $\frac{1}{4}$-inch tube

stainless steel bulk-head connector positioned on the reactor top provided a leak-proof continuation of the exit stream from the inside of the reactor to a Milton-Roy controlled volume pump with a delivery rate variable from 0-400 mls/min. The pump was placed 3 feet below the reactor assembly. As a result, the liquid from the reactor was siphoned under gravity to the pump inlet. The quantity of the liquid pumped was controlled by manipulating the stroke length of the plungers. A back pressure valve adjusted for 60 psig was installed in the line near the pump outlet to insure consistent performance of the pump. These arrangements permitted withdrawal of a known quantity of liquid, while retaining the catalyst inside.

Temperature control: A 16 x 12 inch pyrex glass jar filled with water served as the constant temperature bath. A 1500 watt heater, an electric stirrer and a bimetallic sensing element in conjunction with an electronic controller were used to maintain a constant water temperature in the bath. A mercury thermometer placed near the thermoregulator indicated the bath temperature. The set up was tested at 125° F for 24 hours. The temperature remained constant within ± 0.1 and the set up was considered satisfactory over an 80-120° F range.

The water feed stream was preheated by passing a two foot length of the inlet line through the water bath. This arrangement ensured that the water feed was at about the same temperature as the contents of the reactor. Similar arrangement was not found

necessary for the ester feed because of its small size. During test runs excellent temperature control was attained and the reactor contents were at essentially the same temperature as the water bath.

Reactor support: A triangular frame of angle-iron mounted on the top of the temperature bath jar held it in a fixed position and from it the reactor was suspended in the jar. In this position, about 8 inches of the reactor was immersed in the water bath.

The temperature bath and the accompanying assembly was placed about 3 feet above the ground level on a bench to permit convenient observation of the reactor operation.

V-B REACTANTS AND THE CATALYST

V-B-1 Ion Exchange Resins:

Ion exchange resins are high molecular weight polyacids or polybases which are virtually insoluble in most aqueous and nonaqueous media. In addition to ion exchange phenomenon, their utility encompasses catalytic applications. Since a cation exchange resin owes its capacity for exchanging ions to an acidic functional group, it may be expected to promote reactions which can be catalysed by conventional acids.

Of the numerous types of ion exchange resins synthesized, the most important types are those prepared by suspension copolymerization of styrene plus variable amounts of divinylbenzene

which is used as a crosslinking agent. The percentage of divinylbenzene in the backbone of the resin catalyst is commonly referred to as the degree of crosslinkage. These resins are mechanically strong and chemically inert. The styrene-divinylbenzene network gives a maximum resistance to oxidation, reduction, mechanical wear and breakage and is insoluble in common solvents. In addition, it can be easily formed in the shape of spheres or beads of good hydraulic properties. These resins appear to offer several advantages:

- Simplicity with which they can be removed from the reaction medium by filteration.
- Elimination of the neutralization of the reaction mixture.
- Acid catalysis corrosion problems are reduced.
- Cost reduction: the catalyst can be used repeatedly without regeneration and in many instances with no loss of the catalyst activity.

They are however unsuitable for application at temperatures higher than 120° C.

The strongly acidic sulfonic acid resins, prepared by treating the styrene-divinylbenzene copolymer with hot concentrated sulfuric acid are generally employed as acid catalysts. Their structure is

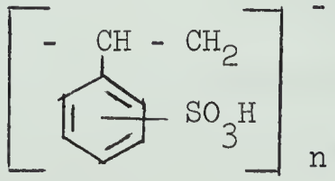

The important resins among those commercially available resins are Dowex - 50 and Dowex - 50W, manufactured by the Dow Chemical Co., and Amberlyst - 15 and IR - 120, manufactured by the Rohm and Haas Co. Their properties and methods of evaluation are available in the corresponding company brochures and elsewhere. (17, 20, 51)

When immersed in water, dry resin particles swell to an extent determined by the degree of crosslinking. As it swells into a jelly-like mass, its structure becomes more porous and diffusion within the resins becomes faster.

Dowex 50 W - x8 was chosen as the catalyst because it is readily available in the hydrogen form and can be obtained graded as to size. The resins were obtained from the Dow Chemical Co. in three size ranges. Some of the resin properties are:

Degree of Crosslinking	:	8 %
Active group	:	Nuclear sulfonic $H^+SO_3^-$
Ionic form	:	H^+
Physical form	:	Spheres
Size range	:	20-50, 50-100, 100-200 mesh
Sphericity	:	90 %
Effective pH range	:	1-14
Total exchange capacity	:	5 meq/gm dry resin
	=	no. of ionic sites per gm of dry resin.

Measurement of particle diameter: Considerable variation in the size of the particles in the samples received was observed. However further attempts to obtain a sharper size separation met little success because very small resin particles had a tendency to adhere to relatively bigger particles. The average diameter for each sample was therefore measured as the mean of about one hundred particles.

by using the equation $$d_{avg} = \frac{\sum d^3}{\sum d^2} \qquad (V.1)$$

This equation gives the mean specific area diameter, which is the diameter of a sphere having a specific surface area equal to the average specific area of the particles. The diameter of the wet resin particles were measured by using a microscope.

About two grams of wet resin was put on a filter paper to remove the bulk of water from the particles. The quantity of resin was then symmetrically divided on the filter paper into eight equal parts. One of the parts was taken as a representative sample. The particles were spread on a glass slide and focused under a microscope. The micrometer consisted of a movable table with micrometer motion controls and an eye-piece with a slide wire and a scale. To avoid any biased selection, only those particles which crossed or touched the horizontal reference line were taken for measurement. The particles were essentially spherical. The

diameter measured was the horizontal distance travelled by the slide wire between two diametrically opposite vertical tangents to the projected circle. For each sample, about one hundred particle diameters were measured. The results are given below

mesh size	Average diameter, cms.
20.50	0.06090
50.100	0.02536
100.200	0.00566

The details of the measurements are given in TABLE (B-1) of Appendix B.

Measurement of resin density: About ten gms of an oven-dry sample of resin was accurately weighed and put in a long graduated cylinder. Water was then slowly added for the rehydration of the resin. After twenty-four hours, the excess water was drained off the resins were transferred to a filter paper and then quickly into a graduated cylinder in which a known volume of water was present. The resins were allowed to settle and the change in the level of water gave the desired resin volume. The density was then calculated by dividing the mass of the oven-dry resin by the volume of the wet resin. The density was measured for all three size ranges. The results are as follows:

Mesh size	Density $gms \cdot ml^{-1}$
20.50	0.7988
50.100	0.7975
100.200	0.7937
mean	0.7960

V-B-2 Reactants:

The ethyl acetate used was 99.997 % pure with

B.P. = 76.9 - 77° C

Specific gravity = 0.894

Molecular Weight = 88.107

It was obtained from the Fischer Scientific Co.

Distilled water of an average pH of 6.8 was used in the reaction. This was mainly to prevent the degradation of the resin.

V-C EXPERIMENTAL PROCEDURE

V-C-1 Measurement of Ester Conversions:

Calibration of flowmeters: The calibration of the rotameters for Ethyl acetate and water and the controlled volume pump for the effluent stream are presented in FIGURES (B-1) to (B-4) of Appendix B.

An experimental run: A typical experimental run to measure the ester conversion proceeded as follows.

- The storage tanks for distilled water and ethyl acetate were filled, whenever necessary, to ensure an ample supply of the reactants for 3 to 4 runs. At the start of a run, the feed pumps were put on to fill the overhead feed tanks.
- A known quantity of the desired size of the oven-dry resin was introduced in the reactor followed by two liters of distilled water. The reactor was covered and the liquid level inside was noted. The reactor was then placed in the water bath, which was maintained at the desired temperature.

Inlet and outlet connections were made and the reactor stirrer was started and adjusted to the desired speed. Within a short time the reactor temperature reached the bath temperature. Also in the meantime the feed pumps filled the overhead feed tanks to the constant level of the overflow lines.

- The effluent stream pump was primed and its stroke length was adjusted for the desired flow. To make up for the depletion of the liquid level in the reactor caused by the priming of the effluent stream pump, fresh distilled water was introduced into it from the feed tank.
- The needle valves in the feed lines were then opened to permit the flow of the reactants. Simultaneously, the effluent stream pump was started. The rotameters were quickly adjusted to the desired flow rates of the reactants.
- The reaction had now started and was allowed to reach a steady state. During the transition period, steady conditions of flow and temperature were maintained and the stirrer speed was frequently checked. A constant liquid level in the reactor indicated that inflow was equal to outflow. After about three reactor volumes had passed through, samples of the effluent stream were collected and analysed for the ester conversion. The analysis was continued till three consecutive samples taken at intervals of one half the residence time in the reactor agreed within $\pm$ 1%.

Analytical methods: The analysis of the effluent stream consisted in measuring the acetic acid produced in the reaction. One mole of acetic acid was formed for each mole of the ester reacted. No attempt was made to analyse for the ethanol and the unreacted ethyl acetate. Twenty-five mls of the effluent stream were titrated against sodium hydroxide of known strength (xN) using phenolphthalein as an indicator. The volume of xN NaOH used was converted to an equivalent amount of 1/40 N NaOH for consistency in reporting the data. The NaOH solutions used were frequently standardised by titrating them against a standard solution of oxalic acid.

Careful checks were made to ascertain the extent of auto-catalysis, if any, of the reaction. The acetic acid produced in the reaction in turn may catalyse the reaction. Data were not available in the literature for the rate of hydrolysis of ethyl acetate catalysed by acetic acid. However, the rate was experimentally found to be negligible for the residence times and reaction conditions employed in the study. This was also observed previously, by Harned and Pfanstiel (26).

It was observed experimentally that distilled water (pH=6.8) kept in contact with the resin approached a constant acidity of pH=4.1. The final pH was found to be independent of the resin size, temperature and the resin: water ratios employed in the experiments. The water in contact with the resin quickly approached the pH of 4.1 and remained constant thereafter. This observation was further confirmed in a continuous system. Distilled water was passed through a resin bed at a

constant flow rate (residence time in the bed - 5 minutes) for about 1.5 hours. Throughout this period the pH of the outgoing water remained steady at 4.1. Smith and Amundson (54) noted the same phenomenon and applied necessary corrections in their analysis.

This increase in the acidity of the water in contact with the resin can be attributed to the presence of minute quantities of metallic ions (as salts) in the distilled water. It is believed that these cations replace the H^+ ions in the resin phase and the H^+ ions in turn pass into the aqueous phase causing a decrease in the pH. This also explains why the pH of the resin-treated distilled water was independent of all the variables mentioned in the previous paragraph.

The above process of ion exchange is accompanied by a decrease in the activity of the resin. However, calculations showed that during an average service of a batch of resin, its catalytic activity would decrease by about 1.1%. This deactivation was not considered to be significant and the resin activity was assumed to be constant over the duration of its use. The day-to-day variations in the quality of distilled water were minor.

The acid water of pH-4.1 was used to make a 5% solution of ethyl acetate. No conversion of the ester was noticed even after four hours of stirring at 100° F.

In the analyses of the experimental data it was therefore assumed that the acetic acid produced in the reaction was due solely to the catalytic effect of the ion exchange resins. To account for the acidity of the water in contact with the cationic resins, 0.52 mls of 1/40 N NaOH were subtracted from the readings for the resin catalysed reaction. This quantity was sufficient to neutralize 25 mls of the acid water of pH = 4.1.

V-C-2 Residence Time Distribution in the Reactor:

With a view to evaluate the parameter m, the residence time distributions of liquid in the reactor were measured for different stirrer speeds by introducing a step change in the feed concentration. Initially the steady-state tracer concentration in the reactor was CN(0) and then at $\Theta=0$, the concentration in the inflow was reduced to zero. The response was measured to this negative step function as the system approached a new steady state. If $CN(\Theta)$ is the tracer concentration in the outflow as a function of time the response of the proposed model is (41):

$$\frac{CN(\Theta)}{CN(0)} = I(\Theta) = 1 - F(\Theta)$$

$$= me^{-m\Theta} \qquad (V.2)$$

where, $\Theta = \frac{t}{\bar{t}}$

The tracer chosen was hydrocholoric acid; the use of a salt was undesirable because it would have replaced the hydrogen

ions from the resin. The residence time distributions were measured with a known quantity of resin in the system. It was thought that the presence of solid particles may have some influence on the flow pattern.

Measurement of the tracer concentration: The effluent concentration of HCl was measured as the impedence of the solution between two electrodes placed in a impedance cell. The cell consisted of two 26-guage platinum wires, 1/8 inch long, placed 1/2 inch apart in the same plane and encased in a cylindrical lucite tube of 1/4 inch i.d. The electrodes were plated with platinum black. The construction of the cell permitted a free flow of the liquid through the cell.

The cell was calibrated with HCl solutions of known strengths. Each standard HCl solution was maintained at 80° F by using the water bath because the impedance of the solution was highly sensitive to the temperature. The solution was withdrawn at a steady flow by the effluent pump; the flow rate had no detectable effect on the impedance over a moderate range. An impedance bridge which supplied an a.c. at 1000 c/s was used for the measurement. This high frequency prevented the generation of gases on the electrodes. The calibration curves of the impedance versus strength of HCl solutions is shown in TABLE (C-1) and FIGURE (C-1) of Appendix C.

The response was studied by recording the variation of impedance at a location near the discharge from the reactor after the negative step function was introduced in the feed stream. Prior to each run the resin particles were kept in the HCl solution of the initial concentration CN(O) to insure that the liquid in the particles was the same as the feed liquid. The reactor was filled to a volume of slightly more than two litres. The effluent stream pump was then started to withdraw the liquid from the reactor at a predetermined rate. This solution as it passed through the cell gave the initial concentration CN(O). When the liquid level dropped exactly to the reference level for two liters, the valve for distilled water feed to the reactor was quickly opened and the flow adjusted to the desired value. Considering the relatively high residence time in the reactor - 15 to 45 minutes - the small delay in this procedure was assumed to have a negligible effect on the response.

The transport lag in the system was taken into account. A fluid element leaving the reactor had to pass through nine mls of transport section, consisting of the filter and $\frac{1}{4}$ inch stainless steel tubing, before it entered the impedance cell. It was assumed that there was no backmixing in this section. Therefore, 9/q minutes after the step change was imposed (where q is the flow rate of the effluent stream in mls/min), the time was noted as θ=0 and the observations started. The impedance of the solution was then

noted at fixed time intervals. This was continued for about three residence times for each run.

V-D EXPERIMENTAL RESULTS

V-D-1 Residence Time Distribution

The residence time distributions were measured for three different conditions. The experimental observations are presented in TABLES (C-2) to (C-4) of Appendix C.

The experimentally observed quantities were Θ and the impedance IMP(Θ). The corresponding tracer concentration CN(Θ) were read from the calibrations curve, FIGURE (C-1). The quantity $\frac{CN(\Theta)}{CN(0)} = I(\Theta)$, when plotted versus Θ on semilog graph paper should give, according to equation (V.2), a straight line of slope=m and intercept=m. These plots are shown in FIGURES (V-3) to (V-5). The results and experimental conditions are shown in TABLE (V-1).

The results show that for all the conditions studied, the parameter m=1, indicating that nearly perfect backmixing occurs in the reactor under those conditions.

V-D-2 Significance of Liquid Film Mass Transfer

Two sets of runs were carried out to evaluate the importance of liquid film mass transfer on the overall conversion. Turbulence in the flow field was controlled by varying the stirrer speed. In

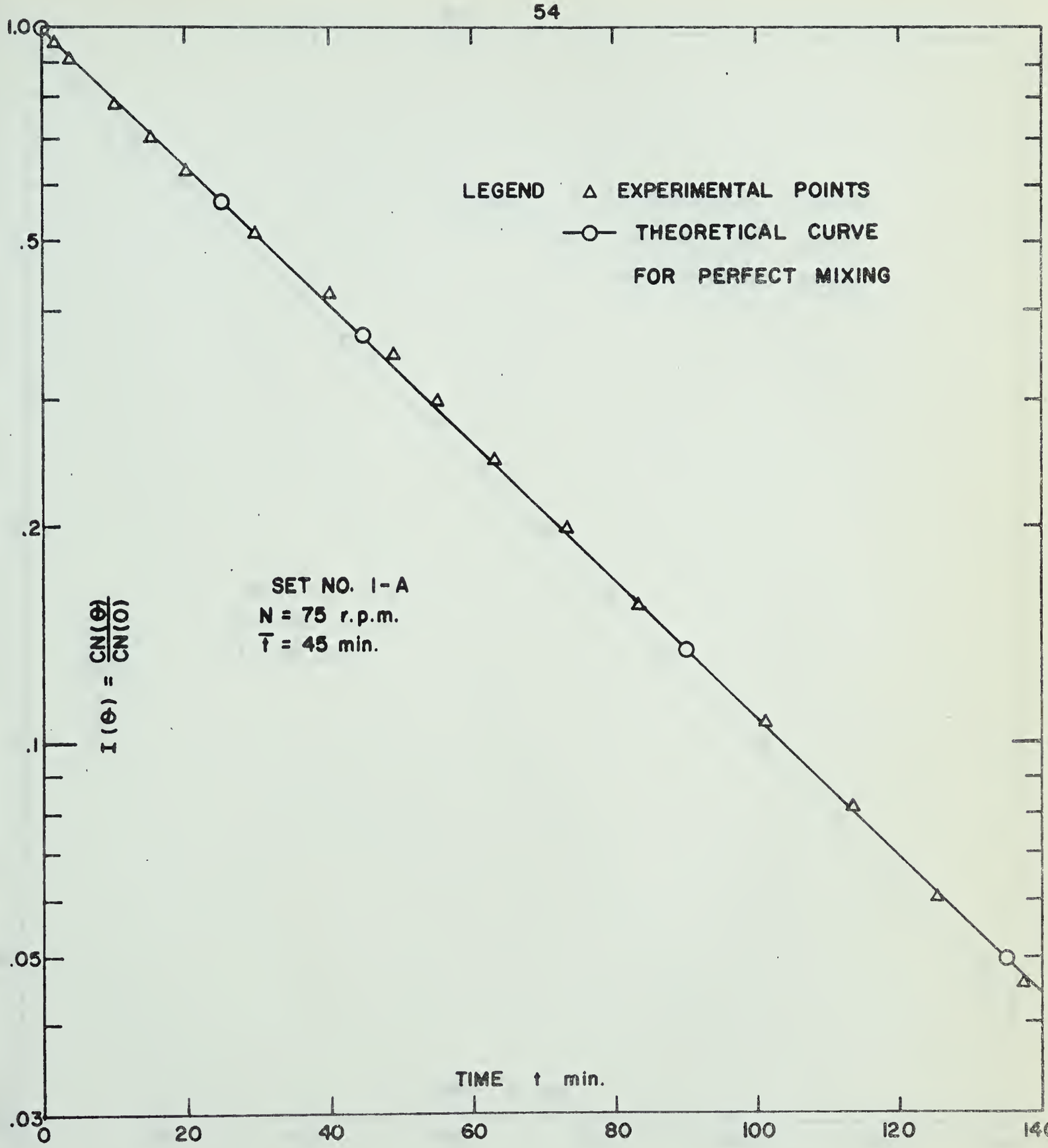

FIGURE V - 3 : REACTOR RESPONSE TO A STEP CHANGE IN THE FEED CONCENTRATION

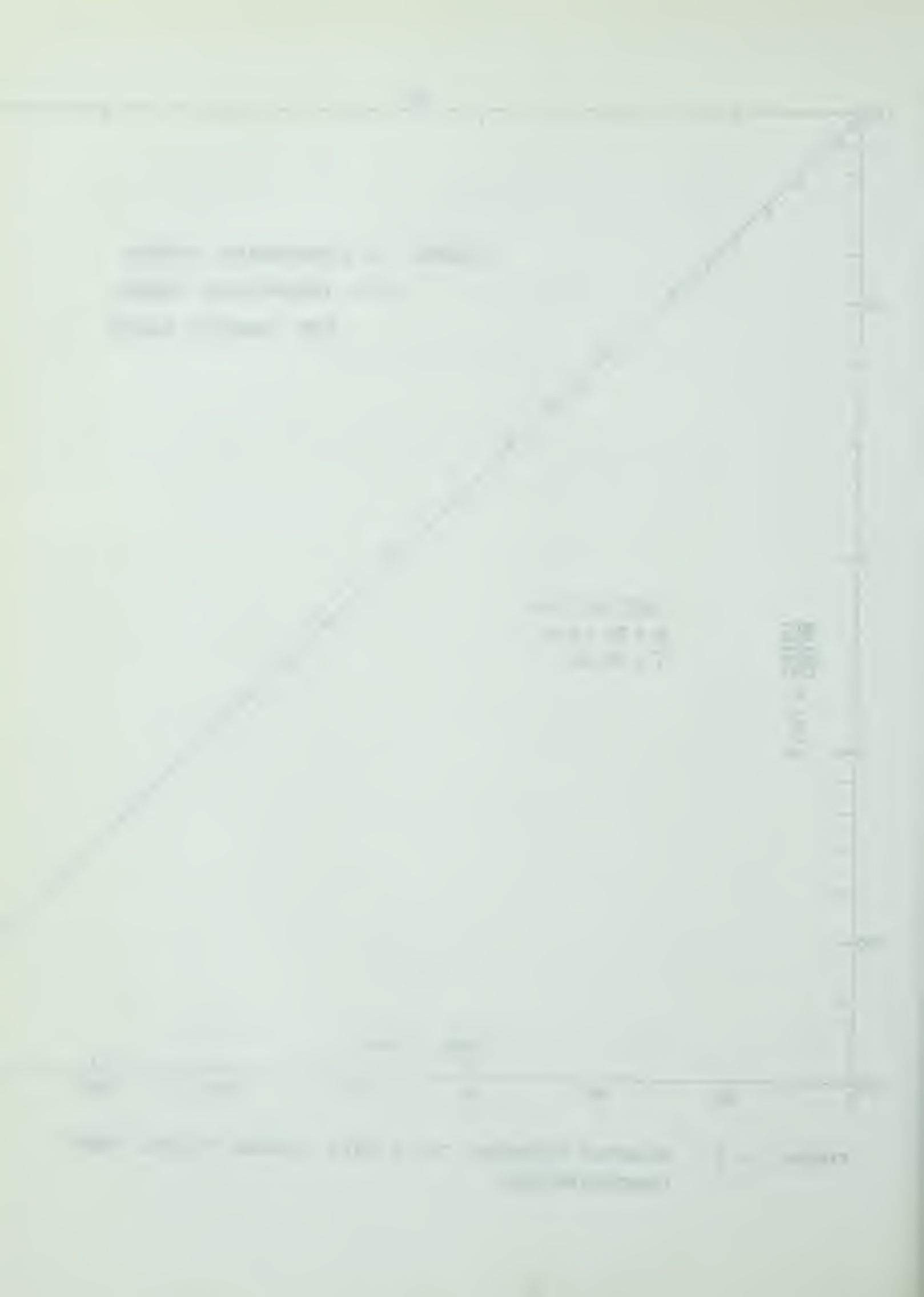

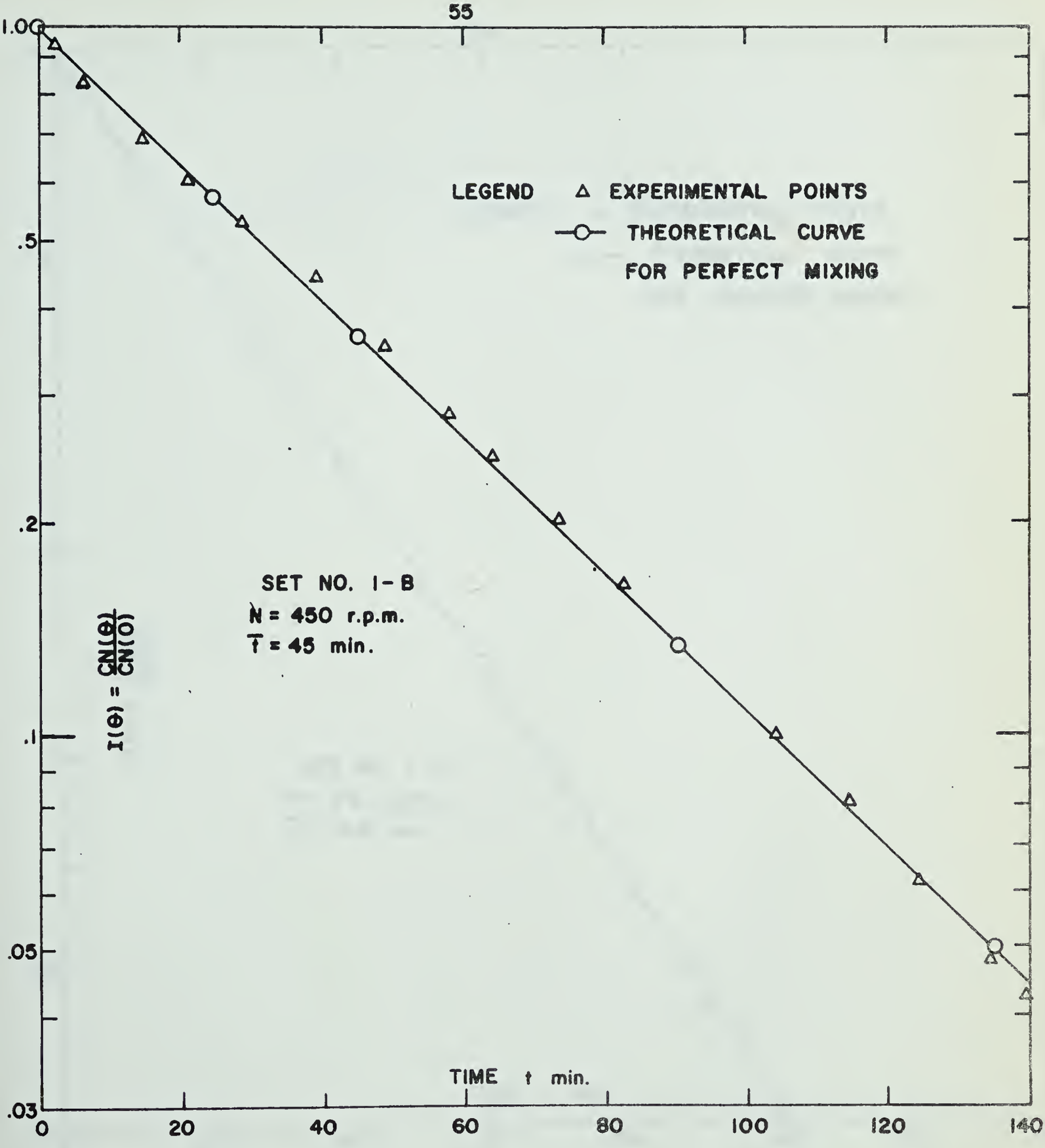

FIGURE V-4 : REACTOR RESPONSE TO A STEP CHANGE IN THE FEED CONCENTRATION

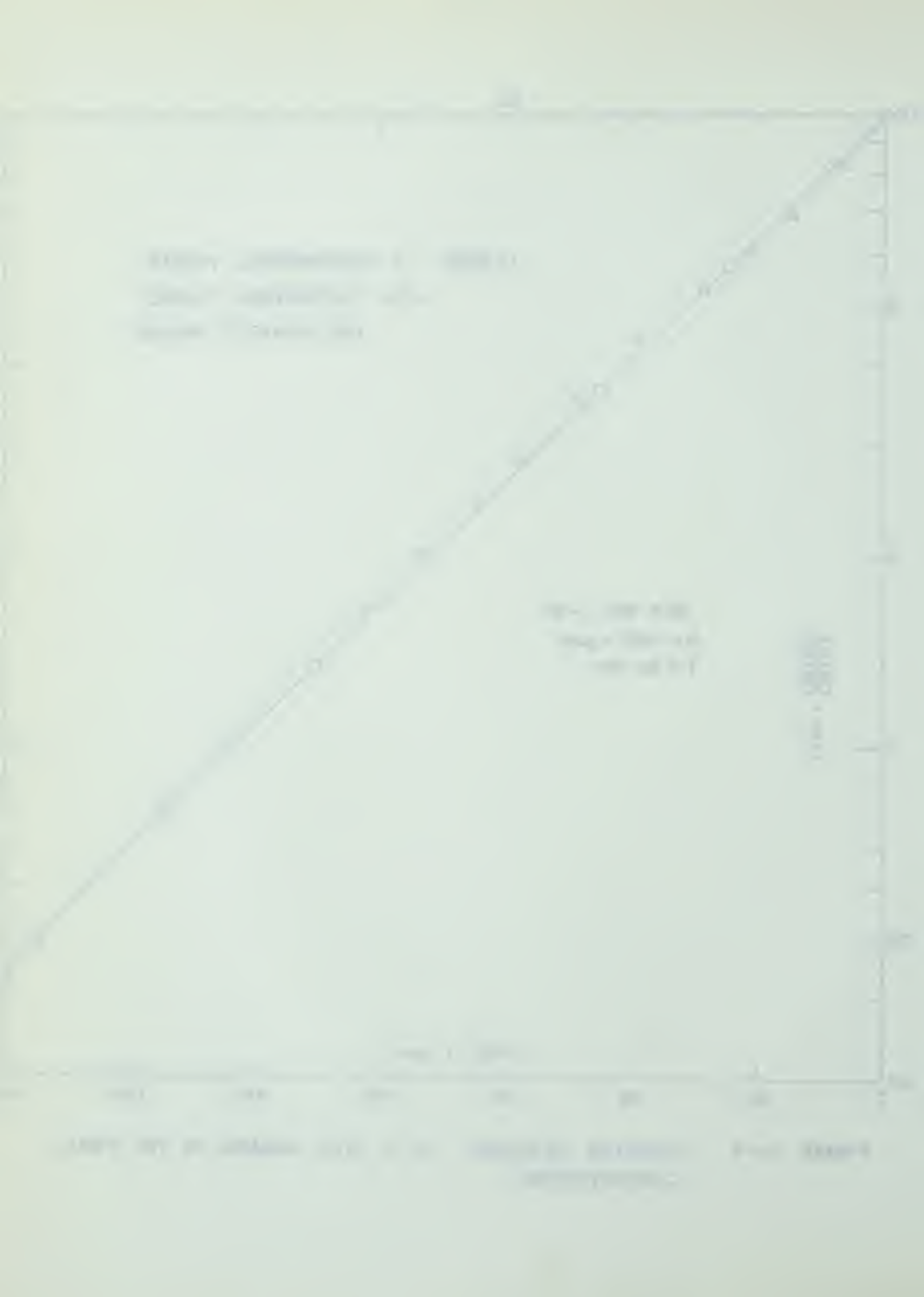

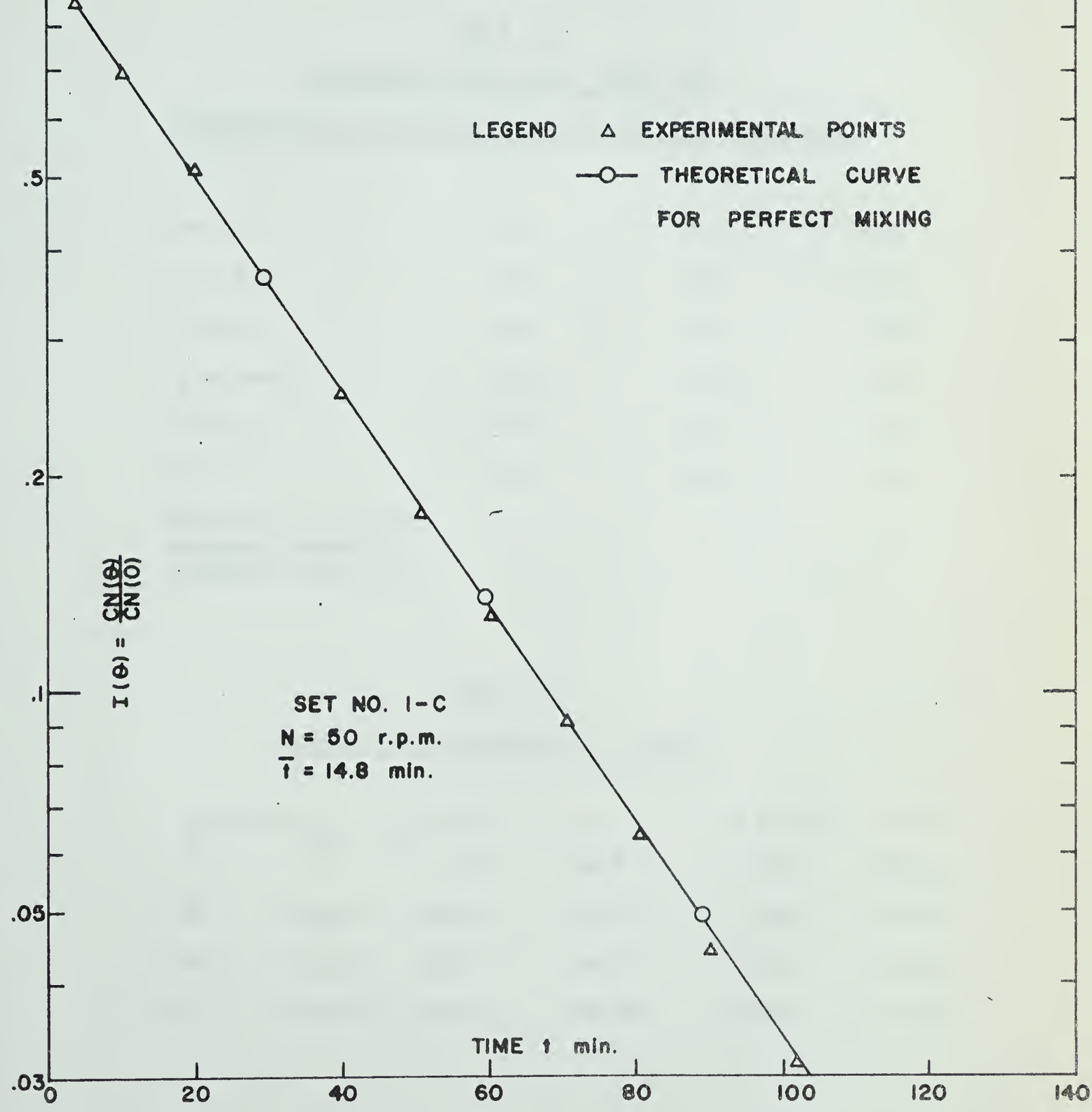

FIGURE V - 5 : REACTOR RESPONSE TO A STEP CHANGE IN THE FEED CONCENTRATION

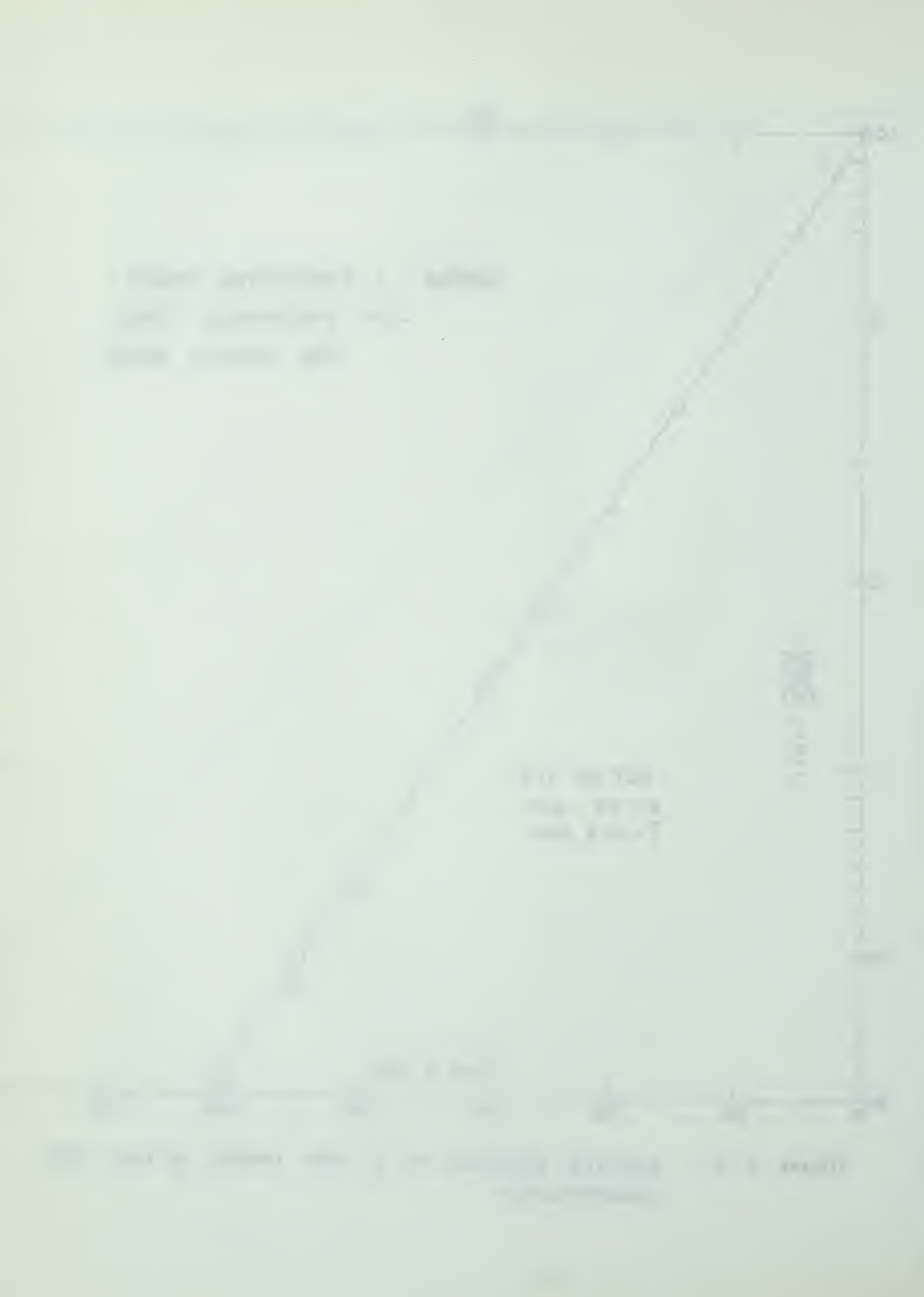

TABLE V-1

EXPERIMENTAL CONDITIONS DURING THE

INVESTIGATION OF NON-IDEAL REACTOR OPERATION AND RESULTS

Set No.	1-A	1-B	1-C
N r.p.m.	75	450	55
$\bar{t}$ min	45	45	14.8
q mls·min^{-1}	44.5	44.5	135
W gms	97	97	97
T ^{o}F	80	80	80
Fraction of the feed entering perfectly backmixed region m	1	1	1

TABLE V-3

TEMPERATURE DEPENDENCE OF k AND D

T		$\frac{1}{T} \times 10^3$	w	$k \times 10^2$	$D \times 10^5$
^{o}F	^{o}K	^{o}K^{-1}	cm$^{-\frac{1}{2}}$	min^{-1}	cm^2/min
80	300.00	3.3333	36.52	3.997	2.9967
100	311.11	3.2142	40.60	10.206	6.1915
120	322.22	3.1034	44.98	23.726	11.7272

each set the turbulence was varied over a wide range and its effect on the conversion measured. If a significant film mass transfer resistance existed, a change in the conversion with increase in the stirrer speed would be noticed.

A known amount of the catalyst was introduced in the reactor. The resin of the smallest size was used so that the mass transfer resistance, if any, would be predominantly evident. The flow rate, q, and temperature, T, were maintained constant throughout a set, in which the only variable was the stirrer speed. At each speed, the conversion of ethyl acetate was measured after a steady state was reached. The experimental conditions for the two sets and the results are presented in TABLES (C-5) and (C-6) of Appendix C. The results are plotted in FIGURE (V-6). A reference to the graphs shows that in both the sets, there is a sharp increase in the conversion from a stirrer speed of 100 to 175 r.p.m. It was observed during experiments that at speeds lower than 100 r.p.m. the resin particles were completely settled on the reactor bottom. For stirrer speeds between 100 and 175 r.p.m. the particles were partially in suspension, the degree of suspension increasing with increase in the stirrer speed, and for more than 200 r.p.m. they were almost completely suspended in the bulk of fluid. At this speed, however, the particles were not uniformly distributed throughout the reaction mixture. With increase in agitation, the uniformity in the catalyst distribution increased and for more than 275 r.p.m. the particles were completely mixed in the bulk.

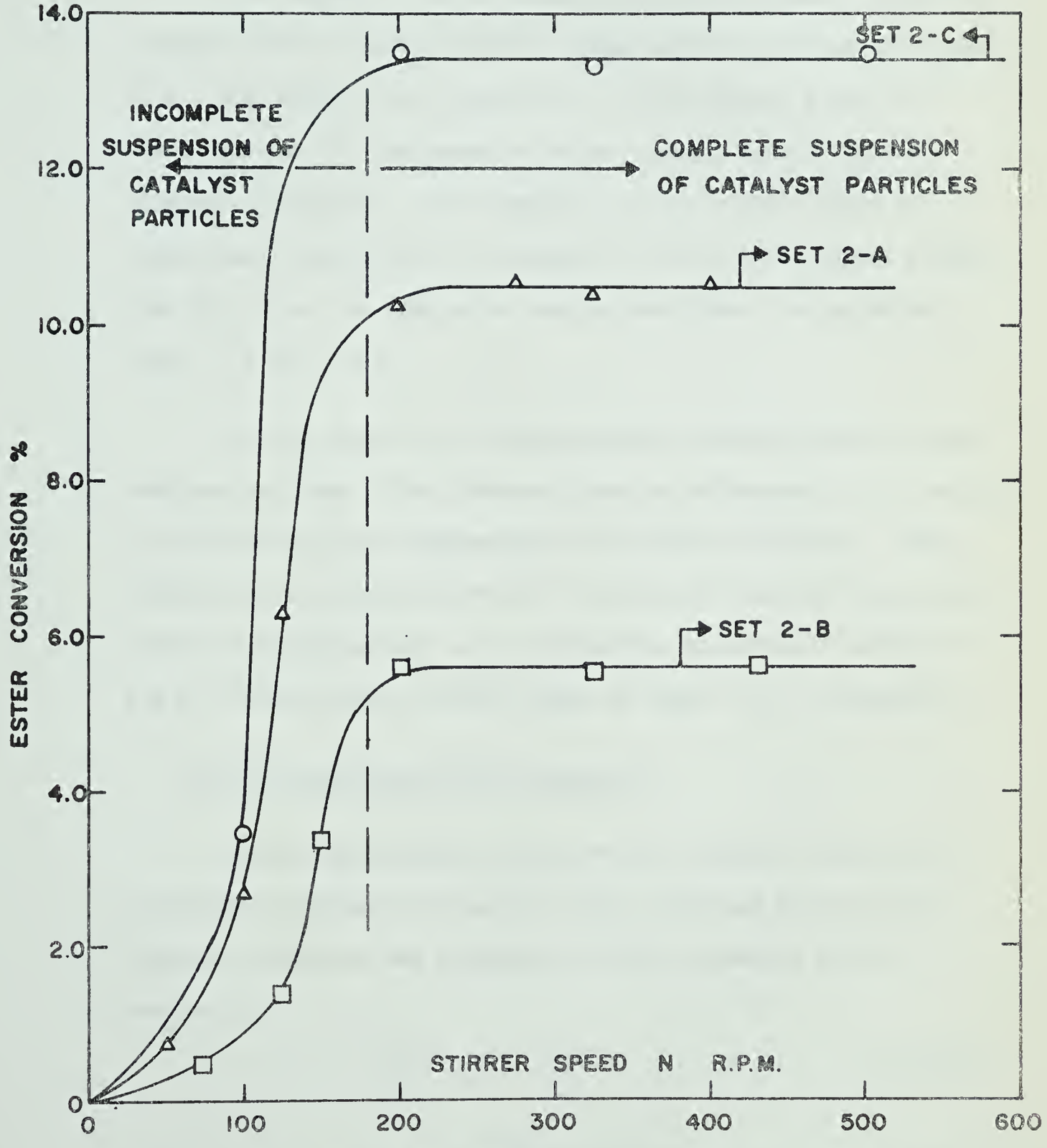

FIGURE V-6 : EVALUATION OF THE FILM MASS TRANSFER RESISTANCE

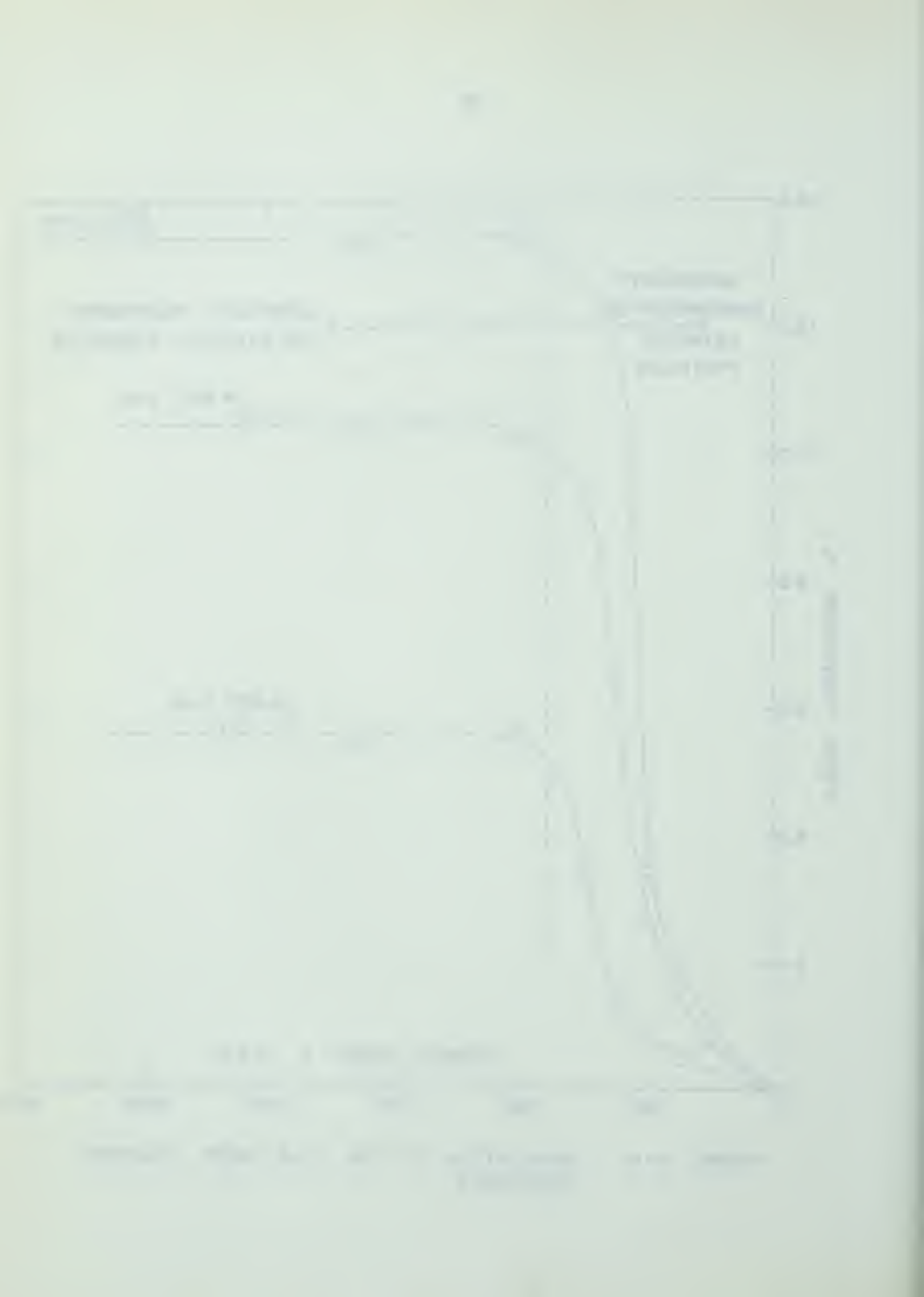

The effect of stirrer speed on the mass transfer coefficient between 0-200 r.p.m. is therefore complicated by the unavailability of all the catalyst for conversion. The conversion after the sharp increase in that range of stirrer speed, remains almost constant thereafter. It is therefore concluded that there is no significant mass transfer resistance for the stirrer speeds greater than 200 r.p.m. No conclusion can be drawn about the agitation range of 0-200 r.p.m.

In the second set of observations a lesser quantity of the catalyst was used. This, however, made no difference in the results. In both the sets the temperature in the reactor was 80° F. Four additional runs were made at 100° F between 100 and 500 r.p.m. No effect of agitation rate on the conversion was noticed above 200 r.p.m. These results are also shown in TABLE (C-7) of Appendix C.

V-D-3 Evaluation of Rate Constants

Having established that under the conditions studied for the system, nonideal flow did not exist (m=1) and the film mass transfer resistance was negligible ($K = \infty$), equation (IV.14) reduced to

$$\frac{C_i}{A_o} = 1 + \frac{q}{Q} \qquad \text{(IV.18)}$$

where,

$$Q = \frac{3WD}{R^2 \varsigma}(wR \cdot \coth(wR) - 1) \qquad \text{(IV.15)}$$

$$w^2 = \frac{k}{D}$$

This linear equation permits the evaluation of the rate constants, k and D, from experimental results.

Four sets of experiments were performed at a constant temperature of 80° F, with different but known amounts (W) and sizes (R) of the catalyst. For each set, the ester conversions were measured at different flow rates, q. During all these runs the stirrer speed was 600 r.p.m. The experimental data are given in TABLES (C-8) to (C-11) of Appendix C. Each set of runs were plotted as $\frac{C_i}{A_o}$ versus q. The plots are shown in FIGURE (V-7). The functional relation between the variables is linear and the best straight lines for the experimental data of each set were found by the least square method. These lines were forced to pass through the point (0, 1) as it should according to the equation (IV.18). The slopes of these lines is equal to $\frac{1}{Q}$. Thus the values of Q were obtained with the corresponding values of W and R. In the expression (IV.15) for Q, the two unknown parameters are k and D. By trial and error, the best values of the parameters were calculated, which gave the minimum standard deviation for the experimental data. The results are shown in TABLE (V-2). They indicate that the least-square-lines are approximated very closely by the theoretical equations. Details of the calculation procedures are given in Appendix C.

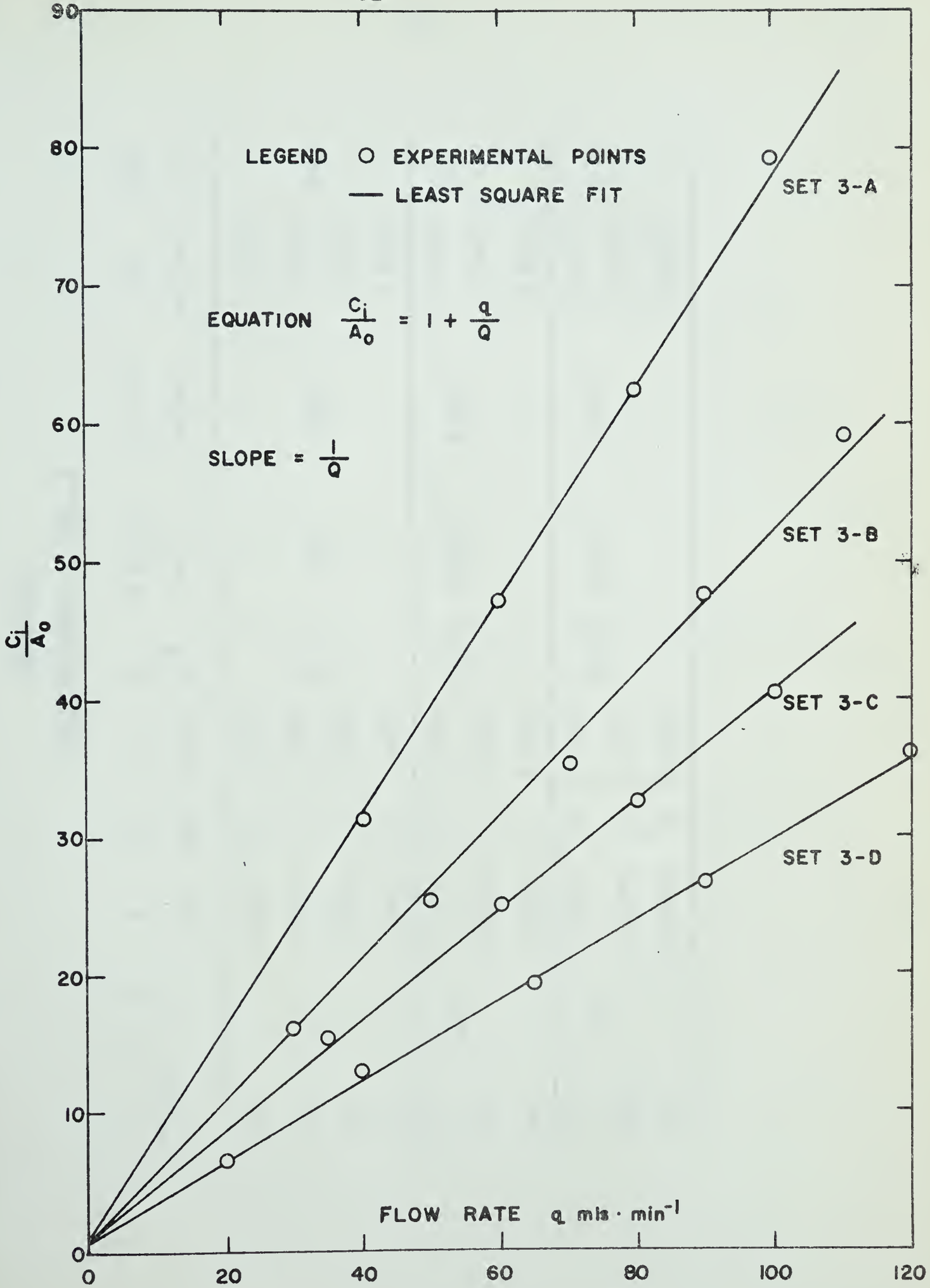

FIGURE V-7 : $\frac{C_i}{A_o}$ VERSUS q AT 80° F.

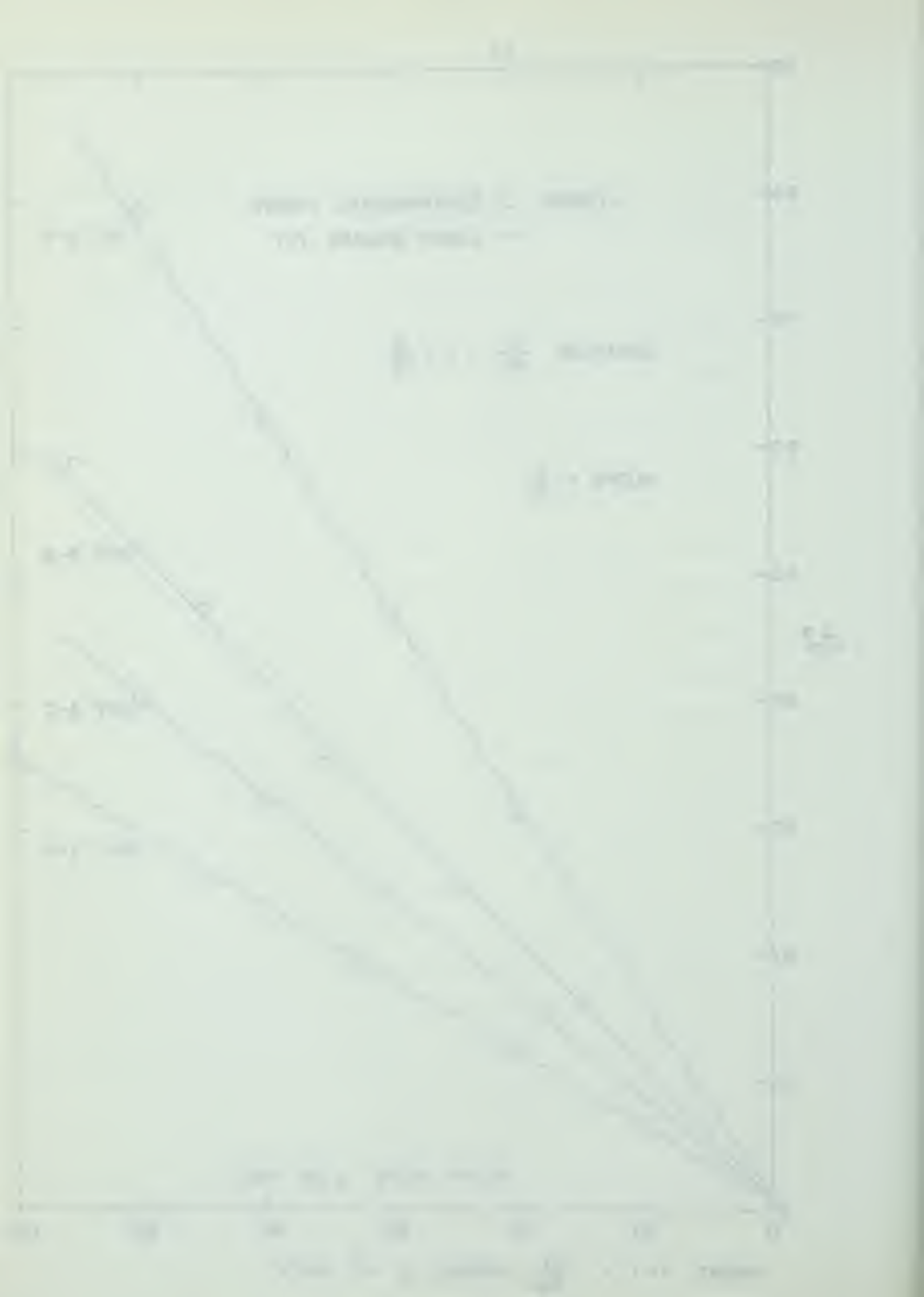

TABLE V-2

RATE CONSTANTS k AND D

Set No.	T °F	R cms	W gms	Q mls/min	w $cm^{-\frac{1}{2}}$	k x 10^2 min^{-1}	D x 10^{-5} cm^2/min	QC mls/min	RSD %
3-A		0.03045	28	1.2926				1.3021	
3-B	80	0.03045	42	1.9466	36.52	3.997	2.9967	1.9532	0.67
3-C		0.01268	51	2.5289				2.5248	
3-D		0.00283	68	3.4428				3.4119	
4-A		0.03045	80	9.3100				9.3440	
4-B	100	0.01268	43	5.5137	40.60	10.206	6.1915	5.4181	1.6
4-C		0.00283	70	8.8417				8.9672	
5-A		0.03045	80	21.2787				21.3296	
5-B	120	0.01268	43	12.7251	44.98	23.726	11.7272	12.5583	0.27
5-C		0.00283	70	20.6343				20.8615	

k and D as function of temperature: The effect of temperature on k and D was investigated by also determining the parameters at 100° F and 120° F. The experimental procedure was the same as above. At each temperature three sets of runs were performed. For each set W, R and N were fixed and the conversions were measured as a function of the flow rate, q.

TABLES (C-12) to (C-17) show the experimental conditions and data. The plots of $\frac{C_i}{A_o}$ versus q are shown in FIGURES (V-8) and (V-9) for 100° F and 120° F, respectively. The results are given in TABLES (V-2) and (V-3).

Both k and D were found to be exponential functions of temperature. This type of temperature variation for the diffusivity, D, appears to be a characteristic of the resin catalyst (52).

The parameters, k and D, are plotted versus $\frac{1}{T}$ in FIGURE (V-10) to obtain the following exponential relations.

$$\log_{10} k = \frac{-3384}{T} + 9.8815$$

or

$$k = 5.665 \times 10^{23} \exp\left(-\frac{15{,}500}{RT}\right) \quad \text{min}^{-1}$$

and

$$\log_{10} D = -\frac{2604}{T} + 4.1577$$

or

$$D = 3.747 \times 10^{9} \exp\left(-\frac{11920}{RT}\right) \quad \text{cm}^2 \cdot \text{min}^{-1}$$

where T is in °K.

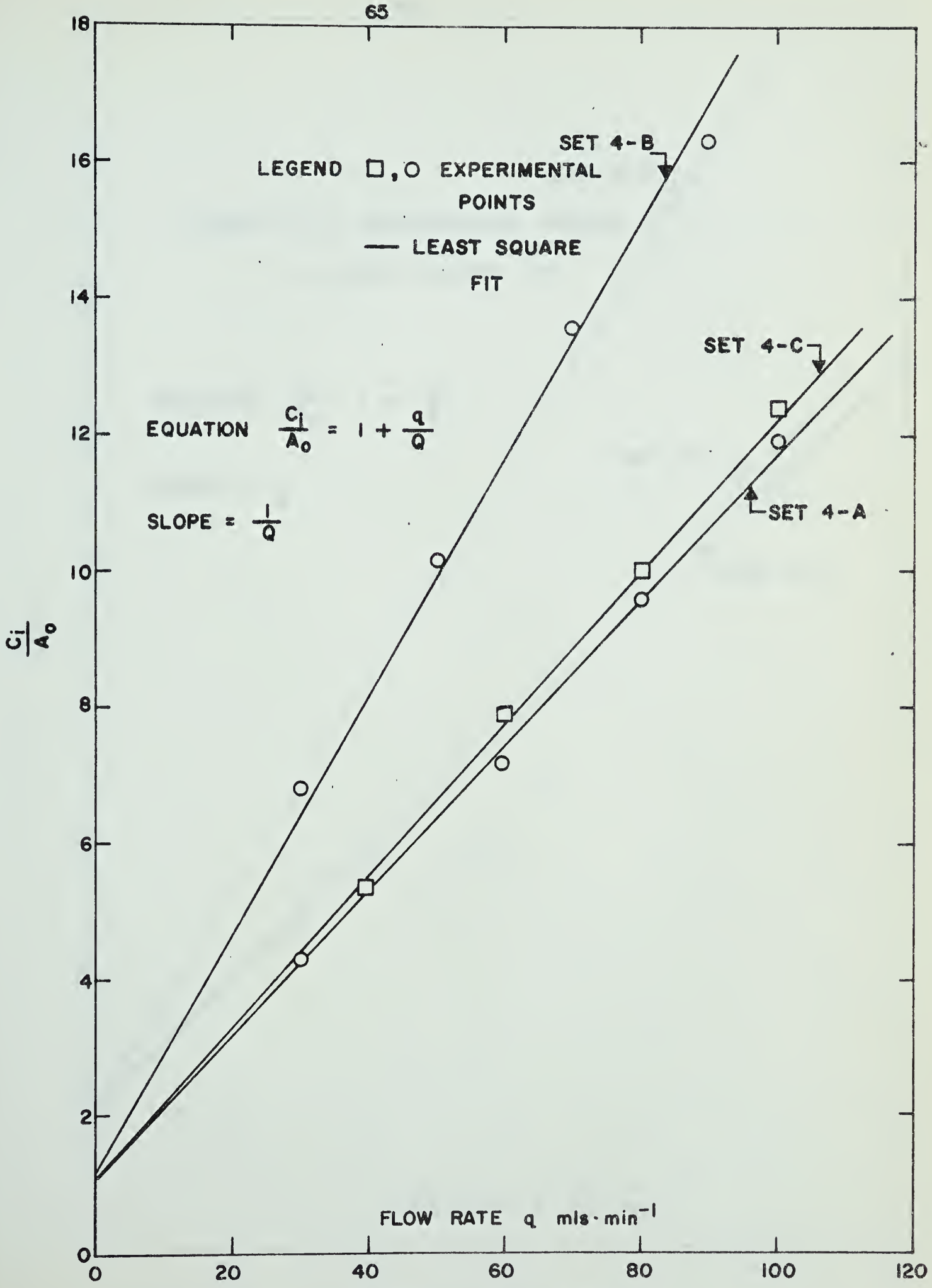

FIGURE V-8 : $\frac{C_i}{A_o}$ VERSUS q AT 100° F.

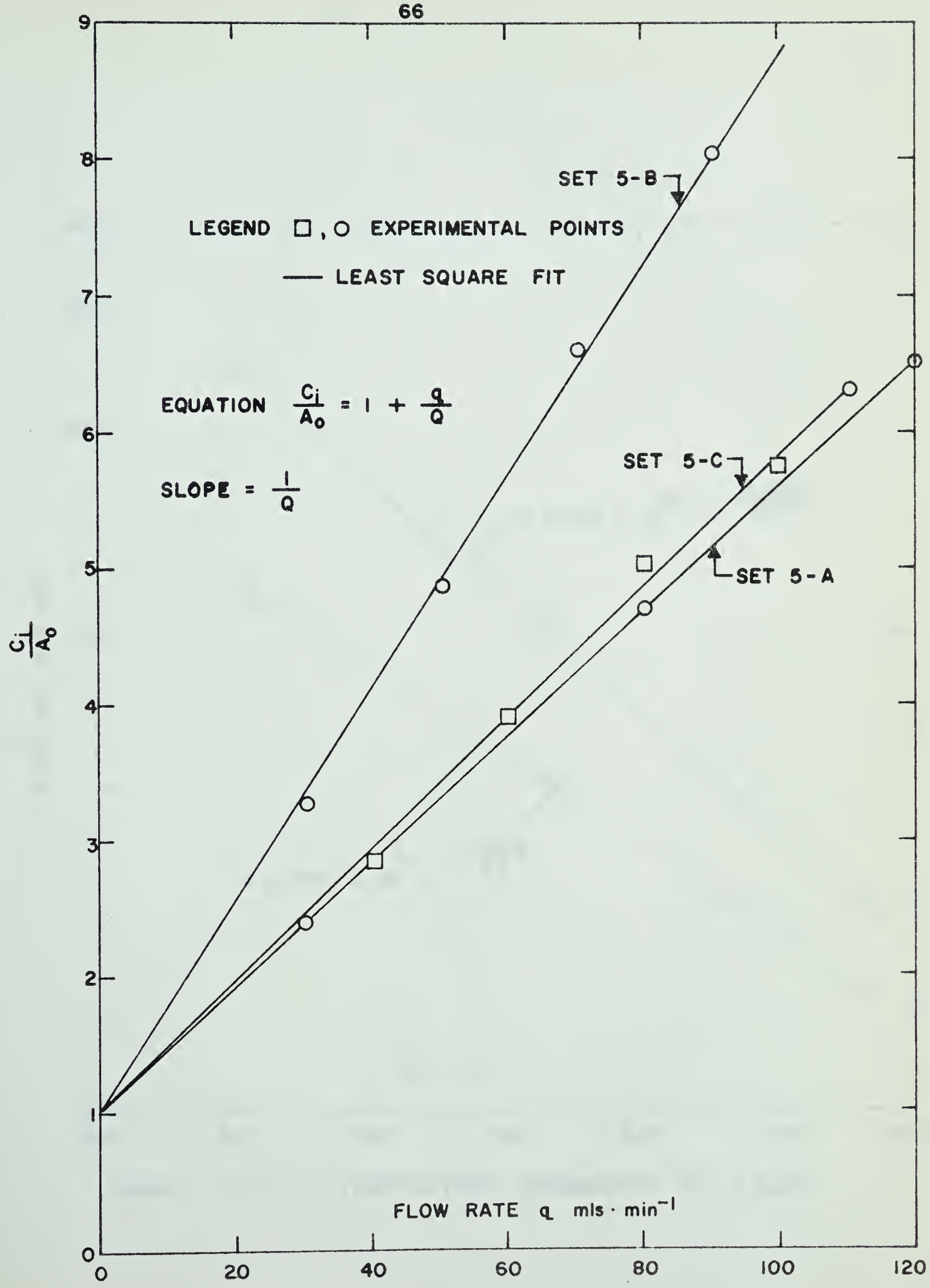

FIGURE V - 9 : $\frac{C_i}{A_o}$ VERSUS q AT 120° F.

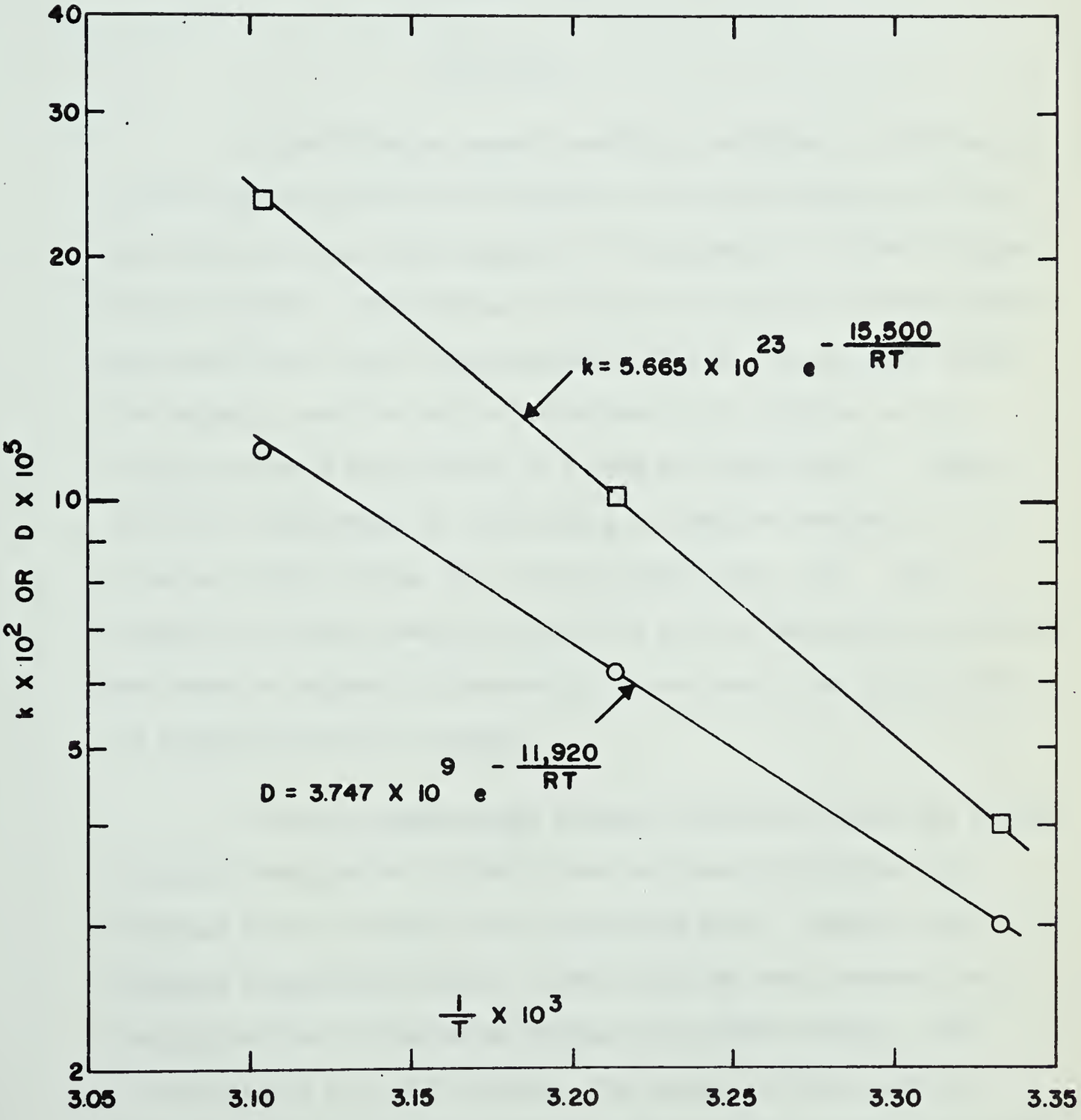

FIGURE V - 10 : TEMPERATURE DEPENDENCE OF k and D

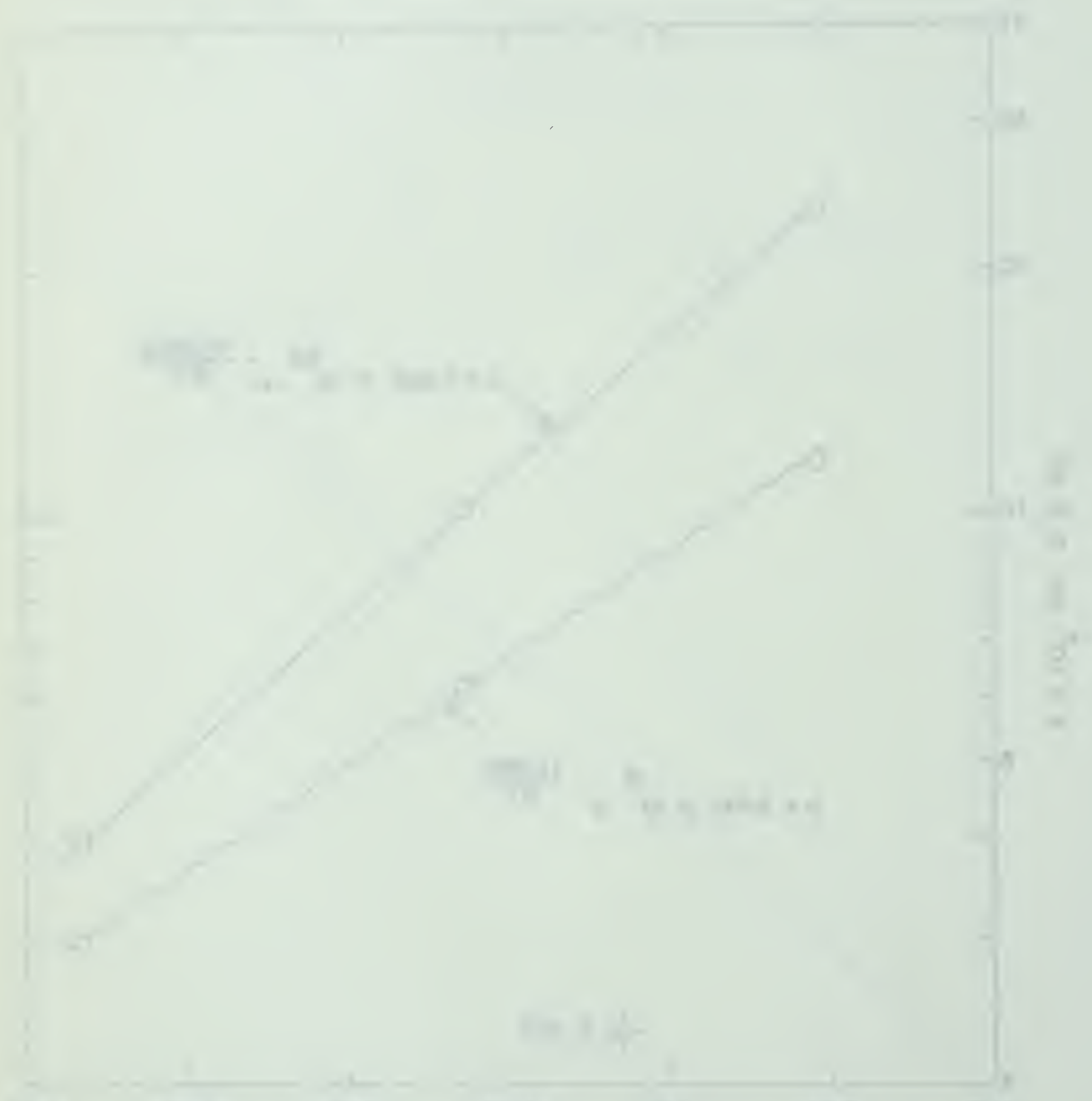

CHAPTER VI

DISCUSSION

Under the experimental conditions employed, no nonideality in the reactor operation was observed. This observation, in retrospect does not seem surprising and is in agreement with that of other workers (59,61). The process of mixing for not very viscous liquids has been shown to be a rapid phenomenon (7,38). In an ideal CFSTR the material near the exit is moved back by the stirrer to the neighbourhood of the entrance in a time much less than $\bar{t}$. Therefore, the requirement for good mixing is that the frequency of rotation of the stirrer must be much greater than $1/\bar{t}$. This condition was amply satisfied under the present experimental conditions and hence no apparent difference in the residence time distributions at varying speeds was observed.

The only experimental evidence available showing the actual nonideal behaviour of a CFSTR is the work done by Cholette and Cloutier (10) to confirm their theoretical model. However, they employed a specially designed vessel which had such features that would give rise to dead water regions and by-pass streams. The reactor had an i.d. of 30 inches. The liquid left the vessel by overflow in the outlet line placed to give a liquid depth of 30 inches. The feed inlet was in the centre, 12 inches from the surface of the liquid and the agitator, a $2\frac{1}{2}$ inch turbine model, was placed in between,

at a distance of 6 inches from the surface. Apparently, the positions of the inlet, outlet and the stirrer, contributed significantly to the response of the vessel. They obtained m=0.8 at 150 r.p.m. Their results however would be applicable only to their particular set up. In general, it can be concluded that except, possibly, for very viscous materials, very short residence times or special configuration of the reactor system, the agitator speed has little influence on mixing. Usually other factors like heat transfer preclude the use of very low agitation rates.

The mass transfer resistance in the external film was negligible for agitator speeds of more than 200 r.p.m., as evidenced by FIGURE (V-6). The reaction rate was therefore not influnced by the film diffusion and the simultaneous mass transfer and chemical reaction within the catalyst particle was the rate limiting step. Comments on the effect of film diffusion at agitator speeds less than 200 r.p.m. is not possible because, in that region, the interfacial area was not independent of the agitation rates. Then, obviously, the total amount of the catalyst was not measurably productive. For a meaningful analysis of such a phenomenon the rate must be expressed per unit of catalyst on which the measured conversion occurs. Amount of the effective catalyst, however, was not possible to determine.

Very few investigators working with similar systems have observed external mass transfer as a rate limiting process. Siato et al (See (49)) observed deviation from the first order kinetics of the inversion of sucrose indicating an effect of external diffusion. However, the later investigation of Reed and Dandroff (49) for the same reaction system indicated no effect of film diffusion over a wide range of Reynold Nos. Engel and Hougen (18) observed very strong external diffusion effects for particles of 0.00256 cms diameter at 80° F and 580 r.p.m., while for 0.01153 cms diameter at 126° F and 175 r.p.m. the film diffusion was negligible. In the present study the external mass transfer resistance was observed to be negligible even for 0.00283 cms diameter particles at 100° F. The descrepancy cannot be simply explained. However, it should be noted that Engel and Hougen worked with amyl acetate while the present work was concerned with ethyl acetate.

The last phase of the study was concerned with evaluating the parameters k and D and their dependence on temperature. Initial observations indicated the overall reaction rate per unit mass of catalyst as measured experimentally was almost independent of the particle size of the catalyst and hence, was limited by the relatively slow chemical reaction; the internal diffusion had no significant influence on the reaction rate. As a result of this it was found, while calculating the parameters k and D from the experimental data, that for small particles the diffusivity can be varied over relatively

wide limits without markedly affecting the value of Q. However, the effect of diffusivity increased with the increase in the particle size.

The effectiveness factors calculated from equation (II.5) for different particle sizes at different temperatures are shown in TABLE (VI-1) and FIGURE (VI-1).

For the ion exchange resin used in this study, the diffusivity was also found to be an exponential function of temperature, though less strong than the reaction rate constant. The parameters w and η are therefore only weakly dependent on temperature. With other solid catalysts for which the internal diffusivity is not an exponential function of temperature, the effectiveness factor, η , would be expected to decrease more rapidly and the overall reaction rate to increase more slowly with increase in temperature.

A reference to TABLE (Vl-1) shows that for the resin particles below 0.0254 cms in diameter and 120° F the effectiveness factors are very near to unity and the rigorous rate expression.

$$\text{Rate} = \eta k C \frac{W}{S}$$

can be approximated by

$$\text{Rate} = k C \frac{W}{S}$$

with deviations of only up to 2.1%

TABLE VI-1

EFFECTIVENESS FACTORS

T °F	R cms	w cm^{-1}	wR	η
	0.03045		0.1112	0.9262
80	0.01268	36.52	0.0450	0.9860
	0.00283		0.0103	0.9993
	0.03045		0.1238	0.9110
100	0.01268	40.60	0.0515	0.9827
	0.00283		0.0115	0.9991
	0.03045		0.1370	0.8938
120	0.01268	44.98	0.0570	0.9789
	0.00283		0.0127	0.9989

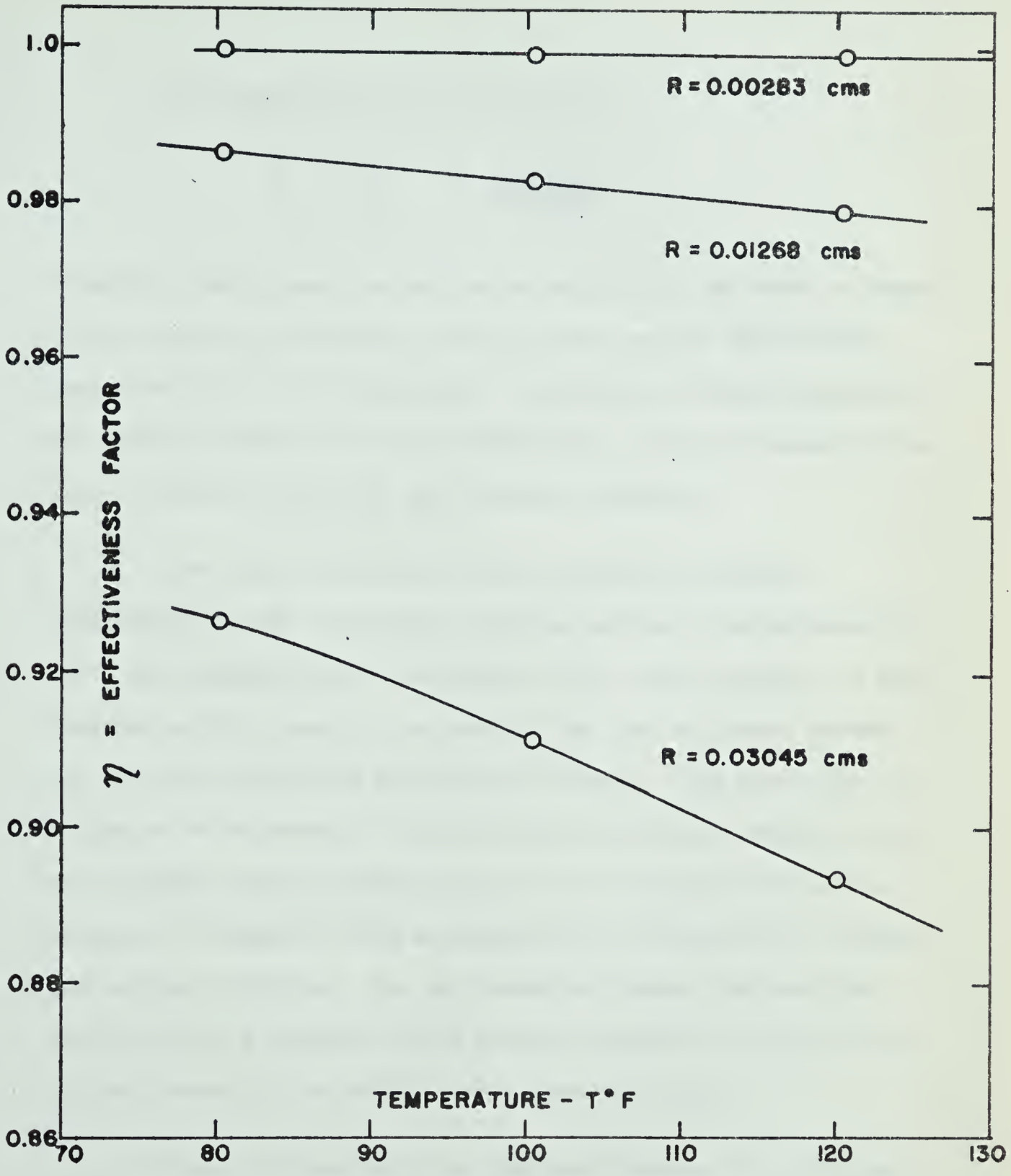

FIGURE VI-1 : EFFECTIVENESS FACTORS

The equations (A.9) and (A.10) give

$$\frac{C}{C_s} = \frac{C}{C_o} = \frac{R}{r} \frac{\text{Sinh}(wr)}{\text{Sinh}(wR)}$$

from which the internal concentration profile for the ester in terms of the surface concentration (which in this case is the effluent concentration) can be calculated. The results of these calculations are shown in TABLE (VI-2) and FIGURE (VI-2). The flat nature of the curves indicate relatively fast internal diffusion.

The high effectiveness factors provide an indirect confirmation of the observation that the external film diffusion is not a rate limiting step. As Petersen (48) says, "Resistance to mass transfer within a catalyst is greater than the resistance between the external surface and the bulk fluid phase. This means that if diffusion to the external surface limits the overall reaction rate, then internal diffusion must also limit the reaction rate and the designer is obliged to make an analysis which includes both external and internal diffusion. One can therefore dismiss the practical possibility of a system in which external diffusion is controlling in coexistance with an effectiveness factor of unity."

Since the above work was finished, Bochner et al (8), who studied the esterification of salicylic acid and methanol using Dowex 50W-x8 resins as the catalyst, observed that the external and internal diffusion of the reaction species had no significant

TABLE VI-2

CONCENTRATION PROFILES $(\frac{C}{C_o})$ IN THE CATALYST PARTICLES

	T °F	80			100			120		
$\frac{r}{R}$	R cms	0.03045	0.01268	0.00283	0.03045	0.01268	0.00283	0.03045	0.01268	0.00283
0.1		0.8219	0.9655	0.9982	0.7667	0.9575	0.9978	0.7467	0.9482	0.9973
0.2		0.8270	0.9665	0.9983	0.7929	0.9588	0.9979	0.7538	0.9498	0.9974
0.3		0.8355	0.9682	0.9984	0.8025	0.9609	0.9980	0.7655	0.9524	0.9976
0.4		0.8475	0.9706	0.9985	0.8167	0.9639	0.9982	0.7822	0.9560	0.9977
0.5		0.8631	0.9738	0.9987	0.8353	0.9677	0.9984	0.8040	0.9606	0.9980
0.6		0.8824	0.9776	0.9989	0.8583	0.9724	0.9986	0.8311	0.9663	0.9983
0.7		0.9056	0.9821	0.9991	0.8860	0.9780	0.0989	0.8638	0.9731	0.9986
0.8		0.9327	0.9873	0.9994	0.9186	0.9844	0.9992	0.9026	0.9810	0.9990
0.9		0.9614	0.9933	0.9997	0.9565	0.9918	0.9996	0.9478	0.9899	0.9995
1.0		1.0000	1.0000	1.0000	1.0000	1.0000	1.0000	1.0000	1.0000	1.0000

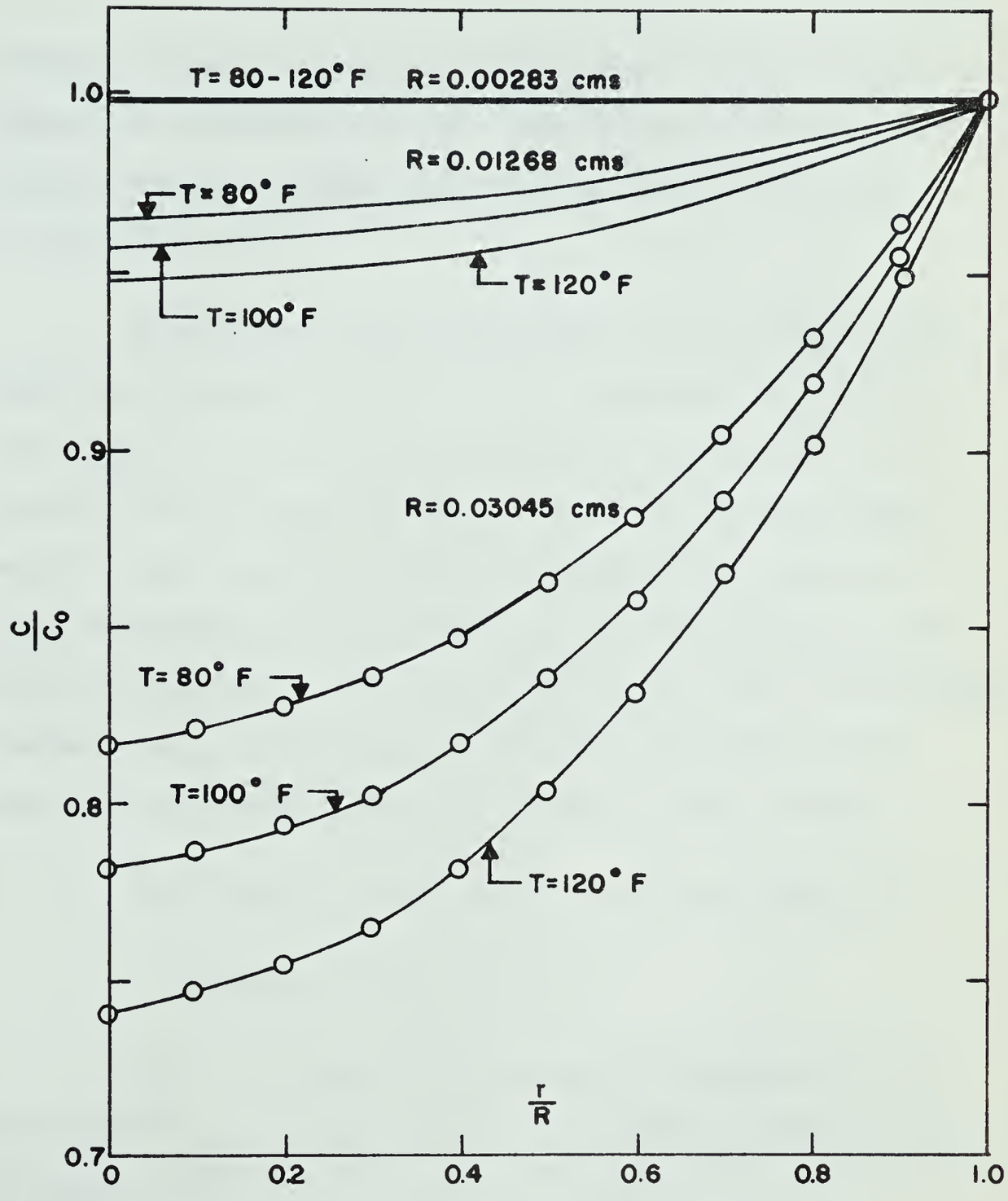

FIGURE VI - 2 : CONCENTRATION PROFILE OF ETHYL ACETATE IN THE RESIN PARTICLES

influence on the overall reaction rate. They demonstrated that the competitive chemisorption of water and salicylic acid was the rate limiting step and a Langmuir type equation fitted the date for 0 - 84.5 % conversion.

It was not the aim of the present study to evaluate such models and formulate the actual reaction mechanism. The ester concentrations and the conversions in the reaction were small. It is possible that the ester concentration within the catalyst volume would be higher than that in the surrounding liquid. However, a linear distribution law may correctly relate concentrations in the bulk liquid and pore liquid (8). In such a case, then, the calculated chemical reaction rate constant, k, would be the product of the distribution coefficient and the true reaction rate constant.

From FIGURE (V-10) the value of the rate constant is

$$k(\text{resin}) = 0.041 \text{ min}^{-1} \text{ at } 25^{\circ} \text{ C}$$

For an equivalent H^{+} ion concentration the value of k for the hydrolysis of ethyl acetate in a homogeneous medium using HCl acid is (26):

$$k(\text{HCl}) = 0.0409 \text{ min}^{-1} \text{ at } 25^{\circ} \text{ C}$$

$$\therefore \quad \frac{k(\text{resin})}{k(\text{HCl})} \cong 1.0 \text{ at } 25^{\circ} \text{ C}$$

Bernhard and Hammett (5) obtained k(resin)/k(HCl) = 0.92 at 25° C, which is in reasonable agreement with the above value. Saletan and White (52) obtained the ratio equal to 1.84 for the esterification of acetic acid and ethanol at 25° C. The value of E, the energy of activation for the reaction, however agrees more closely with that of Davies and Thomas (16) as shown below:

$E = 15{,}500$ cal·gmmole^{-1} (present work)

$E = 17{,}500$ cal·gmmole^{-1} (Bernhard and Hammett (5))

$E = 15{,}540$ cal·gmmole^{-1} (Davies and Thomas (16))

The following comparison of the values of the effective diffusivity, D, shows good agreement in the order of magnitude.

Ethyl Acetate $D = 3.1 \times 10^{-5}$ cm^2·min^{-1} at 25° C (present work)

Ethyl Formate $D = 5.0 \times 10^{-5}$ cm^2·min^{-1} at 25° C (Smith and Amundson(54)

Ethanol $D = 1.5 \times 10^{-5}$ cm^2·min^{-1} at 25° C (Saletan and White(52))

The "activation energy" for the diffusivity D of ethyl acetate in Dowex 50WX8 was found to be 11,920 cal·gmmole^{-1} (FIGURE (V-10)) as compared to that of ethanol in Dowex 50-X8 equal to 9,850 cal·gmmole^{-1} (12). In light of the fact that different types of resins were employed by different workers, further comparison is not pertinent. However, the general agreement with the previous works in the order of magnitudes of k and D and the relatively small scatter in the fit of the experimental data to the proposed equations provides a good, though only partial, verification of the model.

It should be noted that the effective diffusivity, D, is different than the true diffusional coefficient. In reality the diffusional process in solids is an impressively complex matter. The effective diffusivity takes into account the porosity of solid. In addition, all the pore volume may not be effective and different portions of the surface are characterized by different accessibilities. The transport within the solid involves flow splitting and covergence and multidirectional flow paths of which the individual contributions to the flow resistance are unknown. One may lump all these factors into some parameters; they are calculational conveniences and do not throw any direct light on the flow mechanism. In view, therefore, of the limitations attendant upon employing any sophisticated model, further refinement hardly seems profitable from the engineering point of view. The use of effective diffusivity enables one to describe the diffusion process independent of the shape, size and distribution of the pores.

A complete verification of the mathematical model is still to be achieved. The absence of any significant diffusional resistance in the reaction and any nonideality in the liquid flow through the reactor left only a simple model to be verified. If the proposed model were realistic, one would expect to obtain m=1 for all the experimental runs performed at high stirrer speeds. In other words, the best straight line passing through the experimental points on the plots of Q versus q (FIGURES (V-7) to (V-9)) should intercept

the vertical axis at unity. The values of the intercepts thus obtained from the experimental data were found to be varying between 0.7 to 1.2. It is possible that the proposed model is inadequate. However, it is thought that more experimental runs, particularly at low flow rates, q, should be performed for a meaningful evaluation of the model. This was not feasible with the present set up due to the equipment limitations.

A necessary condition for a meaningful evaluation of the complete model is that the experiments should be carried out at agitator speeds at which the catalyst particles are completely suspended in the reactor volume. The intensity of turbulence at these speeds is, however, usually sufficient to eliminate nonideality in the flow patterns and the external film resistance. While not much can be done about the nonideality in flow, it is possible that by judicious choice of certain factors the external mass transfer resistance can be significantly increased. For example even when the particles are suspended in the bulk of liquid, the relative motion between the two phases may be decreased by eliminating baffles and using an appropriate agitator. A higher ester may be employed. Also since the reaction rate increases exponentially with temperature, while mass transfer increases little more than linearly one would anticipate that at sufficiently high temperatures the rate might become mass transfer controlled for all catalysts.

It is theoretically possible to incorporate other modes of flow in a mathematical model, but the quantitative expressions become too complex to be of any practical use. For example, accounting a fraction of the reactor as a plug-flow region would introduce exponential terms in the model equation and the parameters in this equation cannot be easily determined by experiments.

Presence of a dead water region in the vessel where there are no solids does not affect the conversion. Finally, the problem becomes very difficult when the solid particles are settled, at the reactor bottom. Then a fraction of the solids which have settled is also effective in the reaction. The total amount of catalyst effective in this case remains virtually indeterminate as noted previously.

NOMENCLATURE

Ephemeral notation whose bearing does not extend beyond the immediate context is not included.

A_o = Concentration of acid in product stream, gmmoles·ml^{-1}

C = Concentration of ester in the resin particle, gmmoles·ml^{-1}

C_i = Concentration of ester in feed, gmmoles·ml^{-1}

C_o = Concentration of ester in product stream, gmmoles·ml^{-1}

C_s = Concentration of ester on the external surface of the resin particle, gmmoles·ml^{-1}

C^* = Concentration of ester in exit stream of the perfectly backmixed part of a CFSTR

$CN(\Theta)$ = Tracer concentration at time Θ, gmmoles·ml^{-1}

D = Effective diffusivity of ester in the resin phase, cm^2·min^{-1}

E = Energy of activation, cal·gmmole^{-1}

$F(\Theta)$ = Residence time distribution function

IMP = Impedance of HCl solution in the lucite cell, ohms

K = Mass transfer coefficient for ester diffusion through liquid film, cms·min^{-1}; K^*; at terminal speed

N = Stirrer speed, r.p.m.

Q = $\frac{3WD}{R^2\varrho}(wR\cdot\coth(wR) - 1)$, mls·min^{-1}

R = Radius of resin particle, cms

R_v = Reaction rate per unit volume of the catalyst, gmmoles·ml^{-1} per minute

T = Temperature

V = Volume of N/40 NaOH required to neutralize acetic acid in 25 mls of product stream, mls

W = Weight of resin catalyst, gms

$X(100)$ = Percentage conversion of ester

d = Diameter of resin particle; d_{avg} = the surface area average diameter of the resin particles, cms

k = Chemical reaction rate constant, min^{-1}

m = Fraction of feed by-passing the catalyst in a CFSTR

q = Feed rate; q_e = ester feed rate, q_w = water feed rate, $mls \cdot min^{-1}$

r = Space variable in a resin particle; distance from the centre, cms

t = Time, min

$\bar{t}$ = Average residence time of a reaction mixture in CFSTR, min

w = $\sqrt{\frac{k}{D}}$

z = $(wR \cdot \coth(wR) - 1)$

θ = Reduced time, $t/\bar{t}$

η = Effectiveness factor of a catalyst

ρ = Density of resin catalyst, $gms \cdot ml^{-1}$

BIBLIOGRAPHY

1. "Advances in Catalysis" Vol. 1-15, Academic Press.
2. Barker, G.E., White, R.R.; Chem. Eng. Progrs. Symp. series, 48, No.4, 75 (1952).
3. Barker, J.J., Treybal, R.E.; A.I.Ch.E. Journal, 6, 289 (1960).
4. Bernhard, S.A., Hammett, L.P.; J.Am.Chem.Soc., 75, 1798 (1953).
5. Ibid; 75, 5834 (1953).
6. Bernhard, S.A., Garfield, E., Hammett, L.P.; Ibid, 76, 991 (1954).
7. Biggs, R.D.; A.I.Ch.E. Journal, 9, 636 (1963).
8. Bochner, M.B., et al; I & EC Fundamentals, 4, No.3, 314 (1965).
9. Calderbank, P.H., Moo-Young, M.B.; "International Symp. on Distillation," England (1960).
10. Cholette, A. Cloutier, L.; Can.J.Ch.E. 105, (1959).
11. Cholette, A. Blanchet, J.; Ibid, 1 (1960).
12. Crank, J.;"The Mathematics of Diffusion," Clarendon Press (1956).
13. Dankwerts, P.V.; Chem. Eng. Sc., 2, 1 (1953).
14. Dankwerts, P.V.; Jenkins, J.V.; Place, G.; Ibid, 3, 26 (1954).
15. Dankwerts, P.V.; International Series of Monographs on Chemical Engineering, 1, 93 (1957).
16. Davies, C.W., Thomas, G.; J.Chem.Soc., 1607 (1952).
17. "Dowex: Ion Exchange", Dow Chemical Co., (1958).
18. Engel, A.J., Hougen, O.A.; A.I.Ch.E. Journal, 9, 724 (1963).
19. Ford, F.E., Pertmutter, D.D.; Ibid, 9, 371 (1963).
20. Frisch, N.W.; Chem. Eng. Sci., 17, 735 (1963).

21. Gamson, G.W., Thodos, G., Hougen, O.A., Trans. of Am. Inst. Chem. Engrs., 39, 1 (1964).

22. Gilliland, E.R., Mason, E.A.; Ind. Eng. Chem., 41, 1191 (1949).

23. Ibid; 44, 218 (1952).

24. Golub, L.L.; Univ. Microfilms (Ann Arbor, Mich.), L.C. Card No. Mix 58-526; Disst. Absts, 18, 979 (1958).

25. Handloss, A.E., Baron, T.; A.I.Ch.E. Journal, 3, 283 (1957).

26. Harned, H.S., Ptanstiel, R.; J.Am.Chem.Soc., 44, 2193 (1922).

27. Harriott, P.; Can. J. Ch. E., 40, 61 (1962).

28. Ibid; A.I.Ch.E. Journal, 8, 93 (1962).

29. Haskell, V.C., Hammett, L.P.; J.Am. Chem. Soc., 71, 1284 (1949).

30. Hixon, A.W., Wilkens, G.A.; Ind. Eng. Chem., 25, 1196 (1933).

31. Hixon, A.W., Baum, S.J.; Ibid, 33, 478 (1941).

32. Ibid; 34, 120 (1942).

33. Ibid; 34, 194 (1942).

34. Hixon, A.W., Drew, T.B., Knox, K.L.; Chem. Eng. Progr., 50, 592 (1954).

35. Humphrey, D.W., Van ness, H.C.; A.I.Ch.E. Journal, 3, 283 (1957).

36. Hyman, D.; "Advances in Chemical Engineering," 3, 120-204 (1962). Academic Press.

37. Johnson, A.I., Huang Chen-Jung; A.I.Ch.E. Journal, 2, 412 (1956).

38. Johnson, J.P., Edwards, L.J.; Trans, Faraday Soc., 45, 286 (1949).

39. Journal of Catalysis: monthly Publications.

40. Kunin, R.;"Ion Exchange Resins," John Wiley & Sons, Inc. (1958).

41. Levenspiel Octave;"Advances in Chemical Engineering," 4, 95-199 (1963), Academic Press.

42. Levesque, C.L., Craig, A.M.; Ind. Eng. Chem., 40, 96 (1948).

43. Marangozis, J., Johnson, A.I.; Can.J.Ch.E.; 40, 231 (1962).

44. Miller, D.N.; Ind. Eng. Chem., 56, 18 (1964).

45. Murphree, E.W.; Ind. Eng. Chem., 15, 148 (1923).

46. Naor, P., Shinnar, R.; I & EC Fundamentals, 2, 278 (1963).

47. Petersen, E.E.;"Chemical Reaction Analysis", Prentice Hall Inc. (1965).

48. Ibid; 135.

49. Reed, E.W., Dranoff, J.S.; I & EC Fundamentals, 3, No.4, 304 (1964).

50. Riesz, P., Hammett, L.P.; J.Am.Chem. Soc., 76, 992 (1954).

51. Rohm and Haas Co.; Technical notes on IR-120 and Amberlyst 15.

52. Saletan, D.I., White, R.R.; Chem. Eng. Progrs. Symp. series, 48, No. 4, 75 (1952).

53. Sherwood, T.K., Satterfield, C.N.; "The Role of Diffusion in Catalysis," Addison - Weseley Pub. Co., (1963).

54. Smith, N., Amundson, N.; Ind. Eng. Chem., 43, 2156 (1951).

55. Sussman, S.; Ind. Eng. Chem., 38, 1228 (1946).

56. Thiele, E.W.; Ibid, 31, 916 (1939).

57. Thomas, G. Davies, C.W.; Nature, 159, 372 (1947).

58. Wilhelm, R.H., Conklin, L.H., Sauer, T.C.; Ind. Eng. Chem., 33, 453 (1941).

59. Wolf, D., Manning, S.F.; Can.J.Ch.E., 284 (1964).

60. Wolf, D., Resnick, W.; I & EC Fundamentals, 287, (1963).

61. Worrell, G.R., Engleton, L.E.; Can.J.Ch. Eng., 254 (1964).

62. Yang, K.H., Hougen, O.A.; Chem. Eng. Progrs., 46, 146 (1950).

APPENDIX A

DERIVATION OF THE MATHEMATICAL MODEL

The linear differential equation

$$\frac{d^2C}{dr^2} + \frac{2}{r}\left(\frac{dC}{dr}\right) - \frac{kC}{D} = 0 \qquad (A.1)$$

has a general solution of the form (See CHAPTER IV)

$$C = \frac{A}{r}\cosh(wr) + \frac{B}{r}\sinh(wr) \qquad (A.2)$$

where, $w^2 = \frac{k}{D}$

The boundary conditions imposed by the system are:

(1) At the centre of the particle

$$\left(\frac{dC}{dr}\right)_{r=o} = 0 \qquad (A.3)$$

The equation (A.2) now reduces to

$$C = \frac{B}{r}\sinh(wr) \qquad (A.4)$$

(2) At the catalyst surface (See equation (IV. 13))

$$C_i - C_s = \left[\frac{3WD}{R\varsigma mq} + \frac{D}{K}\right]\left(\frac{dC}{dr}\right)_{r=R} \qquad (A.5)$$

Differentiating equation (A.4)

$$\left(\frac{dC}{dr}\right)_{r=R} = \frac{B}{r^2} \frac{(wR \cdot \coth(wR) - 1)}{\sinh(wR)} \qquad (A.6)$$

Also,

$$C_s = (C)_{r=R} = \frac{B}{R} \sinh(wR) \qquad (A.7)$$

Substituting equations (A.6) and (A.7) in equation (A.5) and simplifying,

$$B = \frac{C_i}{(1 + Pz)} \frac{R}{\sinh(wR)} \qquad (A.8)$$

where

$$P = \frac{3WD}{R^2 \zeta mq} + \frac{D}{RK}$$

and

$$z = (wR \cdot \coth(wR) - 1)$$

Equations (A.8) and (A. 4) give

$$\frac{C}{C_i} = \frac{1}{(1 + Pz)} \frac{R}{r} \frac{\sinh(wr)}{\sinh(wR)} \qquad (A.9)$$

At the particle surface

$$r = R$$

$$\therefore \quad \frac{C}{C_i}_{r=R} = \frac{C_s}{C_i} = \frac{1}{1 + Pz} \tag{A.10}$$

Now, according to the model proposed

C^* = Bulk concentration of the ester in the perfectly backmixed part of the reactor.

Therefore, a rate balance for the diffusion of the ester through the liquid film surrounding a particle gives

$$D \left(\frac{dC}{dr}\right)_{r=R} = K(C^* - C_s)$$

Rearranging the above expression

$$\frac{C^*}{C_i} = \frac{C_s}{C_i} + \frac{D}{K} \frac{1}{C_i} \left(\frac{dC}{dr}\right)_{r=R} \tag{A.11}$$

From equations (A.8) and (A.6)

$$\left(\frac{dC}{dr}\right)_{r=R} = \frac{C_i}{R} \frac{z}{(1 + Pz)} \tag{A.12}$$

Substituting (A.12) and (A.10) into (A.11)

$$\frac{C^*}{C_i} = \frac{1}{(1 + Pz)} + \frac{D}{RK} \frac{z}{(1 + Pz)} \tag{A.13}$$

However, from equation (IV.4)

$$\frac{C_o}{C_i} = 1 - m + \frac{mC^*}{C_i}$$

$$\therefore \quad \frac{C_o}{C_i} = 1 - m + \frac{m}{(1 + Pz)} \left[1 + \frac{Dz}{RK}\right] \tag{A.14}$$

Simplifying the above expression

$$\frac{C_o}{C_i} = 1 - \frac{z}{(1 + Pz)} \frac{3WD}{R^2 \varsigma q} \tag{A.15}$$

$$\therefore \quad \frac{A_o}{C_i} = 1 - \frac{C_o}{C_i}$$

$$= \frac{z}{(1 + Pz)} \frac{3WD}{R^2 \varsigma q} \tag{A.16}$$

Rearranging equation (A.16)

$$\frac{C_i}{A_o} = \frac{R^2 \varsigma q}{3WDz} + \frac{R \varsigma q}{3KW} + \frac{1}{m}$$

or

$$\frac{C_i}{A_o} = q \left[\frac{1}{Q} + \frac{R \varsigma}{3KW}\right] + \frac{1}{m} \tag{A.17}$$

where

$$Q = \frac{3WD}{R^2 \varsigma} (wR \cdot \coth(wR) - 1) \tag{A.18}$$

(A.17) and (A.18) are the desired expressions for the proposed model.

Effectiveness Factor:

When $K = \infty$ and $m = 1$, equation (A.17) reduces to

$$\frac{C_i}{A_o} = 1 + \frac{q}{Q} \qquad (A.19)$$

and

$$C_s = C^* = C_o \qquad (A.20)$$

However,

$$C_i = C_o + A_o$$

$$\therefore \quad 1 + \frac{C_o}{A_o} = 1 + \frac{q}{Q}$$

or $$qA_o = QC_o \qquad (A.21)$$

The rate of disappearance of ester

$$= q\,(C_i - C_o)$$

$$= qA_o \qquad \text{gmmoles/min}$$

Therefore, rate of the reaction per unit effective volume of the catalyst is given by

$$R_V = \frac{\rho q A_o}{W} \quad \text{gmmoles} \cdot \text{min}^{-1} \cdot \text{ml}^{-1} \text{ of catalyst}$$

$$= \frac{\rho Q C_o}{W} \quad \text{(Using equation (A.21))} \qquad \text{(A.22)}$$

Now, by definition

$$R_V = \eta k C_s$$

$$= \eta k C_o \quad \text{(Using equation (A.20))} \qquad \text{(A.23)}$$

where,

η = effectiveness factor

Comparing equations (A.22) and (A.23)

$$\eta = \frac{\rho}{W} \frac{3WD}{kR^2\rho} (wR \cdot \coth(wR) - 1)$$

$$\eta = \frac{3}{w^2R^2} (wR \cdot \coth(wR) - 1) \qquad \text{(A.24)}$$

or,

$$\eta = \frac{3D}{kR^2} \left[R\sqrt{\frac{k}{D}} \cdot \coth\left(R\sqrt{\frac{k}{D}}\right) - 1 \right]$$

APPENDIX B

MISCELLENEOUS DETAILS

TABLE B-1

MEASUREMENT OF PARTICLE DIAMETER

(a) Size Range: 20-50 mesh

No.	Diameter $d \times 10^{-2}$ cms	No.	Diameter $d \times 10^{-2}$ cms	No.	Diameter $d \times 10^{-2}$ cms
1	1.6956	2	3.4916	3	6.0200
4	4.4247	5	8.0969	6	4.5451
7	5.1772	8	6.0200	9	4.4247
10	6.3210	11	3.7625	12	5.7190
13	4.4548	14	6.1404	15	4.7558
16	5.8190	17	4.3043	18	6.1805
19	4.6053	20	3.0401	21	6.9631
22	6.0200	23	5.5384	24	8.2183
25	6.3618	26	3.7023	27	2.4090
28	6.4113	29	5.1772	30	3.7324
31	5.3227	32	3.4013	33	2.3789
34	4.6956	35	4.6655	36	4.4648
37	5.9899	38	3.6241	39	6.3210
40	1.2642	41	2.8595	42	4.4648
43	4.3344	44	2.7993	45	6.8026
46	2.5294	47	5.1772	48	4.0635
49	4.3650	50	6.6220	51	6.1404
52	6.1705	53	6.8628	54	6.3812
55	4.0033	56	5.0879	57	7.0735
58	7.5551	59	4.7558	60	6.5618
61	4.0033	62	5.3578	63	6.7424
64	5.5685	65	6.0802	66	7.2240
67	4.2140	68	7.4949	69	4.8160
70	4.5155	71	3.1906	72	7.1036
73	7.1046	74	5.9899	75	1.8060
76	5.1471	77	7.4046	78	5.8695
79	3.3110	80	5.9598	81	7.5250
82	4.4849	83	5.5685	84	7.7056
85	7.2842	86	5.8695	87	2.2274
88	7.4648	89	3.0100	90	4.6354
91	2.7692	92	4.7869	93	5.9297
94	3.3712	95	4.7859	96	2.6187
97	4.0033	98	7.5551	99	4.3645
100	4.7257				

$$\sum_{1}^{100} d_i^2 = 0.2874$$

$$\sum_{1}^{100} d_i^3 = 1.7503 \times 10^{-2}$$

$$\therefore \quad d_{avg} = \frac{\sum d_i^3}{\sum d_i^2}$$

$$= 6.090 \times 10^{-2} \text{ cms}$$

$$R = 0.03045 \text{ cms}$$

and, Relative Standard Deviation

$$= \left[\frac{\sum_{1}^{100} (d_i - d_{avg})^2}{(100 - 1)\, d^2_{avg}} \right]^{\frac{1}{2}} \times 100$$

$$= 28.7\ \%$$

TABLE B-1 (CONTINUED)

MEASUREMENT OF PARTICLE DIAMETER

(b) Size Range: 50-100 mesh

No.	Diameter $d \times 10^{-2}$ cms	No.	Diameter $d \times 10^{-2}$ cms	No.	Diameter $d \times 10^{-2}$ cms
1	1.4308	2	2.5165	3	2.8472
4	2.5524	5	2.7178	6	1.3733
7	2.8832	8	2.5309	9	2.4086
10	1.8478	11	2.7260	12	1.5746
13	2.1714	14	2.6200	15	2.8688
16	1.8263	17	2.5894	18	1.5243
19	2.5165	20	2.0995	21	2.5093
22	1.6893	23	2.5884	24	2.8185
25	1.9000	26	2.4086	27	2.1858
28	2.1383	29	2.4662	30	1.9195
31	3.1825	32	2.7394	33	2.5956

(CONTINUED)

TABLE B-1 (CONTINUED)

MEASUREMENT OF PARTICLE DIAMETER

(b) Size Range: 50-100 mesh

No.	Diameter $d \times 10^{-2}$ cms	No.	Diameter $d \times 10^{-2}$ cms	No.	Diameter $d \times 10^{-2}$ cms
34	2.7681	35	2.5309	36	2.9361
37	2.6028	38	2.4374	39	2.7610
40	2.7466	41	2.2864	42	1.7472
43	2.9048	44	2.6747	45	1.3373
46	3.5734	47	2.1642	48	2.6423
49	2.3367	50	2.4805	51	1.6321
52	1.8615	53	1.5530	54	3.0486
55	2.4158	56	2.7538	57	2.5740
58	2.7034	59	2.8275	60	2.5524
61	2.6603	62	2.4156	63	2.6387
64	2.6315	65	2.5596	66	2.3439
67	1.9772	68	1.8400	69	1.7975
70	2.7897	71	2.3799	72	1.6537
73	2.0923	74	2.4230	75	2.7466
76	2.5940	77	2.6315	78	2.6459
79	2.5596	80	1.6968	81	2.3224
82	2.6028	83	1.5027	84	1.8047
85	2.5956	86	2.7394	87	2.4374
88	2.4158	89	1.5099	90	3.0054
91	2.4158	92	2.1642	93	1.6171
94	1.3733	95	2.4805	96	2.3871
97	2.7034	98	1.8760	99	2.7897
100	2.0923				

$$\sum_{1}^{100} d_i^2 = 0.5766$$

$$\sum_{1}^{100} d_i^3 = 1.4623 \times 10^{-3}$$

$$\therefore \quad d_{avg} = \frac{\sum d_i^3}{\sum d_i^2}$$

$$d_{avg} = 2.536 \times 10^{-2} \text{ cms}$$

$$\therefore \quad R = 0.01268 \text{ cms}$$

and, Relative Standard Deviation

$$= \left[\frac{\sum_{1}^{100} (d_i - d_{avg})^2}{(100 - 1)\, d_{avg}} \right]^{\frac{1}{2}} \times 100$$

$$= 19.5 \ \%$$

TABLE B-1 (CONTINUED)

MEASUREMENT OF PARTICLE DIAMETER

(c) Size Range: 100-200 mesh

No.	Diameter $d \times 10^{-2}$ cms	No.	Diameter $d \times 10^{-2}$ cms	No.	Diameter $d \times 10^{-2}$ cms
1	6.0385	2	8.0014	3	5.4484
4	6.4240	5	2.1074	6	7.1703
7	1.6191	8	2.7756	9	6.7334
10	1.4906	11	7.4787	12	6.3993
13	1.4906	14	5.4484	15	2.5957
16	0.8995	17	2.5186	18	4.1634
19	4.3947	20	3.8550	21	1.3364
22	1.7733	23	7.3245	24	5.7054
25	1.0537	26	3.2125	27	0.8738
28	7.0418	29	5.3713	30	2.5700
31	5.4227	32	4.2405	33	2.7499
34	1.8247	35	4.8059	36	5.7054
37	3.3153	38	4.3934	39	7.8385
40	5.0372	41	3.3667	42	4.2262
43	4.8830	44	6.6007	45	5.9367
46	5.2428	47	1.4135	48	2.2616
49	2.7499	50	2.1845	51	1.5163
52	4.8573	53	1.8761	54	1.6705
55	4.0349	56	3.8807	57	4.7031
58	2.6985	59	3.1354	60	5.5769
61	2.3387	62	1.9275	63	5.7285
64	4.3967	65	2.4415	66	7.9670
67	4.0349	68	7.0161	69	2.2359

(CONTINUED)

TABLE B-1 (CONTINUED)

MEASUREMENT OF PARTICLE DIAMETER

(c) Size Range: 100-200 mesh

No.	Diameter $d \times 10^{-2}$ cms	No.	Diameter $d \times 10^{-2}$ cms	No.	Diameter $d \times 10^{-2}$ cms
70	4.0763	71	2.7756	72	4.5489
73	1.3364	74	3.6237	75	5.0629
76	4.6603	77	2.2359	78	6.0395
79	6.6049	80	7.2731	81	1.4649
82	7.5000	83	6.4764	84	1.5677
85	2.5957	86	2.3644	87	5.2488
88	5.3199	89	1.6705	90	3.3667
91	1.4649	92	5.4484	93	5.4484
94	2.3901	95	5.3456	96	1.4906
97	1.5934	98	1.5163	99	2.5443
100	3.9814				

$$\sum_{1}^{100} d_i^2 = 1.973 \times 10^{-3}$$

$$\sum_{1}^{100} d_i^3 = 1.1167 \times 10^{-5}$$

$$\therefore \quad d_{avg} = \frac{\sum d_i^3}{\sum d_i^2}$$

$$= 5.68 \times 10^{-3} \text{ cms}$$

$$\therefore \quad R = 0.002843 \text{ cms}$$

and, Relative Standard Deviation

$$= \left[\frac{\sum_{1}^{100} (d_i - d_{avg})^2}{(100 - 1)\, d^2_{avg}} \right]^{\frac{1}{2}} \times 100$$

$$= 37.2 \%$$

TABLE B-2

EQUIPMENT DETAILS

	Equipment		Details
(1)	Storage bottle for distilled water	Material : Size :	Pyrex glass 12 gallons
(2)	Storage bottle for ethyl acetate	Material : Size :	Pyrex glass 1 gallon
(3)	Constant head tank for water	Material : Size :	glass 1000 mls
(4)	Constant level tank for ethyl acetate	Material : Size :	glass 500 mls
(5)	Feed pump for water	Material : Type : Size :	monel Centrifugal, Fisher Scientific Co 2 inch diameter turbine capable of supplying 1 gpm at 12 ft. of water head.
(6)	Feed pump for ester	Material : Type : Capacity : Plunger : Discharge Pressure :	Stainless Steel Positive displacement, duplex, Milton Roy Co. 5 mls/min/side 1/10 inch dia. x 1 inch length, 96 s/min. 2000 psia
(7)	Rotameters (a) for water	Material : Range : Type :	glass 0-130 mls·min^{-1} No. 603, Matheson Co.
	(b) for ethyl acetate	Material : Range : Type :	glass 0-5 mls·min^{-1} No. 601, Matheson Co.
(8)	Reactor (a) Vessel	Material : Size :	Pyrex glass $9\frac{1}{2}$ inches height, 6 inches o.d. $5\frac{1}{2}$ inches i.d., 3/4 inch wide flange, ground top.

(CONTINUED)

TABLE B-2

EQUIPMENT DETAILS (CONTINUED)

	Equipment		Details
(8)	Reactor	Material :	Stainless Steel
	(b) Baffles	Size :	$\frac{1}{2}$ inch width, $9\frac{1}{4}$ inches length, 1/8 inch thickness.
		No. :	4
	(c) Filter	Material :	Sintered brass
		Size :	3/4 inch o.D. x $1\frac{1}{2}$ inch long 12-50 microns pores.
	(d) Stirrer I	Material :	Stainless Steel
		Type :	T-line, electric, with speed control.
		Size :	1/50 H.P., 20-6000 r.p.m. 5/16 inch dia. shaft.
	(e) Stirrer II	Material :	Stainless Steel
		Type :	Lightenin' Air Stirrer
		Size :	300-3000 r.p.m. at 30-90 psi air pressure, 5/16 inch dia. shaft.
	(f) Impeller	Material :	Stainless Steel
		Type :	Turbine type
		Size :	1 3/4 inches dia., 3 vanes.
	(g) Reactor cover	Material :	Stainless Steel
		Size :	9 inch dia. x $\frac{1}{4}$ inch thick
	(h) Ring flange	Material :	Stainless Steel
		Size :	$6\frac{1}{4}$ inches i.d., 9 inches o.d., $\frac{1}{4}$ inch thick.
(9)	Constant temperature bath	Material :	Pyrex glass
	(a) Vessel	Size :	10 inch dia. x 12 inches
	(b) Thermometer	Material :	Mercury-glass
		Range :	0-150° F
	(c) Heater	Material :	copper
		Power :	1500 watts

(CONTINUED)

TABLE B-2

EQUIPMENT DETAILS (CONTINUED)

	Equipment		Details
(9)	Constant temperature bath	Material :	-
		Type :	Bimetallic, American Inst. Co.
	(d) Thermoregulator	Sensitivity:	$\pm$ 0.05° F
	(e) Electronic Relay	Material :	-
		Type :	Precision Scientific Co. on-and-off control.
		Capacity :	1650 watts
	(f) Stirrer	Material :	Stainless Steel
		Type :	Sparkless 'Cenco' electric motor stirrer
		Size :	1/100 H.P., 1000 r.p.m., 40 watts, $\frac{1}{4}$ inch dia. shaft, 1 $\frac{1}{2}$ inch dia. impeller
(10)	Effluent pump	Material :	Stainless Steel
		Type :	Positive displacement, duplex, Milton Roy Co., Laboratory model
		Capacity :	80 mls/min/side
		Plunger :	$\frac{1}{4}$" dia. x 1 inch length, 96 s/min.
		Discharge Pressure :	1000 psia
(11)	Back pressure valve	Material :	Stainless Steel
		Type :	Spring loaded, diaphram.
		Size :	$\frac{1}{4}$ inch, 0.6 gpm, 60 psig.
(12)	Impedance Cell	Material :	Lucite
		Size :	1 3/4 inches length, $\frac{1}{4}$ inch i.d. 1 $\frac{1}{2}$ inches o.d.
		Electrodes:	Platinum, coated with platinum black, 26 guage, $\frac{1}{2}$ inch apart, extentending 1/8 inch in the casing.

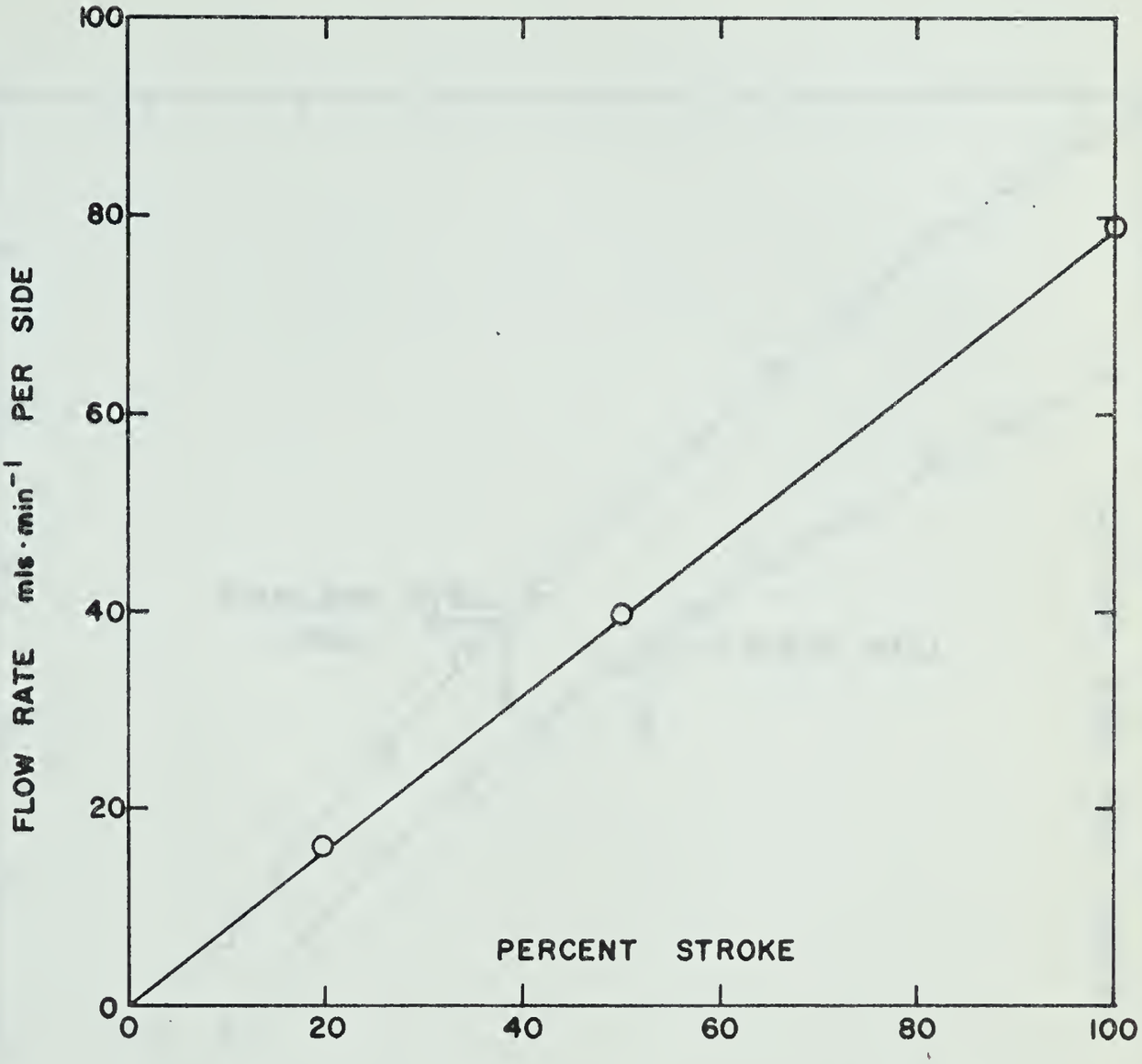

FIGURE B-1 : CALIBRATION OF THE MINIPUMP FOR PRODUCT WITHDRAWAL

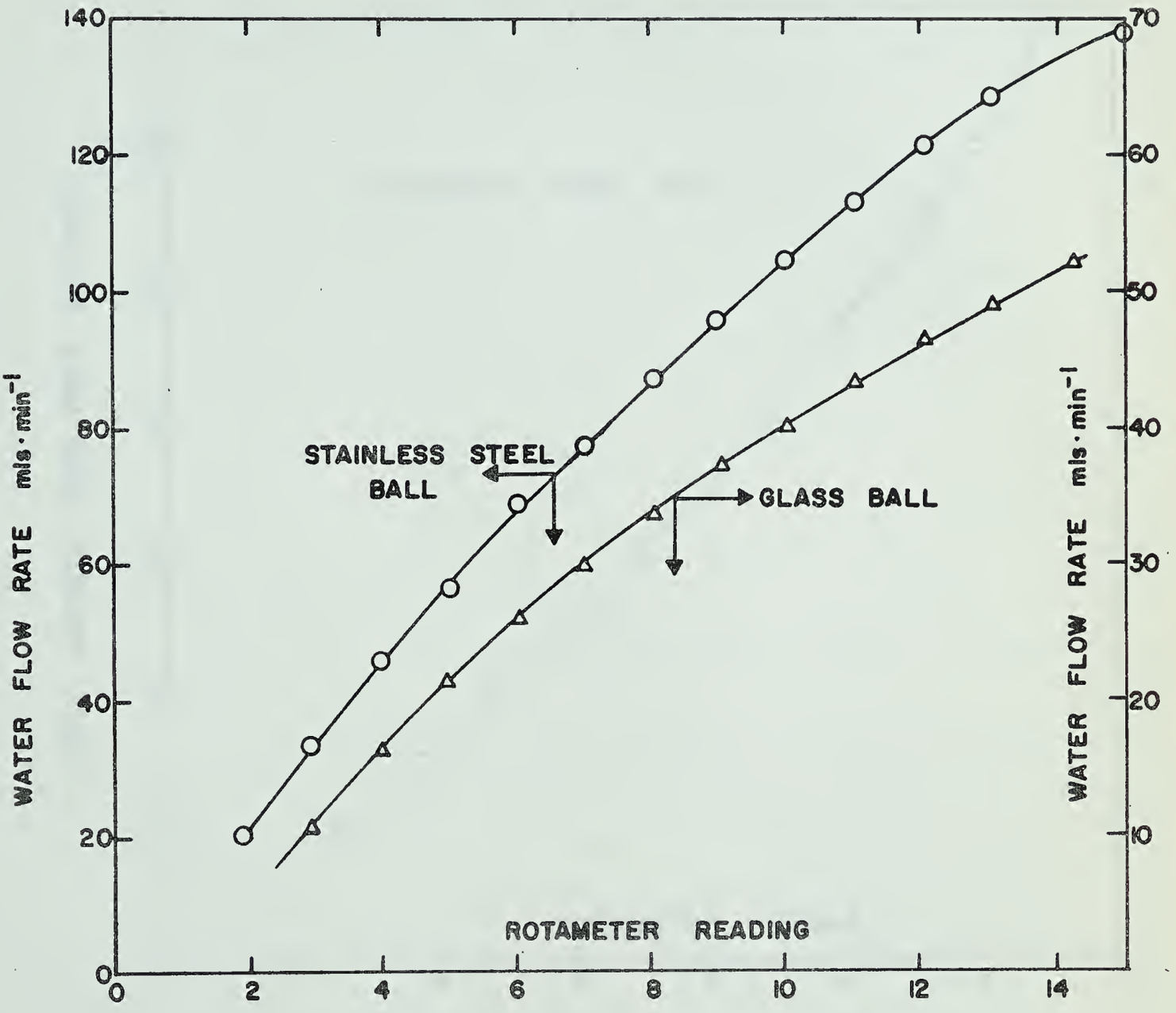

FIGURE B-2 : CALIBRATION OF ROTAMETER FOR WATER FEED

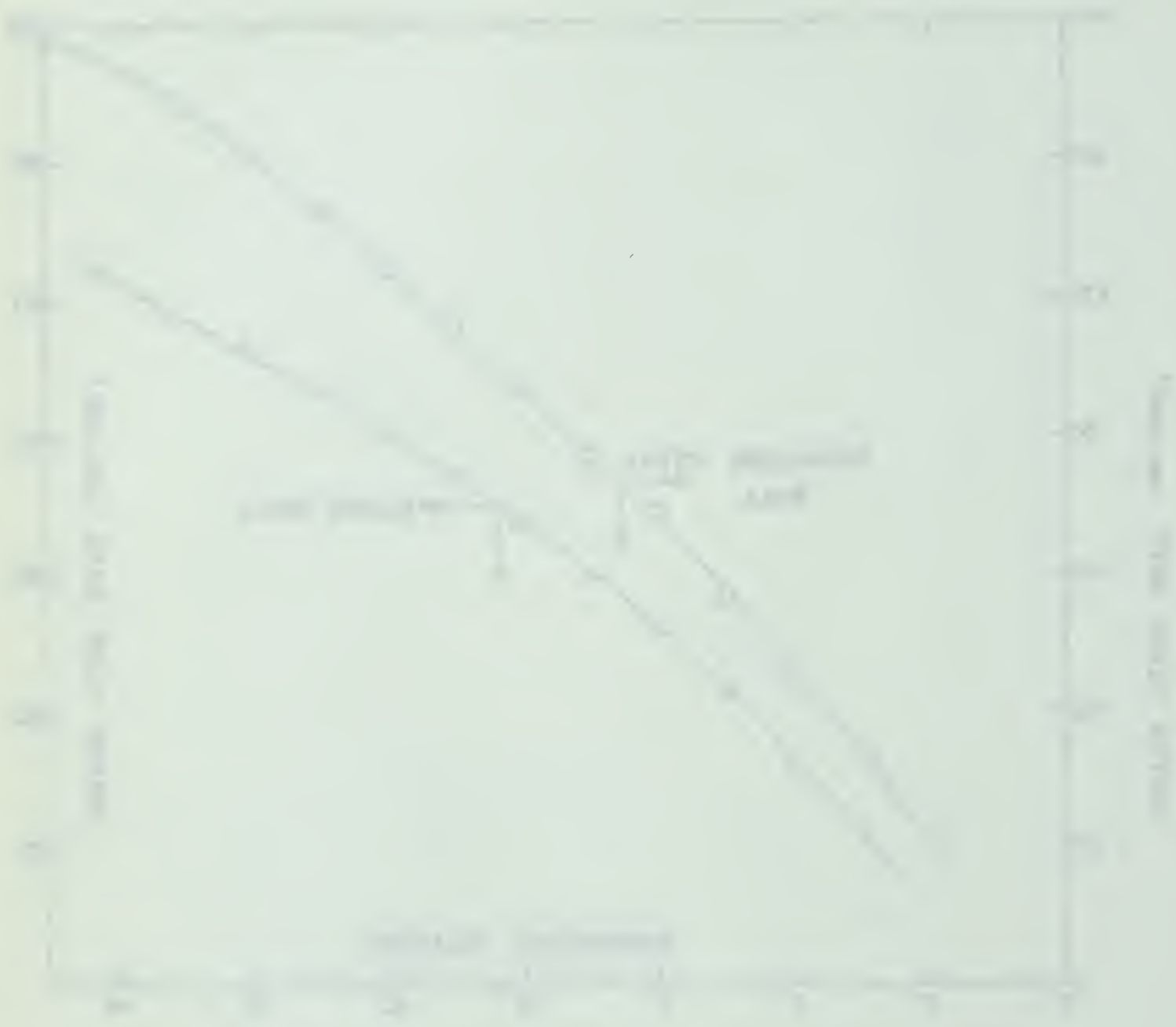

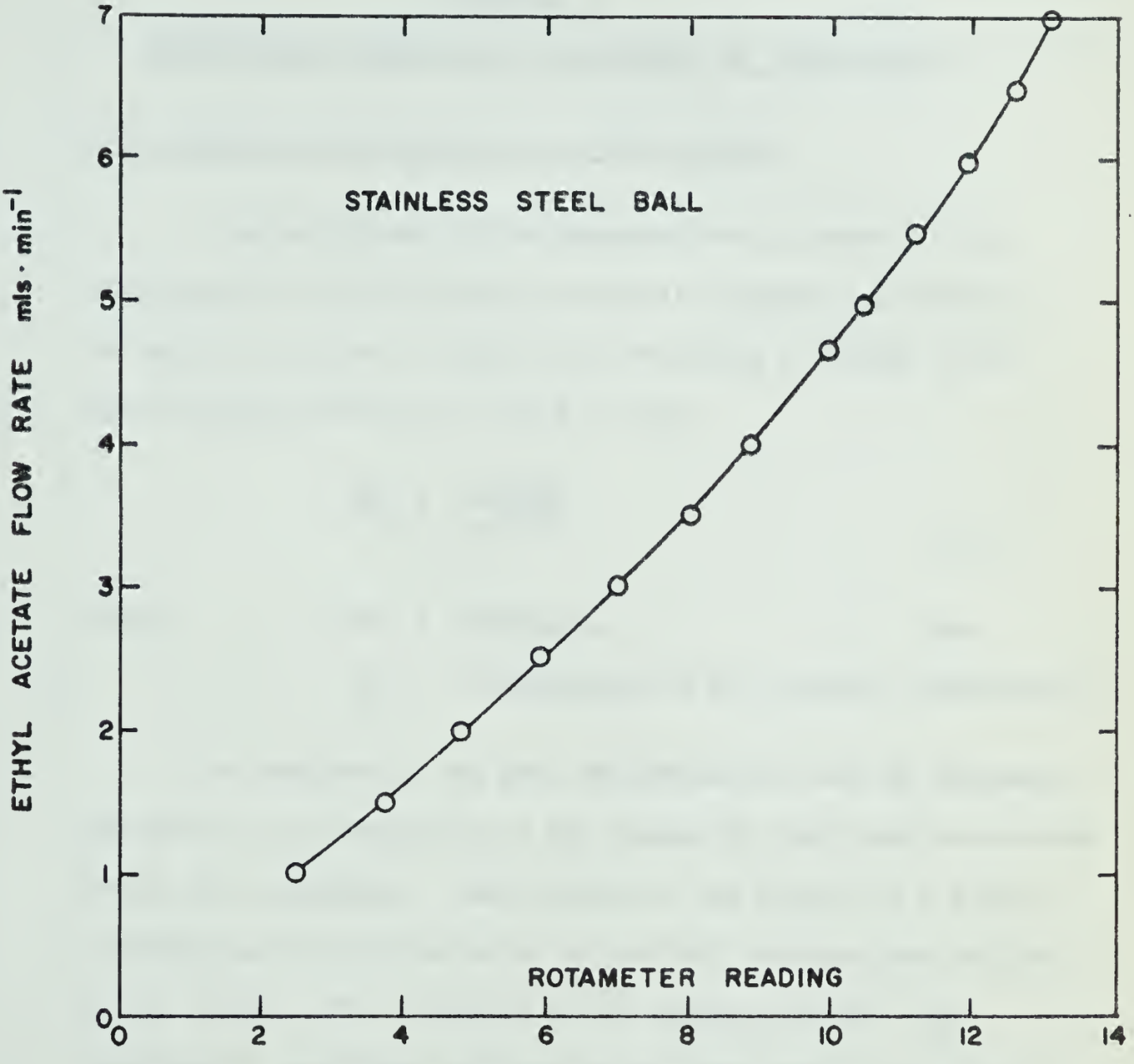

FIGURE B-3 : CALIBRATION OF ROTAMETER FOR ETHYL ACETATE FEED

APPENDIX C

EXPERIMENTAL OBSERVATIONS AND METHODS OF CALCULATIONS

C-1 Response of the Reactor to a Step Function

The calibration of the impedance cell in terms of the concentrations of HCl solution versus its impedance as measured in the cell is given in TABLE (C-1) and shown in FIGURE (C-1). The following relation was found to hold:

$$IMP = \frac{0.02446}{CN^{0.936}} \qquad (C\text{-}1)$$

where, IMP = Impedance, ohms

CN = Concentration of HCl solution, gmmoles·ml^{-1}

The calibration had good reproducibility and the impedance was found to be insensitive to the changes in flow rates encountered during the experiments. The response of the reactor to a sudden introduction of distilled water in 0·1N HCl solution, was followed by the change in the impedance of the effluent stream. The experimental conditions and results for three sets, 1-A, 1-B, 1-C, are given in TABLES (C-2) to (C-4), respectively.

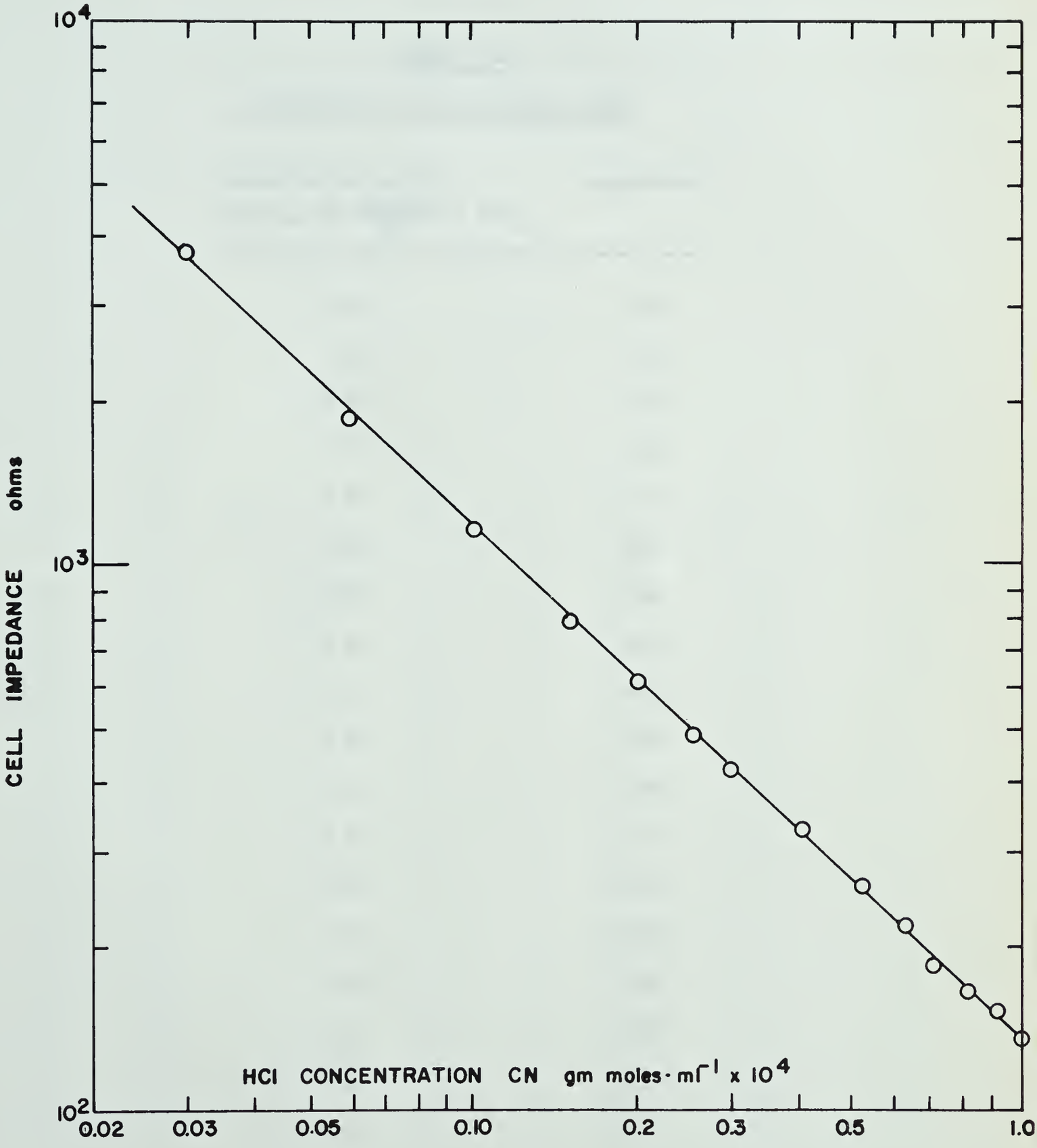

FIGURE C-1 : CALIBRATION OF THE IMPEDANCE CELL;
CONCENTRATION OF HCl SOLUTION VERSUS IMPEDANCE

TABLE C-1

CALIBRATION OF THE IMPEDANCE CELL

Concentration of HCl solution CN $\frac{\text{gmmoles}}{\text{ml}} \times 10^4$	Impedance
1.00	140
0.90	151
0.80	165
0.70	185
0.60	216
0.50	260
0.40	330
0.30	423
0.25	495
0.20	608
0.15	780
0.10	1171
0.06	1845
0.03	3780
1.00	140
0.60	218
0.25	493
0.10	1178

TABLE C-2

RESPONSE OF THE REACTOR TO A STEP FUNCTION

Set No: 1-A

Experimental conditions during the set:

$N = 75$ r.p.m.

$\bar{t} = 45$ min.

$q = 44.5$ mls·min^{-1}

$W = 97$ gms

$T = 80$ ^{o}F

t min	Imp ohms	CN $\frac{gmmoles}{ml} \times 10^4$	$\frac{CN}{CN(0)}$	t min	Imp ohms	CN $\frac{gmmoles}{ml} \times 10^4$	$\frac{CN}{CN(0)}$
0	140	1.000	1.000	24	221	0.585	0.585
1	143	0.966	0.966	25	227	0.570	0.570
2	144	0.956	0.956	27	236	0.549	0.549
3	146	0.937	0.937	28	240	0.540	0.540
4	148	0.919	0.919	29	245	0.530	0.530
5	151	0.895	0.895	30	250	0.520	0.520
6	155	0.865	0.865	31	255	0.510	0.510
7	157	0.851	0.851	32	261	0.499	0.499
8	160	0.831	0.831	33	266	0.490	0.490
9	163	0.812	0.812	34	271	0.481	0.481
10	168	0.783	0.783	36	282	0.464	0.464
11	172	0.760	0.760	37	289	0.454	0.454
12	175	0.745	0.745	38	295	0.445	0.445
13	178	0.732	0.732	39	302	0.436	0.436
14	181	0.717	0.717	40	309	0.426	0.426
15	185	0.700	0.700	42	322	0.410	0.410
16	189	0.684	0.684	43	329	0.401	0.401
17	192	0.673	0.673	44	336	0.3915	0.3915
18	196	0.659	0.659	45	343	0.3825	0.3825
19	200	0.645	0.645	46	350	0.3740	0.3740
20	205	0.630	0.630	48	365	0.3570	0.3570
21	209	0.617	0.617	49	372	0.3500	0.3500
22	212	0.609	0.609	51	389	0.3320	0.3320
23	217	0.596	0.596	53	403	0.3175	0.3175

TABLE (C-2) continued

TABLE C-2 (CONTINUED)

t min	Imp ohms	CN $\frac{\text{gmmoles}}{\text{ml}} \times 10^4$	CN / CN(0)	t min	Imp ohms	CN $\frac{\text{gmmoles}}{\text{ml}} \times 10^4$	CN / CN(0)
55	422	0.3010	0.3010	95	979	0.1200	0.1200
57	440	0.2870	0.2870	97	1020	0.1150	0.1150
59	458	0.2730	0.2730	99	1058	0.1110	0.1110
61	477	0.2620	0.2620	101	1102	0.1064	0.1064
63	497	0.2490	0.2490	103	1153	0.1012	0.1012
65	520	0.2370	0.2370	105	1204	0.0961	0.0961
67	543	0.2250	0.2250	109	1310	0.0888	0.0888
69	568	0.2150	0.2150	113	1428	0.0810	0.0810
71	591	0.2060	0.2060	117	1556	0.0738	0.0738
73	614	0.1975	0.1975	121	1695	0.0670	0.0670
75	640	0.1880	0.1880	125	1838	0.0605	0.0605
77	668	0.1790	0.1790	129	1986	0.0552	0.0552
79	700	0.1700	0.1700	133	2151	0.0501	0.0501
81	730	0.1624	0.1624	137	2330	0.0457	0.0457
83	760	0.1550	0.1550	141	2530	0.0415	0.0415
85	793	0.1480	0.1480	145	2745	0.0380	0.0380
87	827	0.1415	0.1415	149	2970	0.0351	0.0351
89	863	0.1352	0.1352	155	3350	0.0320	0.0320
91	899	0.1300	0.1300	158	3540	0.0317	0.0317
93	940	0.1245	0.1245				

TABLE C-3

RESPONSE OF THE REACTOR TO A STEP FUNCTION

Set No: 1-B

Experimental conditions during the set:

N	=	450	r.p.m.
$\bar{t}$	=	45	min.
q	=	44.5	mls·min^{-1}
W	=	97	gms
T	=	80	^{o}F

t min	Imp ohms	CN $\frac{\text{gmmoles}}{\text{ml}} \times 10^4$	CN CN(0)	t min	Imp ohms	CN $\frac{\text{gmmoles}}{\text{ml}} \times 10^4$	CN CN(0)
0	140	1.000	1.000	55	415	0.307	0.307
1	140	1.000	1.000	58	443	0.284	0.284
3	145	0.945	0.945	61	474	0.263	0.263
5	151	0.895	0.895	64	506	0.244	0.244
7	158	0.843	0.843	67	539	0.227	0.227
9	165	0.800	0.800	70	572	0.2155	0.2155
11	171	0.765	0.765	73	608	0.200	0.200
13	178.5	0.729	0.729	76	647	0.186	0.186
15	186	0.697	0.697	79	687	0.174	0.174
17	194	0.666	0.666	82	735	0.161	0.161
19	202	0.639	0.639	85	781	0.150	0.150
21	210	0.615	0.615	88	841	0.139	0.139
23	217	0.596	0.596	91	895	0.1305	0.1305
25	225	0.574	0.574	94	952	0.123	0.123
27	236	0.549	0.549	97	1010	0.116	0.116
29	245	0.530	0.530	99	1055	0.1113	0.1113
31	256	0.508	0.508	104	1180	0.099	0.099
33	266	0.490	0.490	109	1320	0.088	0.088
35	277	0.473	0.473	114	1460	0.079	0.079
37	289	0.454	0.454	119	1635	0.0698	0.0698
39	301	0.436	0.436	124	1805	0.0620	0.0620
41	314	0.420	0.420	129	2008	0.0545	0.0545
43	327.5	0.402	0.402	134	2225	0.0483	0.0483
45	341	0.385	0.385	139	2490	0.0423	0.0423
47	355	0.368	0.368	144	2780	0.0376	0.0376
49	369	0.3525	0.3525	149	3100	0.0340	0.0340
52	391	0.329	0.329	154	3445	0.0316	0.0316

TABLE C-4

RESPONSE OF THE REACTOR TO A STEP FUNCTION

Set No: 1-C

Experimental conditions during the set:

N	= 55	r.p.m.
$\bar{t}$	= 14.8	min.
q	= 135	mls·min^{-1}
W	= 97	gms
T	= 80	^{o}F

t min	Imp ohms	CN $\frac{\text{gmmoles}}{\text{ml}} \times 10^{4}$	CN / CN(0)	t min	Imp ohms	CN $\frac{\text{gmmoles}}{\text{ml}} \times 10^{4}$	CN / CN(0)
0	140	1.000	1.000	26	713	0.167	0.167
1	146	0.937	0.937	27	760	0.155	0.155
2	156	0.858	0.858	28	810	0.145	0.145
3	167	0.788	0.788	29	863	0.135	0.135
4	178	0.732	0.732	30	929	0.126	0.126
5	189	0.685	0.685	31	989	0.1185	0.1185
6	201	0.643	0.643	32	1049	0.112	0.112
7	214	0.603	0.603	33	1110	0.1055	0.1055
8	227	0.570	0.570	34	1180	0.099	0.099
9	242	0.536	0.536	35	1260	0.0925	0.0925
10	257	0.506	0.506	36	1350	0.086	0.086
11	274	0.476	0.476	37	1445	0.080	0.080
12	293	0.447	0.447	38	1550	0.074	0.074
13	314	0.420	0.420	39	1650	0.069	0.069
14	336	0.391	0.391	40	1760	0.064	0.064
15	358	0.365	0.365	41	1870	0.0595	0.0595
16	380	0.341	0.341	42	1990	0.055	0.055
17	404	0.318	0.318	43	2120	0.051	0.051
18	430	0.294	0.294	44	2270	0.047	0.047
19	458	0.273	0.273	45	2410	0.044	0.044
20	487	0.256	0.256	46	2560	0.041	0.041
21	518	0.2375	0.2375	47	2720	0.0385	0.0385
22	553	0.221	0.221	48	2900	0.036	0.036
23	587	0.212	0.212	49	3100	0.034	0.034
24	633	0.190	0.190	50	3300	0.0325	0.0325
25	672	0.178	0.178	51	3500	0.031	0.031

C-2 Sample Calculations for Ester Conversion

If, (a) Sample size of the effluent stream = 25 mls

(b) Normality of acetic acid in the effluent stream = NA

(c) Normality of NaOH used for titration = 1/40

(d) mls of N/40 NaOH used for titrating 25 mls of effluent stream = VS

(e) mls of N/40 NaOH required for titrating 25 mls of water kept in contact with the resins = 0.52

then,

(f) mls of N/40 NaOH necessary to titrate acetic acid in the 25 mls of effluent stream = V

= VS-0.52

and

$$NA = \frac{V}{(25)(40)} = V \times 10^{-3}$$

therefore, Concentration of acetic acid in the effluent stream = A_o

= $V \times 10^{-6}$ gmmoles·ml^{-1}

Now,

$$C_i = \frac{q_e \rho_e / m_e}{q_e + q_w}$$

$$= \frac{q_e \rho_e}{q M_e}$$

where,

C_i = Influent concentration of ethyl acetate gmmoles·ml^{-1}

M_e = Molecular weight of ethyl acetate

= 88.11

q_e = Flow rate of ethyl acetates mls·min^{-1}

q_w = Flow rate of water mls·min^{-1}

q = Total influent flow rate mls·min^{-1}

= $q_e + q_w$

ρ_e = Density of ethyl acetate gms·ml^{-1}

= 0.892

Since one mole of ethyl acetate hydrolysed yields one mole of acetic acid,

% conversion of ethyl acetate = X(100)

$$= \frac{A_o}{C_i} \times 100$$

detailed calculations for Set 3-A

Run No. 3-A-4

$$C_i = \frac{q_e \rho_e}{q M_e}$$

$$= \frac{(5)(0.892)}{(100)(88.11)}$$

$$= 5.0732 \times 10^{-4} \text{ gmmoles·ml}^{-1}$$

V = 6.41 mls

$$\therefore \quad A_o = V \times 10^{-6}$$

$$= 6.41 \times 10^{-6} \quad \text{gmmoles} \cdot \text{ml}^{-1}$$

$$\text{and } X(100) = \frac{(6.41 \times 10^{-6})}{(5.0732 \times 10^{-4})} \times 100$$

$$= 1.26$$

$$\frac{C_i}{A_o} = \frac{5.0732 \times 10^{-4}}{6.41 \times 10^{-6}}$$

$$= 79.15$$

Similar results for the other runs in set 3-A are given in TABLE (C-8). Also, the above calculations for the experimental runs made to evaluate the significance of external film diffusion are shown in TABLES (C-5) to (C-7).

The functional relation between $\frac{C_i}{A_o}$ and q is given by (equation (IV.18)):

$$\frac{C_i}{A_o} = 1 + \frac{q}{Q}$$

This is an equation of a straight line with slope equal to $\frac{1}{Q}$ and intercept of unity with the vertical axis. The best fit of the experimental data of $\frac{C_i}{A_o}$ vs q was taken as the line which passes through (0,1) and gives the least sum of squares of the deviations of the individual observations from the line. It can be shown that for

TABLE C-5

SIGNIFICANCE OF EXTERNAL FILM DIFFUSION

Set No: 2-A

Experimental conditions during the set:

$T = 80$ °F

$W = 95$ gms

$R = 0.00283$ cms

$q_w = 38.4$ mls·min^{-1}

$q_e = 1.6$ mls·min^{-1}

$q = 40.0$ mls·min^{-1}

$C_i = 5.0732 \times 10^{-4}$ gmmoles·ml^{-1}

$\bar{t} = 50$ min

Run No.	N r.p.m.	V* mls	A_o $\frac{\text{gmmoles}}{\text{ml}} \times 10^6$	X(100) % conversion	$\frac{C_i}{A_o}$
A-1	50	3.91	3.91	0.77	129.75
A-2	100	14.01	14.01	2.76	36.21
A-3	125	32.12	32.12	6.33	15.79
A-4	150	50.22	50.22	9.90	10.10
A-5	200	52.46	52.46	10.34	9.67
A-6	275	53.77	53.77	10.60	9.43
A-7	325	52.93	52.93	10.44	9.58
A-8	400	53.64	53.64	10.57	9.46
A-9	475	53.48	53.48	10.54	9.49

* V = mls of N/40 NaOH necessary to titrate acetic acid in 25 mls of the effluent stream.

TABLE C-6

SIGNIFICANCE OF EXTERNAL FILM DIFFUSION

Set No. 2-B

Experimental conditions during the set:

$T = 80$ °F

$W = 48$ gms

$R = 0.00283$ cms

$q_w = 38.4$ mls·min^{-1}

$q_e = 1.6$ mls·min^{-1}

$q = 40.0$ mls·min^{-1}

$C_i = 5.0732 \times 10^{-4}$ gmmoles·ml^{-1}

$\bar{t} = 50$ min

Run No.	N	V	A_o	X(100)	$\frac{C_i}{A_o}$
	r.p.m.	mls	$\frac{\text{gmmoles}}{\text{ml}} \times 10^6$	% conversion	
B-1	75	2.58	2.58	0.51	196.64
B-2	125	6.88	6.88	1.36	73.74
B-3	150	16.86	16.86	3.32	30.09
B-4	200	28.47	28.47	5.61	17.82
B-5	320	27.92	27.92	5.50	18.17
B-6	420	28.61	28.61	5.64	17.33
B-7	500	28.53	28.53	5.62	17.78

TABLE C-7

SIGNIFICANCE OF EXTERNAL FILM DIFFUSION

Set No. 2-C

Experimental conditions during the set:

T	=	100	^{o} F
W	=	48	gms
R	=	0.00283	cms
q_w	=	38.4	mls·min^{-1}
q_e	=	1.6	mls·min^{-1}
q	=	40.0	mls·min^{-1}
C_i	=	5.0732×10^{-4}	gmmoles·ml^{-1}
$\bar{t}$	=	50	min

Run No.	N	V	A_o	X(100)	$\frac{C_i}{A_o}$
	r.p.m.	mls	$\frac{\text{gmmoles}}{\text{ml}} \times 10^6$	% conversion	
C-1	100	17.37	17.37	3.42	29.21
C-2	200	68.46	68.46	13.50	7.41
C-3	350	67.46	67.46	13.30	7.52
C-4	500	68.28	68.28	13.46	7.43

$$e^2 = \sum_{1}^{n} \left[\left(\frac{C_i}{A_o} \right)_k - \left(1 + \frac{q_k}{Q} \right) \right]^2$$

n = number of runs in a set

to be minimum, the slope of the line is

$$\frac{1}{Q} = \frac{\sum \left(\frac{C_i}{A_o} \right)_k \left(q \right)_k - \left(q \right)_k}{\sum \left(\frac{C_i}{A_o} \right)_k^2}$$

Thus for set 3-A we have the following values (See TABLE (C-8)):

Run No. k	$\frac{C_i}{A_o}$	q	$(\frac{C_i}{A_o})q$	$\left(\frac{C_i}{A_o}\right)^2$
3-A-1	31.43	40	1257.2	1600
3-A-2	47.10	60	2826.0	3600
3-A-3	62.40	80	4992.0	6400
3-A-4	79.15	100	7915.0	10000
n = 4	220.08	280	16990.2	21600

$$\therefore \quad \frac{1}{Q} = \frac{(16990.2) - (280)}{(21600)}$$

$$= 0.7736$$

$$\therefore \quad Q = 1.2926$$

For each set, the values of Q are obtained in this manner. Thus at 80^{o} F we have the following values (See TABLES (C-8) to (C-11):

Set No.	W gms	R cms	Q mls·min^{-1}
3-A	28	0.03045	1.2926
3-B	42	0.03045	1.9466
3-C	51	0.01268	2.5289
3-D	68	0.00283	3.4428

The equation

$$Q = \frac{3WD}{R^2\varsigma} \left(wR \cdot \coth(wR) - 1\right) \qquad \text{(IV.15)}$$

where,

$$w^2 = \frac{k}{D}$$

was then used to evaluate the parameters k and D from the experimental data shown above - both, k and D, being independent of W and R. The equation has two unknowns, w and D, and there are four sets of observations, Hence, the 'best' values of w and D were obtained by the following trial-and-error-calculations procedure.

(1) Assume a reasonable but arbitary value of w.

(2) Using equation (IV.15) calculate D for each set of experimental values of Q, W and R. This gives, say, D_1, D_2, D_3 and D_4.

(3) Calculate the mean D :

$$D_m = \frac{\sum_{1}^{4} D_i}{4}$$

(4) Calculate the standard deviation of D_i's with respect to D_m, using the following formula

$$S.D. = \left[\frac{\sum_{1}^{4} (D_i - D_m)^2}{4 - 1} \right]^{\frac{1}{2}}$$

(5) Change the value of w and repeat steps (2) to (5).

(6) Select the range of w within which the minimum standard deviation as calculated in step (4) lies.

(7) Now vary w by much smaller values and repeat steps (1) to (6).

Thus progressively the range of w was narrowed down and smaller jumps were given in varying w. In the final set of calculations the successive values of w differed by only 0.01. Eventually, the value of w which gave the minimum standard deviation of D_i's with respect to the mean, D_m (Step-4), was chosen as the best value and the corresponding D_m as the best value for diffusivity, D.

Using the 'best' values of w and D, Q's were calculated using equation (IV-15) and were denoted QC. The final values for 80° F were as follows:

Set No.	Q mls·min^{-1}	D x 10^5 cm^2·min^{-1}	QC mls·min^{-1}
3-A	1.2926	2.9805	1.3021
3-B	1.9466	2.9719	1.9532
3-C	2.5289	2.9978	2.5248
3-D	3.4428	3.0366	3.4119
	mean	2.9967	

$w = 36.52$

$D = 2.9967 \times 10^{-5}$ cm^2·min^{-1}

$k = w^2 D$

$= 3.997 \times 10^{-2}$ min^{-1}

The Relative Standard Deviation (RSD) of the above fit was calculated by using the following expression

$$RSD = \left[\frac{\sum_{1}^{4} (D_i - D_m)^2}{(4 - 1) D_m^2} \right]^{\frac{1}{2}} \times 100$$

$= 0.67$ %

Results of similar calculations for 100° F & 120° F are shown in TABLE (V-2).

TABLE C-8

EVALUATION OF k AND D

Set No. 3-A

Experimental conditions during the set:

$T = 80$ ^{o}F

$W = 28$ gms

$R = 0.03045$ cms

$N = 600$ r.p.m.

$C_i = 5.0732 \times 10^{-4}$ gmmoles·ml^{-1}

Run No.	q_e mls/min	q_w mls/min	q mls/min	$\bar{t}$ min.	V mls	A_o $\frac{\text{gmmoles}}{\text{ml}} \times 10^6$	$\frac{C_i}{A_o}$	X(100) % conversion
A-1	2.0	38	40	50	16.14	16.14	31.43	3.18
A-2	3.0	57	60	33.33	10.77	10.77	47.10	2.12
A-3	4.0	76	80	25	8.13	8.13	62.40	1.60
A-4	5.0	95	100	20	6.41	6.41	79.15	1.26

The least square fit of the equation (IV.18) gives

$$\frac{1}{Q} = 0.7736$$

$$\therefore \quad Q = 1.2926 \text{ mls·min}^{-1}$$

TABLE C-9

EVALUATION OF k AND D

Set No. 3-B

Experimental conditions during the set:

$T = 80$ ^{o}F

$W = 42$ gms

$R = 0.03045$ cms

$N = 600$ r.p.m.

$C_i = 5.0732 \times 10^{-4}$ gmmoles·ml^{-1}

Run No.	q_e mls/min	q_w mls/min	q mls/min	$\bar{t}$ min.	V mls	A_o $\frac{\text{gmmoles}}{\text{ml}} \times 10^6$	$\frac{C_i}{A_o}$	X(100) % conversion
B-1	1.5	28.5	30	66.67	31.53	31.53	16.09	6.21
B-2	2.5	47.5	50	40.00	20.08	20.08	25.26	3.96
B-3	3.5	66.5	70	28.57	14.42	14.42	35.18	2.84
B-4	4.5	85.5	90	22.22	10.67	10.67	47.55	2.10
B-5	5.5	104.5	110	18.17	8.57	8.57	59.20	1.69

The least square fit of the equation (IV.18) gives

$$\frac{1}{Q} = 0.5137$$

$$\therefore \quad Q = 1.9466 \quad \text{mls·min}^{-1}$$

TABLE C-10

EVALUATION OF k AND D

Set No. 3-C

Experimental conditions during the set:

$T = 80$ °F

$W = 51$ gms

$R = 0.01268$ cms

$N = 600$ r.p.m.

$C_i = 5.0732 \times 10^{-4}$ gmmoles/ml

Run No.	q_e mls/min	q_w mls/min	q mls/min	$\bar{t}$ min.	V mls	A_o $\frac{\text{gmmoles}}{\text{ml}} \times 10^6$	$\frac{C_i}{A_o}$	X(100) % conversion
C-1	1.75	33.25	35	57.14	32.71	32.71	15.51	6.45
C-2	3.0	57	60	33.33	20.25	20.25	25.05	3.99
C-3	4.0	76	80	25	15.71	15.71	32.29	3.10
C-4	5.0	95	100	20	12.56	12.56	40.39	2.41

The least square fit of equation (IV.18) gives

$$\frac{1}{Q} = 0.3954$$

$$\therefore \quad Q = 2.5289 \quad \text{mls} \cdot \text{min}^{-1}$$

TABLE C-11

EVALUATION OF k AND D

Set No. 3-D

Experimental conditions during the set:

$T = 80$ $^{\circ}F$

$W = 68$ gms

$R = 0.00283$ cms

$N = 600$ r.p.m.

$C_i = 5.0732 \times 10^{-4}$ gmmoles·ml^{-1}

Run No.	q_e mls/min	q_w mls/min	q mls/min	$\bar{t}$ min.	V mls	A_o $\frac{\text{gmmoles}}{\text{ml}} \times 10^6$	$\frac{C_i}{A_o}$	X(100) % conversion
D-1	1.0	19	20	100	75.59	75.59	6.71	14.90
D-2	2.0	38	40	50	38.91	38.91	13.04	7.67
D-3	3.25	61.75	65	30.77	25.99	25.99	19.52	5.12
D-4	4.5	85.5	90	22.22	18.94	18.94	26.79	3.73
D-5	6.0	114	120	16.67	14.02	14.02	36.19	2.76

The least square fit of equation (IV.18) gives

$$\frac{1}{Q} = 0.2905$$

$$\therefore \quad Q = 3.4428 \text{ mls·min}^{-1}$$

TABLE C-12

EVALUATION OF k AND D

Set No. 4-A

Experimental conditions during the set:

$T = 100$ ^{o}F

$W = 80$ gms

$R = 0.03045$ cms

$N = 600$ r.p.m.

$C_i = 4.0586 \times 10^{-4}$ gmmoles·ml^{-1}

Run No.	q_e mls/min	q_w mls/min	q mls/min	$\bar{t}$ min.	V mls	A_o $\frac{\text{gmmoles}}{\text{ml}} \times 10^6$	$\frac{C_i}{A_o}$	X(100) % conversion
A-1	1.2	28.8	30	66.67	97.23	97.23	4.17	23.98
A-2	2.4	57.6	60	33.33	56.56	56.56	7.18	13.93
A-3	3.2	76.8	80	25	42.29	42.29	9.60	10.42
A-4	4.0	96.0	100	20	34.09	34.09	11.91	8.40

The least square fit of equation (IV.18) gives

$$\frac{1}{Q} = 0.1074$$

$$\therefore \quad Q = 9.3100 \text{ mls·min}^{-1}$$

TABLE C-13

EVALUATION OF k AND D

Set No. 4-B

Experimental conditions during the set:

$T = 100$ ^{o}F

$W = 43$ gms

$R = 0.01268$ cms

$N = 600$ r.p.m.

$C_i = 4.0586 \times 10^{-4}$ gmmoles·ml^{-1}

Run No.	q_e mls/min	q_w mls/min	q mls/min	$\bar{t}$ min.	V mls	A_o $\frac{\text{gmmoles}}{\text{ml}} \times 10^6$	$\frac{C_i}{A_o}$	X(100) % conversion
B-1	1.2	28.8	30	66.67	59.70	59.70	6.80	14.71
B-2	2.0	48.0	50	40.00	39.93	39.93	10.16	9.84
B-3	2.8	67.2	70	28.57	29.93	29.93	13.56	7.37
B-4	3.6	86.4	90	22.22	23.52	23.52	17.26	5.79

The least square fit of equation (IV.18) gives

$$\frac{1}{Q} = 0.1814$$

$$\therefore \quad Q = 5.5137 \quad \text{mls·min}^{-1}$$

TABLE C-14

EVALUATION OF k AND D

Set No. 4-C

Experimental conditions during the set:

$T = 100$ ^{o}F

$W = 70$ gms

$R = 0.00283$ cms

$N = 600$ r.p.m.

$C_i = 4.0586 \times 10^{-4}$ gmmoles·ml^{-1}

Run No.	q_e mls/min	q_w mls/min	q mls/min	$\bar{t}$ min.	V mls	A_o $\frac{\text{gmmoles}}{\text{ml}} \times 10^6$	$\frac{C_i}{A_o}$	X(100) % conversion
C-1	1.6	38.4	40	50	75.90	75.90	5.35	18.69
C-2	2.4	57.6	60	33.33	51.44	51.44	7.89	12.67
C-3	3.2	76.8	80	25	40.66	40.66	9.98	10.02
C-4	4.0	96.0	100	20	32.81	32.81	12.37	8.08

The least square fit of equation (IV.18) gives

$$\frac{1}{Q} = 0.1131$$

$$\therefore \quad Q = 8.8417 \quad \text{mls·min}^{-1}$$

TABLE C-15

EVALUATION OF k AND D

Set No. 5-A

Experimental conditions during the set:

$T = 120$ $^{\circ}F$

$W = 80$ gms

$R = 0.03045$ cms

$N = 600$ r.p.m.

$C_i = 4.0586 \times 10^{-4}$ gmmoles·ml^{-1}

Run No.	q_e mls/min	q_w mls/min	q mls/min	$\bar{t}$ min.	V mls	A_o $\frac{\text{gmmoles}}{\text{ml}} \times 10^6$	$\frac{C_i}{A_o}$	X(100) % conversion
A-1	1.2	28.8	30	66.67	170.09	170.09	2.39	41.84
A-2	2.0	48.0	50	40	128.05	128.05	3.17	31.54
A-3	3.2	76.8	80	25	86.42	86.42	4.70	21.28
A-4	4.4	105.6	110	18.17	64.38	64.38	6.30	15.87

The least square fit of equation (IV.18) gives

$$\frac{1}{Q} = 0.0470$$

$$\therefore \quad Q = 21.2787 \text{ mls·min}^{-1}$$

TABLE C-16

EVALUATION OF k AND D

Set No. 5-B

Experimental conditions during the set:

$T = 120$ ^{o}F

$W = 43$ gms

$R = 0.01268$ cms

$N = 600$ r.p.m.

$C_i = 4.0586 \times 10^{-4}$ gmmoles·ml^{-1}

Run No.	q_e mls/min	q_w mls/min	q mls/min	$\bar{t}$ min.	V mls	A_o $\frac{\text{gmmoles}}{\text{ml}} \times 10^6$	$\frac{C_i}{A_o}$	X(100) % conversion
B-1	1.2	28.8	30	66.67	124.24	124.24	3.27	30.58
B-2	2.0	48.0	50	40	83.29	83.29	4.87	20.53
B-3	2.8	67.2	70	28.57	61.38	61.38	6.61	15.13
B-4	3.6	86.4	90	22.22	50.43	50.43	8.05	12.42

The least square fit of equation (IV.18) gives

$$\frac{1}{Q} = 0.0786$$

$$\therefore \quad Q = 12.7251 \text{ mls·min}^{-1}$$

TABLE C-17

EVALUATION OF k AND D

Set No. 5-C

Experimental conditions during the set:

$T = 120$ $^{\circ}F$

$W = 70$ gms

$R = 0.00283$ cms

$N = 600$ r.p.m.

$C_i = 4.0586 \times 10^{-4}$ gmmoles·ml^{-1}

Run No.	q_e mls/min	q_w mls/min	q mls/min	$\bar{t}$ min.	V mls	A_o $\frac{\text{gmmoles}}{\text{ml}} \times 10^6$	$\frac{C_i}{A_o}$	X(100) % conversion
C-1	1.6	38.4	40	50	142.23	142.23	2.85	25.09
C-2	2.4	57.6	60	33.33	103.79	103.79	3.91	25.57
C-3	3.2	76.8	80	25	80.53	80.53	5.04	19.84
C-4	4.0	96.0	100	20	70.59	70.59	5.75	17.39

The least square fit of equation (IV.18) gives:

$$\frac{1}{Q} = 0.0485$$

$$\therefore \quad Q = 20.6343 \quad \text{mls·min}^{-1}$$